5-1995

Late Quaternary Glacial Geology, Shoreline Morphology, and Tephrochronology of the Iliamna/Naknek/Brooks Lake Area, Southwestern Alaska

Karen B. Stilwell
Utah State University

LATE QUATERNARY GLACIAL GEOLOGY, SHORELINE MORPHOLOGY, AND TEPHROCHRONOLGY OF THE ILIAMNA/NAKNEK/BROOKS LAKE AREA, SOUTHWESTERN ALASKA

by

Karen B. Stilwell

A thesis submitted in partial fulfillment
of the requirements for the degree

of

MASTER OF SCIENCE

in

Geology

Approved:

UTAH STATE UNIVERSITY
Logan, Utah

1995

ABSTRACT

Late Quaternary Glacial Geology, Shoreline Morphology, and Tephrochronology of the Iliamna/Naknek/Brooks Lake Area, Southwestern Alaska

by

Karen B. Stilwell, Master of Science

Utah State University, 1995

Major Professor: Darrell Kaufman
Department: Geology

This study focuses on the late-Wisconsin Brooks Lake glaciation, lake-level fluctuations, and volcanic deposits in the Iliamna/Naknek/Brooks Lake area on the northern Alaska Peninsula, southwestern Alaska. The Brooks Lake glaciation consists of five stades, from youngest to oldest: Kvichak, Iliamna, Newhalen, Iliuk, and Ukak. This thesis reassigns the type Mak Hill moraine to a pre-late-Wisconsin glaciation, and considers the moraine enclosing Naknek Lake an early-late-Wisconsin deposit correlative to either the Kvichak stade, Iliamna stade, or both. The presence in the Iliamna Lake valley, and the absence in the Naknek Lake valley of a two-fold earliest-late-Wisconsin Kvichak/Iliamna glacial sequence suggest that the two glacial systems responded differently to climate change, or glacier/bed dynamics due to differing ice sources and glacier configurations. Plant macrofossils dated at 26,155 ± 285 ^{14}C yr BP afford a new maximum-limiting age on the type Kvichak moraine. Slope angles on the type Kvichak and Iliamna moraines are less steep (~11-15°) than on younger Newhalen, Iliuk, and Ukak moraines (~18-20°), indicating that a considerable length of time separated the Iliamna and Newhalen stades.

Correlation of this time-stratigraphic marker with other better dated Alaskan glacial sequences suggests that the interstadial occurred ~13-14 ka.

Following late-Wisconsin deglaciation of the Iliamna and Naknek lake basins, lake levels lowered, creating a flight of wave-cut terraces. Horizontal terraces, formed during latest-Wisconsin/early-Holocene time, at ~40 m above Iliamna Lake, and ~15 and ~30 m above Naknek Lake, suggest that these shorelines are not tilted as a result of glacial-isostatic rebound or regional tectonism. The most prominent terraces above both lakes lay about halfway between the highest terrace and present-day lake level. If these terraces are correlative, then this indicates some climate control on lake-level fluctuations.

Electron-microprobe analysis of six late-Pleistocene tephra samples allows five samples to be correlated with latest-Pleistocene Lethe tephra, and extends the Lethe ash plume ~125 km westward, and ~150 km northwestward of its presumed source area. Analysis of four early-Holocene black tephras fails to support any correlations, suggesting that there are multiple black tephras in the area. Ash C, a tricolored ash, consists of more than one chemically distinct tephra, and there is little consistency between color zones of the ash at different sites.

(176 pages)

ACKNOWLEDGMENTS

I would especially like to thank Darrell Kaufman for making available to me ideas, encouragement, assistance, and funding (NSF Grant #OPP-9217634) to undertake and complete this research. I would also like to thank the Geological Society of America and the American Alpine Club for additional financial support. I give a special thanks to Caleb Thompson for his assistance in the field; to Pat McClenahan and Robin Leatherwood (Katmai National Park Service), the Fish and Wildlife Service in King Salmon, and Chris Foote (Fisheries Institute at University of Washington) for lodging, equipment, and field support; to James Riehle and Charles Meyer for electron-microprobe analysis of tephras; and also to Peter Lea, Chris Waythomas, Don Fiesinger, Steve Simms, Donald Dumond, Richard Bland, and DeAnne Pinney for their input.

Karen B. Stilwell

CONTENTS

LIST OF TABLES

LIST OF FIGURES

CHAPTER 1
INTRODUCTION

Around the globe, pronounced climate change is the most prominent characteristic of late-Quaternary time. Most notably, during the height of the Last Glacial Maximum, the Laurentide Ice Sheet, which was centered over Canada, was high enough to divert the jet stream southward, African lakes were virtually dry, lakes in the southwestern portion of the United States were at a maximum, and all glaciers advanced from mountainous areas. Because high latitudes are affected most by global climate change, these areas are crucial to understanding the global climate system. Mountainous regions in Alaska were dramatically affected during the late Wisconsin (approximately 25,000 to 10,000 years ago). Glaciers advanced, scouring the landscape and leaving behind moraines that provide clues for geologists to determine the timing and driving mechanisms behind climate change and glaciations.

The Iliamna/Naknek/Brooks Lake study area (Chapter 2) is located on the northern Alaska Peninsula in southwestern Alaska to the west of Kodiak Island and to the east of Bristol Bay. The physiography of the northern Alaska Peninsula is characterized in the west by broad, extensive lowlands, termed the Bristol Bay lowlands, east-west trending lakes basins in the central portion, and on the east side of the peninsula by rugged, active volcanoes of the Aleutian Range that support present-day glaciers.

This thesis addresses late-Wisconsin glaciation, lake-level fluctuations during the Pleistocene-Holocene transition, and tephras left by late-Quaternary volcanic eruptions on the northern Alaska Peninsula. Glaciers advanced and retreated several times to deposit moraines ascribed to the late-Wisconsin Brooks Lake glaciation of Muller (1952). These deposits are the most prominent geomorphic features in the area. Following deglaciation of the lake basins, lake levels lowered, creating a flight of beach ridges and wave-cut terraces that rim the numerous lakes in the region. These beach ridges and wave-cut terraces

are also notable geomorphic features. Volcanoes acted independently of climate, erupting numerous ashes that are scattered throughout the study area. These deposits provide a detailed record of late-Quaternary volcanism and help to constrain the ages of glacial advances and lake-level changes.

This thesis is composed of five chapters that help to unravel the late-Quaternary geomorphic and geochronologic context of the glacial advances and lake-level fluctuations that have significantly shaped the present-day landscape of the Iliamna/Naknek/Brooks Lake area. In this thesis, I also evaluate the role of regional and global climate change in this area. Chapter 2, the heart of the thesis, delves into the area's late-Wisconsin glacial history. The third chapter addresses the morphology, ages, and elevations of postglacial emerged shorelines around Iliamna and Naknek lakes. Finally, Chapter 4 presents major-element chemistries, correlations, and ages of volcanic ashes in the region. Each of these three chapters includes an abstract, introduction, methods, results and discussion, and summary and conclusion section. References are combined at the close of the thesis, followed by two appendices containing complete data sets used in the study.

CHAPTER 2
LATE WISCONSIN GLACIAL HISTORY OF THE ILIAMNA/NAKNEK/BROOKS LAKE AREA, SOUTHWESTERN ALASKA

ABSTRACT

During the late Wisconsin (~30-10 ka), portions of the Cordilleran Ice Sheet advanced westward from Cook Inlet across a low topographic divide into the Iliamna Lake valley on the northern Alaska Peninsula. Higher mountains at the head of Naknek and Lake Clark valleys diverted the ice sheet, but supported a confluent system of local-mountain glaciers. Muller (1952) originally defined the Brooks Lake glaciation, including the Iliuk (youngest) stade, in the Naknek Lake valley, whereas Detterman and Reed (1973) identified three additional stades of the Brooks Lake glaciation based upon moraines in the Iliamna Lake valley: The Kvichak (oldest) and Iliamna moraines deposited by the Cordilleran Ice Sheet, and the Newhalen moraine (younger, but pre-Iliuk) derived from glaciers in the Lake Clark drainage. Riehle and Detterman (1993) recently correlated moraines in the Iliamna Lake valley with moraines in the Naknek Lake valley, and assigned the type Mak Hill moraine (Muller, 1952) to the Kvichak stade. In this thesis, I present an alternative correlation of glacial deposits that reassigns the type Mak Hill moraine to a pre-late-Wisconsin glaciation based upon: (1) a ^{14}C age of about 39 ka on peat from the Naknek River valley that apparently postdates the Mak Hill moraine (Mann and Peteet, 1994) and (2) the presence of a thick (~2 m) eolian unit, presumably late Wisconsin, atop Mak Hill drift that is absent from younger deposits. The moraine enclosing Naknek Lake is considered an early-late-Wisconsin deposit formed by ice originating in local mountains. The advance is correlative to either the Kvichak stade, Iliamna stade, or both. The lack of a

two-fold earliest-late-Wisconsin Kvichak/Iliamna glacial sequence in the Naknek Lake valley suggests that the glacial systems responded differently to climate change and/or glacier-bed dynamics due to differing ice sources and glacier configurations. Moreover, younger Newhalen and Iliuk moraines are found only in valleys with a local mountain-glacier source.

Plant macrofossils underlying outwash associated with the type Kvichak moraine afford a new maximum-limiting age of 26,155 $\pm$ 285 ^{14}C yr BP on the earliest stade of the Brooks Lake glaciation. This age agrees with a recently reported maximum-limiting age of 26,570 $\pm$ 320 ^{14}C yr BP for peat underlying outwash graded to the Naknek moraine (Mann and Peteet, 1994). Slope angles on the type Kvichak and Iliamna moraines are less steep (~11-15°) than on younger Newhalen and Iliuk moraines (~18-20°), suggesting a considerable length of time separated the Iliamna and Newhalen stades. Moraine-crest widths show a general broadening from younger to older moraines. Surface-clast pitting, which requires tens of thousands of years for pit development, does not distinguish between moraines of different stades. Soil-oxidation thickness also does not differentiate moraines, but appears to be a function of parent material. Radiocarbon ages and the time-stratigraphic marker derived from slope angles provide a basis for correlation with other Alaskan late-Wisconsin glacial sequences and the late-Wisconsin eolian record of the Bristol Bay region. Correlations suggest that the interstadial separating the Iliamna and Kvichak stades occurred at ~22-17 ka, and the interstadial separating the Iliamna and Newhalen stades occurred at ~13-14 ka. Equilibrium-line altitudes in the Naknek Lake valley were lowered between 250-650 m during the Iliuk stade, and approximately 420-820 m during early-late-Wisconsin stades.

INTRODUCTION

Glaciers fluctuate in response to changes in their mass balance. Moraines deposited at stable ice-front positions provide a record of past glacier fluctuations and a proxy for past climate change. Correlating moraines across long distances affords a means for assessing climate change throughout a particular region. This study assesses late-Wisconsin (approximately 25-10 ka, where ka is an abbreviation for thousands of years before present) glacier and climate fluctuations between two valleys located on the upper Alaska Peninsula, southwestern Alaska (Fig. 1).

The upper Alaska Peninsula retains a rich history of late-Wisconsin glacier fluctuations. This glaciation, the Brooks Lake glaciation of Muller (1952), consists of five stades, suggesting that the record of late-Wisconsin glaciation is especially well preserved, perhaps offering more resolution than any other recognized late-Wisconsin glacial sequence in Alaska (see Hamilton, 1994 for a recent review of glaciations in Alaska). Other late-Wisconsin glacial sequences throughout Alaska are either incomplete coastal records where glaciers terminated in the ocean, or inland records consisting of one to two recognized stades.

The primary objective of this study is to use ^{14}C dating, relative-age criteria, field mapping, stratigraphy, equilibrium-line altitudes, and aerial photographs to reconstruct the glacial history of the Iliamna/Naknek/Brooks Lake area (Figs. 2 and 3). This area was selected primarily because of its rich late-Wisconsin glacial history, as well as its relative accessibility.

The Iliamna/Naknek/Brooks Lake study area (Fig. 3) contains the type localities for drift of Wisconsin age mapped along the Alaska Peninsula (Detterman and Reed, 1973; Detterman, 1986; Riehle and Detterman, 1993). A lack of quantified observations has hampered correlations in the study area. River and lake bluffs that expose the underlying

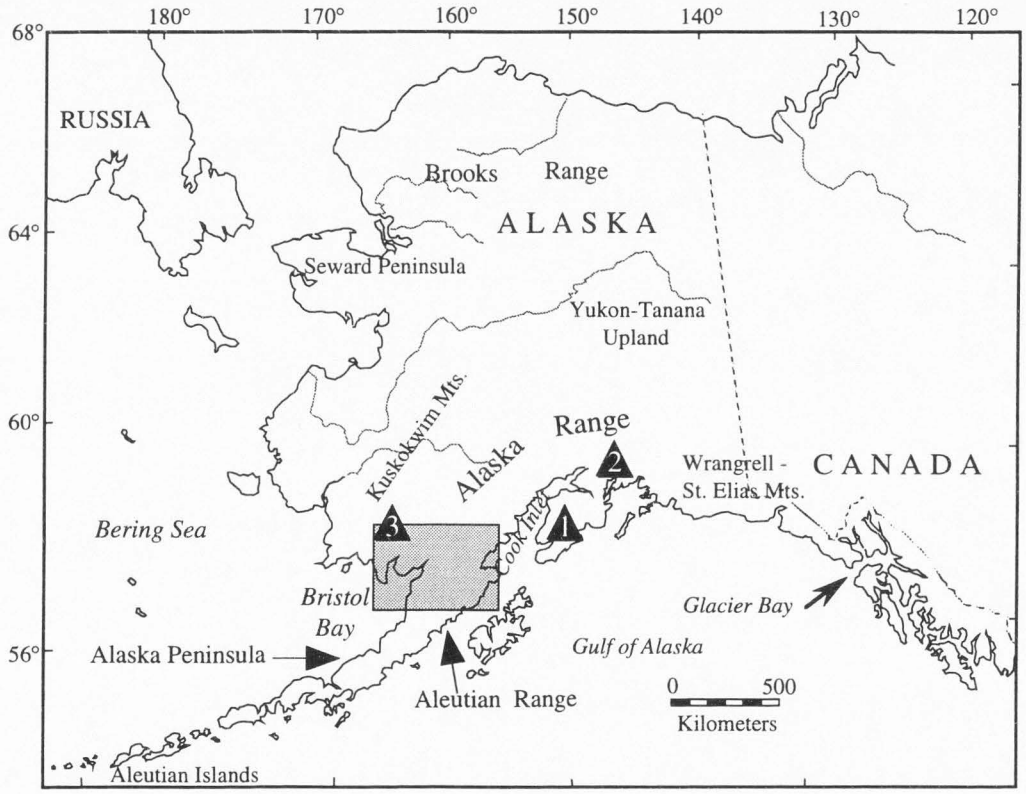

Figure 1. State of Alaska showing location of late-Wisconsin glacial sequences studied throughout Alaska and referred to in text, and location of Bristol Bay area shown in Figure 2. Numbered black triangles refer to smaller mountain ranges referred to in text: (1) Kenai Mountains, (2) Chugach Mountains, and (3) Ahklun Mountains.

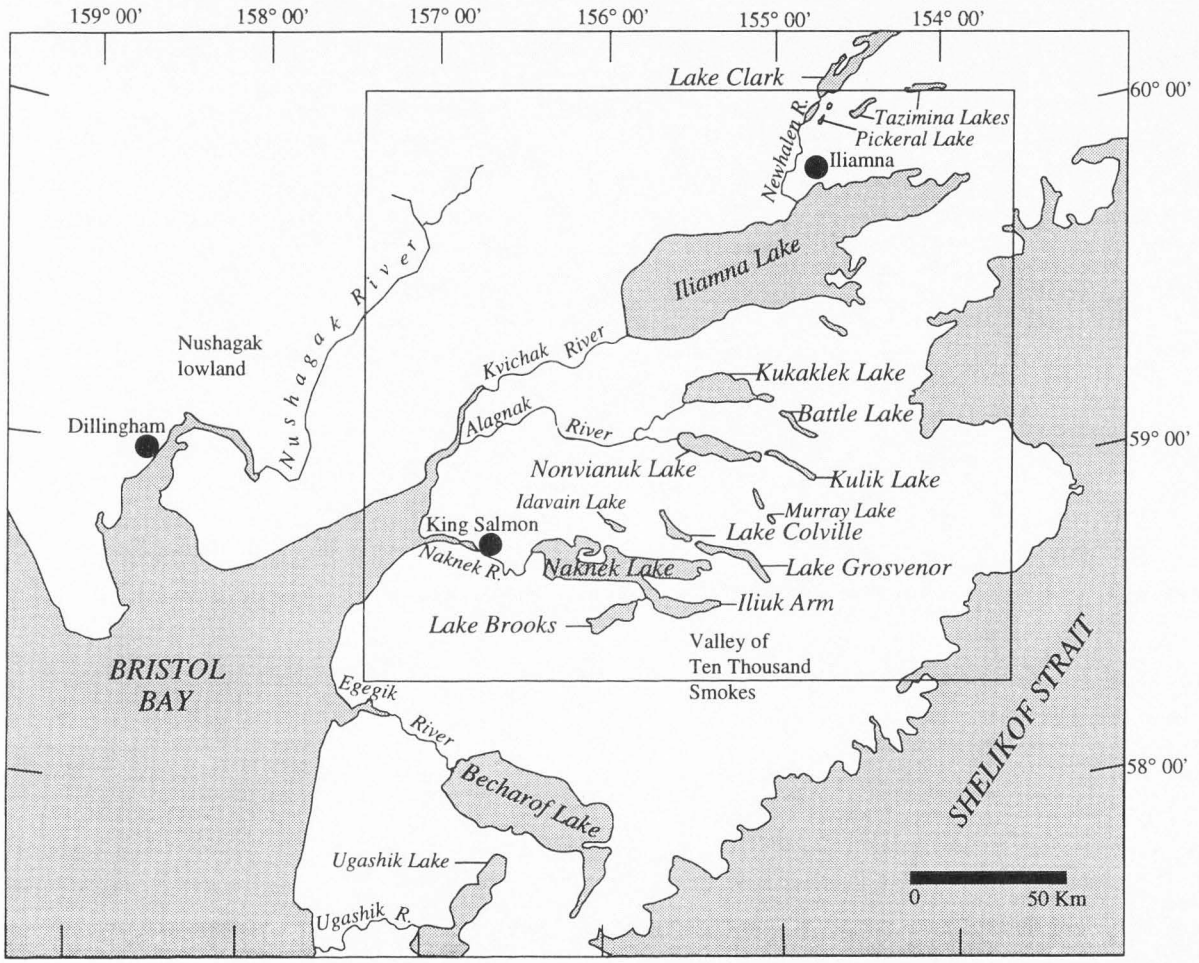

Figure 2. Bristol Bay area, showing location of the Iliamna/Naknek/Brooks Lake study area (Fig. 3), southwestern Alaska, and names of features mentioned in text.

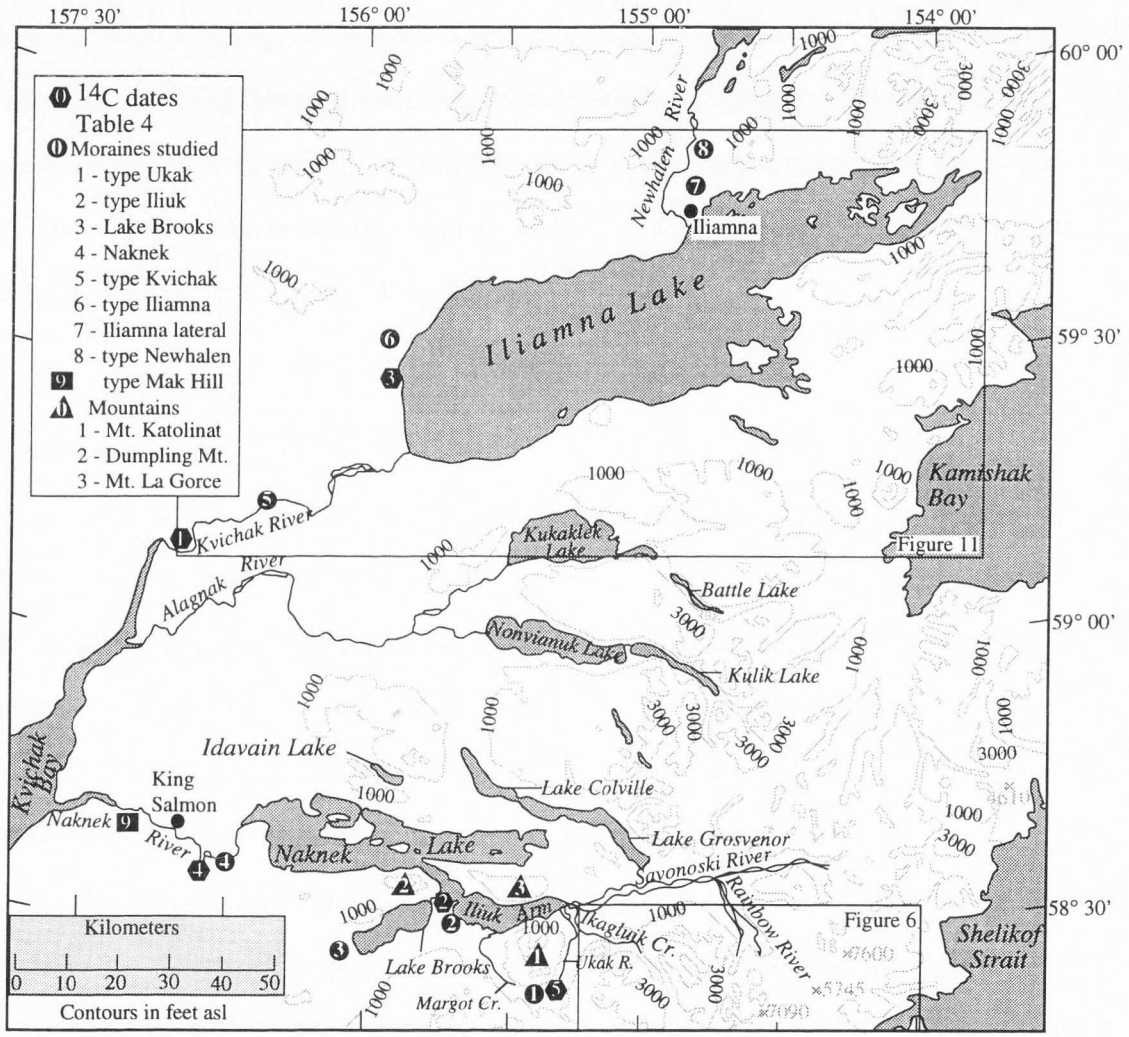

Figure 3. Iliamna/Naknek/Brooks Lake area showing location of the type localities for moraines of Wisconsin age and other moraines studied. Also shown are locations of ^{14}C dates listed in Table 4 and mountains mentioned in text.

sediment offer additional insight into the glacial history of the area. Reconstruction of glacier fluctuations in the study area will facilitate correlations with other late-Wisconsin glacial records throughout Alaska. Correlations, in turn, will enable comparisons of climatic variability that controlled late-Wisconsin glacier fluctuations between moist southwestern Alaska and dry interior Alaska. Likewise, reconstruction of the glacial history will facilitate correlation with the late-Wisconsin eolian record of the Bristol Bay region (for example, Lea and Waythomas, 1990).

BACKGROUND

Modern Geography

The Alaska Peninsula is a 775-km-long projection in southwestern Alaska, between Shelikof Strait to the east and Bristol Bay to the west (Figs. 1 and 2). High volcanic peaks of the Aleutian Range, up to 2300 m above sea level (masl), are the source areas for modern glaciers. Modern lakes, Naknek, Brooks, Iliamna, and Becharof, are remnants of larger glacial lakes dammed by terminal moraines of Wisconsin age, and occupy glacial troughs sculpted by ice flowing from east to west (Detterman, 1986).

Strong winds, frequent cloud cover, high precipitation, and persistent fog typify the climate of the Alaska Peninsula. Intense storms spawned by the Aleutian low pressure zone circulate northeastward along the southeast side of the Peninsula en route to Canada (Detterman, 1986). Mean annual precipitation at King Salmon (Fig. 2) is 48 cm (Detterman, 1986). Modern glaciers along the Alaska Peninsula owe their mass to this high precipitation rate. Interior Alaska, in contrast, is drier and shielded from marine moisture; therefore, local moisture availability is the most critical factor in controlling the mass balance of glaciers in the region.

Glacial Record

About one-half of Alaska was glaciated sometime during the Late Cenozoic, whereas 5% is glaciated presently (Hamilton, 1994). Proximity to moisture of the North Pacific Ocean and the Gulf of Alaska generated extensive glaciers in the southern portion of Alaska, where late-Wisconsin age deposits dominate the glacial-geologic record. Pre-late-Wisconsin glacial records in this region are fragmental due to erosion by subsequent glacier advances, tectonic activity, and dissipation of sediments where glaciers terminated in the ocean (Hamilton, 1994). Portions of the Cordilleran Ice Sheet along with local-mountain ice masses advanced westward across the northern Alaska Peninsula during the late Wisconsin, depositing moraines ascribed to the Brooks Lake glaciation.

Muller (1952) originally defined the Brooks Lake glaciation for the Naknek Lake valley and named the Iliuk (youngest) stade.[1] Detterman and Reed (1973) identified three additional stades of the Brooks Lake glaciation based upon their work in the Iliamna Lake valley: Kvichak (oldest), Iliamna, and Newhalen (youngest). Riehle and Detterman (1993) recently correlated moraines in the Iliamna Lake valley with moraines in the Naknek Lake valley.

The late-Wisconsin glacial history of the Naknek Lake valley is complex, poorly understood, and continually under revision (Table 1). Riehle and Detterman (1993) noted that the number and spacing of moraines do not match those of adjacent valleys. Although Iliamna Lake valley to the north and Becharof Lake valley to the south (Fig. 2) both have a two-fold, earliest-late-Wisconsin Kvichak/Iliamna glacial sequence, the Naknek Lake

---

[1] In an effort to maintain nomenclature consistent with the previous literature addressing the Brooks Lake glaciation, the use of geological climate units (glaciation and stade) are retained throughout this study, even though they have been abandoned by the American Association of Petroleum Geologists (1983).

valley does not. In an attempt to resolve this, Riehle and Detterman (1993) reinterpreted the type Mak Hill moraine, previously ascribed to the early Wisconsin (Muller, 1952), as a Kvichak-age moraine. They defended their interpretation by noting that it allowed the number and spacing of moraines in the Naknek Lake valley to more closely match successions of moraines in adjacent valleys; however, the interpretation violates the principles of stratigraphic nomenclature. According to the American Association of Petroleum Geologists (1983), a type locality cannot be correlated to a deposit of a different age.

The distinction between Newhalen and Iliuk stades is uncertain. For example, Detterman (1986) was unsure whether the Iliuk advance should be classified as part of the Newhalen stade. Similarly, Riehle and Detterman (1993) suggested that the restricted extent of Newhalen drift may represent a minor readvance or stillstand during an overall

TABLE 1. VARIOUS INTERPRETATIONS OF THE GLACIAL HISTORY IN THE NAKNEK LAKE VALLEY, SOUTHWESTERN ALASKA

	Muller (1952)	Detterman (1986)	Pinney and Beget (1991a)	Riehle and Detterman (1993)
			Ukak	
Late Wisconsin	Iliuk	Iliuk	Iliuk	Iliuk
	Undifferentiated	Newhalen		Newhalen
	stades of the	Iliamna		
	Brooks Lake glaciation	Kvichak		Iliamna
pre-late Wisconsin	Mak Hill			Kvichak *

Not addressed

* Riehle and Detterman (1993) mapped the type Mak Hill moraine as Kvichak drift, assigning it to the late Wisconsin

retreat from the preceding Iliamna advance. Finally, Pinney and Begét (1991a) recently discovered a fifth upper-Wisconsin glacial deposit, Ukak drift, which, as of yet, has not been recognized as part of the Brooks Lake glaciation.

This study aims to elucidate some of these uncertainties encompassing glacial mapping of the Brooks Lake glaciation. More specifically, it will: (1) determine the number of earliest-late-Wisconsin glacial advances in the Naknek Lake valley and the position of the maximum late-Wisconsin advance, (2) ascertain whether Newhalen and Iliuk stades are distinguishable, and (3) include the Ukak stade as the latest stade of the Brooks Lake glaciation.

METHODS

Relative-Age Criteria

Relative-age criteria rely on the principle that certain parameters vary with age due to postdepositional modification through time (for a review, see Birkeland and others, 1979). Important assumptions include: (1) variables (slope angles, surface-clast pitting, etc.) depend principally upon the length of postdepositional exposure and (2) the rate of postdepositional modification is comparable at all sampling localities.

The five type localities of the Brooks Lake glaciation were selected for relative-age analysis, providing a basis for correlation with other moraines in the study area (Fig. 3). Relative-age data were collected from three additional moraines: (1) the prominent, complex moraine enclosing Naknek Lake, (2) the single moraine ridge enclosing Lake Brooks, and (3) an Iliamna lateral moraine dissected by the Newhalen River near the village of Iliamna, termed the *Ilimana lateral moraine*. Two to three sites were selected for relative-age study on each of eight moraines: type Kvichak, type Iliamna, type Newhalen, type

Iliuk, type Ukak, the moraine enclosing Naknek Lake, the moraine enclosing Lake Brooks, and the Iliamna lateral moraine (Fig. 3). Sites selected: (1) appeared stable, (2) were relatively accessible, (3) encompassed the highest point on a crest, (4) exhibited the highest primary relief, and (5) had exposed clasts at the surface.

Moraine Morphology. Moraines evolve from an initial sharp form, and become subdued with time. Moraine crest widths and flanking slope angles have been used previously to determine the relative ages of glacial advances in Alaska (for example, Kaufman and Calkin, 1988). Fresh morainal topography and morphologic similarity permit correlation of Salmon Lake drift deposits on the Seward Peninsula with early Wisconsin-age deposits in other parts of Alaska (Kaufman and Hopkins, 1986). Moraine morphology was useful for subdividing the glacial sequence of the Farewell area in the western Alaska Range (Kline and Bundtzen, 1986). TenBrink and Waythomas (1985) used moraine morphology to correlate and map moraines in the Alaska Range. Steeper angles and more irregular topography distinguish deposits of Itkillik II age in the Brooks Range from older deposits of Itkillik I age, which have a smoother topographic expression and broader crests (Hamilton, 1986).

An important assumption underlying morphometric analysis of moraines for relative dating is that their initial form, which is controlled by the mode of deposition, is comparable. Moraines deposited by stagnating ice are irregular and hummocky, whereas moraines deposited at the margin of active ice form single arcuate ridges. Variables controlling the evolution of moraine slope angles and crest widths include the rate at which a moraine is modified, the process of degradation, the orientation, and the regional climate (Kaufman and Calkin, 1988). These factors are assumed constant for all moraines in the study area.

Moraine crest widths were measured by pacing the distance between two points, both one-eye height (150 cm) below the crest of the moraine, along a transect perpendicular to the long axis of the moraine (Fig. 4) (Kaufman and Hopkins, 1986). Three crest widths were measured to characterize the crest width at each site.

Slope angles were measured as the angle of the steepest, straightest segment, between the crest and base of the moraine, which is considered representative of the overall slope of the moraine. Two people stood at opposite ends of the slope segment; one person

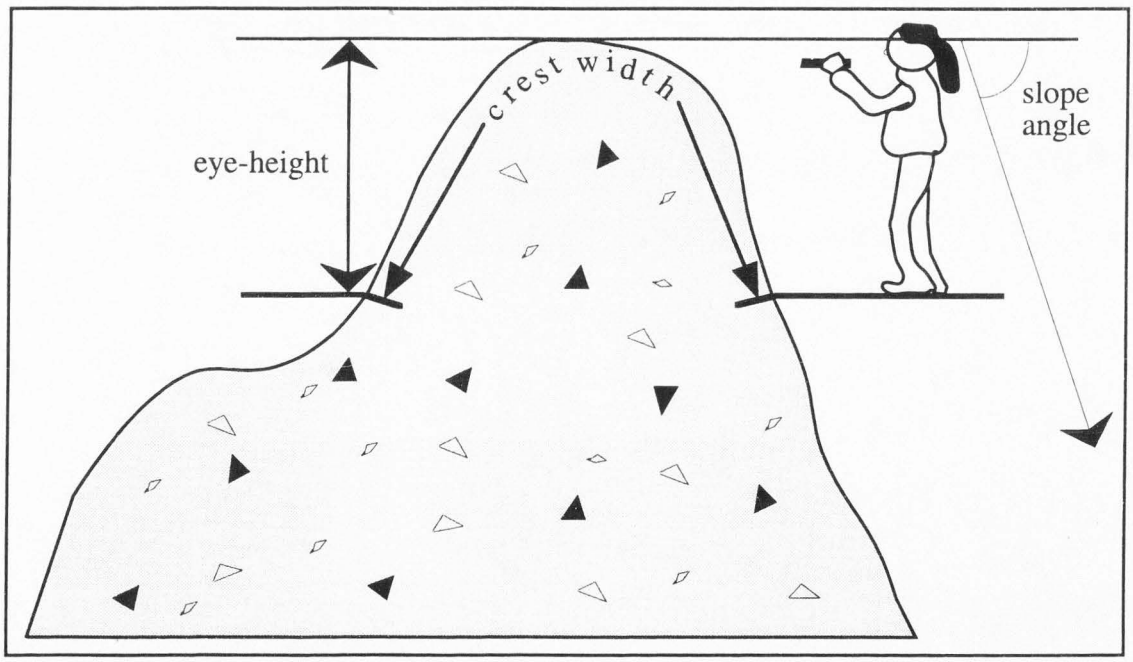

Figure 4. Measurement of crest widths and slope angles for morphometric analysis of moraines.

used a hand-held inclinometer to measure the angle, and the length of the segment was paced (Fig. 4) (Kaufman and Hopkins, 1986; Kaufman and Calkin, 1988). The mean of three distal and three proximal slope angles was used to characterize the distal and proximal slopes of each site.

Surface-Clast Pitting. Clasts on the surface of a moraine develop weathering pits with time (for example, Burke and Birkeland, 1979). Lithology is the most important variable controlling the rate of pit development. Pits form more slowly on basaltic rocks than on granitic rocks (Birkeland and others, 1979). Surface-boulder characteristics distinguish glacial deposits of Pleistocene age on the Seward Peninsula (Kaufman and Hopkins, 1986). Here, criteria such as boulder frequency, tall-boulder frequency, boulder height, and boulder angularity help to differentiate five glacial units (Peck and others, 1990). The availability of surface clasts on most late-Wisconsin moraines in the study area made surface-clast pitting an appropriate relative-age measurement for this study.

Approximately 25 clasts, each with at least 15 cm exposed at the surface, were selected randomly for classification where available. A four-fold pitting classification scheme was devised (Table 2; Fig. 5). In addition to pitting class, clast lithology and largest diameter exposed at the surface were recorded for each clast (Appendix 1). Lithologic categories were then combined into two textural groups: coarse-grained and fine-grained. A parameter, termed the weathering index, was devised and calculated for both textural categories as the mean-weighted pitting class at each site by the equation:

$$\frac{\sum_{p=4}^{p=1} P * N}{\sum N}$$

where **P** = pitting class and **N** = number of clasts in that class.

TABLE 2. SURFACE-CLAST PITTING CLASSIFICATION SCHEME

Figure	Pitting class	Description
5a	1	not pitted, smooth
5b	2	micro-scale pits, grain relief
5c	3	1 or more pits >0.5 cm-deep
5d	4	1 or more pits >1.0 cm-deep

Soil Oxidation Thickness. Soils develop systematically with time, and time-dependant parameters include: oxidation thickness, clay content, reddening, $CaCO_3$ accumulation, morphology, horizon thickness, and clay mineral alteration. Climate, texture, composition of parent material, and loess input affect the rate of soil formation (Birkeland, 1984).

In Alaska, the degree of soil development helps to distinguish Stewart River drift deposits in the Kigluaik Mountains (Kaufman and Hopkins, 1986). Soil oxidation depth varies significantly between Healy, Lignite Creek, and Teklanika River glacial drifts in the northern Nenana Valley (Thorson, 1986). A lack of consistent parent material in the Iliamna/Naknek/Brooks Lake study area, however, precluded the use of most soil parameters for relative dating.

A test pit was dug along crests at each site to unweathered parent material. The soil profile was described, including oxidation thickness and the Muncell color of the B horizon.

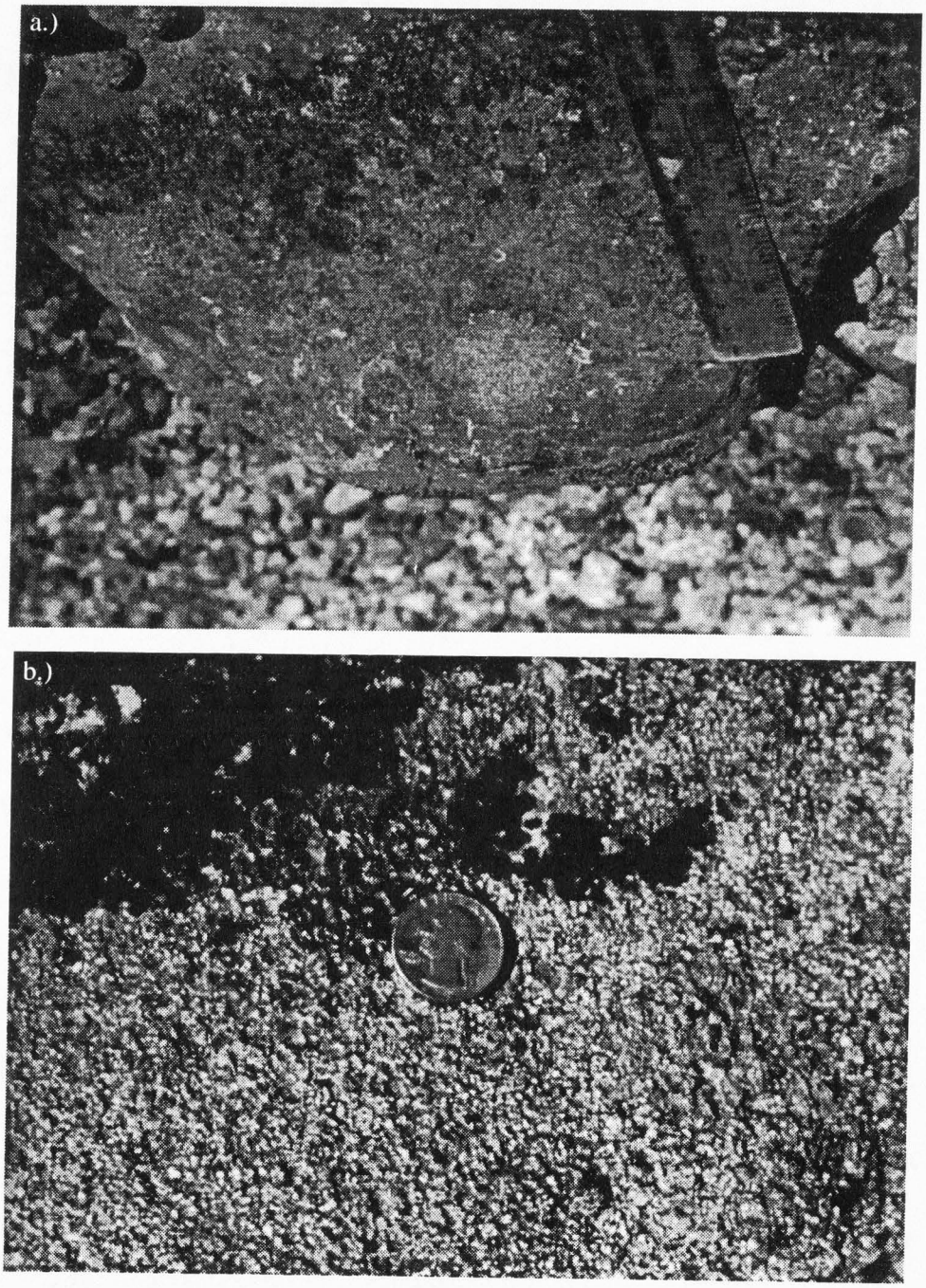

Figure 5. Pitting classification scheme for surface clasts: (a) pitting class 1 (fine-grained), (b) pitting class 2 (coarse-grained), (c) pitting class 3 (coarse-grained), and (d) pitting class 4 (coarse-grained).

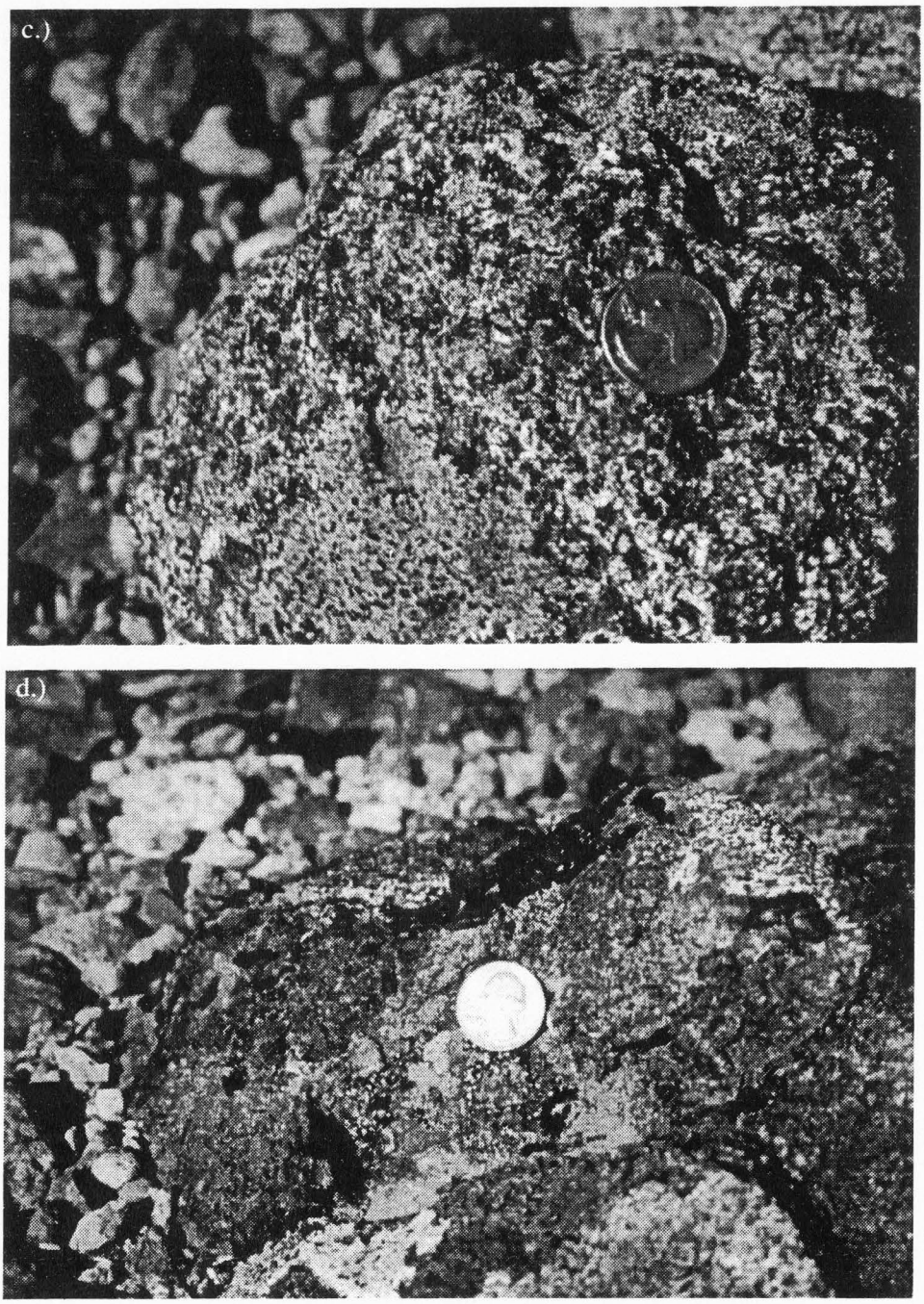

Figure 5 (continued)

^{14}C Dating

Peat and organic-rich silt used for ^{14}C dating were wet sieved at 0.246 mm with purified water and dried at 60° C. Plant macrofossils were hand-picked under a laminar-flow hood. Charcoal found at one site did not require any sample preparation. Samples were dated at the University of Arizona's accelerator mass spectrometry facility.

Equilibrium-Line Altitudes

Comparison of paleo-equilibrium-line altitudes to modern equilibrium-line altitudes has added important information about the magnitude of climate change in many areas (Meierding, 1982; Porter and others, 1983; Lea, 1984; Kaufman and Hopkins, 1986; Leonard, 1989; Rodbell, 1992; Torsnes and others, 1993). Several approaches have been used to estimate equilibrium-line altitudes (ELA) based on reconstructed glaciers. These include: (1) cirque-floor altitudes (which generally overestimate ELA of valley glaciers), (2) maximum altitude of lateral moraines (a minimum estimate of ELA), (3) accumulation area ratios (AAR), (4) toe-to-headwall ratios (THAR), and (5) glaciation thresholds (Andrews, 1975; Meierding, 1982; Porter and others, 1983; Torsnes and others, 1993). The AAR method estimates ELA by assuming that the accumulation area of a glacier is typically 66%, whereas the THAR approach assumes that the ELA is located some fraction of the total vertical distance between the toe and the headwall of the reconstructed glacier.

For this study, the THAR method was used to estimate paleo-ELA for the Iliuk-stade glacier and the Lake Brooks glacier in the Naknek Lake valley. Meierding (1982) found that a THAR of 0.40 was best for late-Pleistocene ELA estimates in the Colorado Front Range. THAR values yielded the smallest standard error in comparison to the AAR approach, which is considered the most accurate technique (Meierding, 1982). The lowest

elevations along the type Iliuk terminal moraine at the head of Iliuk Arm, an Iliuk terminal moraine at Lake Grosvenor, the moraine enclosing Lake Brooks, and the moraine enclosing Lake Colville were obtained from 1:63,360-scale contour maps. The summit altitude of the present-day ice cap to the southeast of Naknek Lake provided a minimum estimate of the paleo-headwall altitude. Present-day ELA was calculated for both the ice cap and for smaller cirque glaciers occupying Mt. Griggs to the west of the ice cap (Fig. 6).

Glacial Mapping

Eight moraines ascribed to the Brooks Lake glaciation were studied in the field. Aerial photographs (1:63,360-scale) were used to map late-Wisconsin glacial deposits from 58° 15' to 60° 00' latitude and 156° 30' to 154° 30' longitude. Moraines were correlated based upon morpho-stratigraphic position, ice source, and morphologic character, supplemented by relative-age data collected in the field. Ice limits were drawn by extrapolating between well-defined moraines.

RESULTS AND DISCUSSION

The glacial reconstruction of this study presents an alternative correlation between glacial deposits from Iliamna Lake valley to Naknek Lake valley, including intervening valleys, which differs somewhat from that of both Detterman and Reed (1973) and Riehle and Detterman (1993) (Fig. 7). Differences from previous interpretations of the Brooks Lake glaciation are presented here by highlighting the most significant map features and conclusions drawn from them. Data that support these correlations are discussed in the following sections of this chapter.

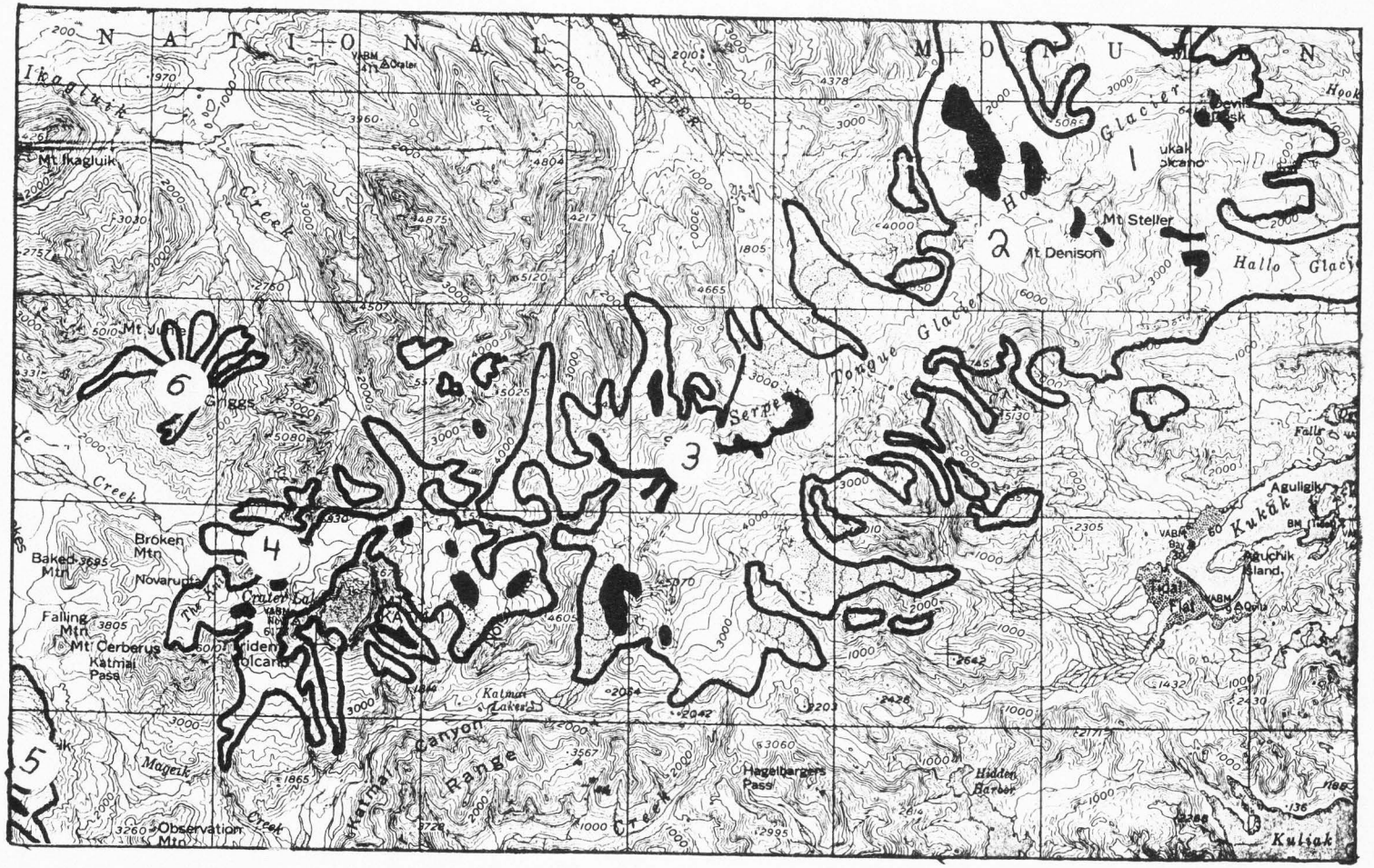

Figure 6. Headwall locations used for equilibrium-line-altitude calculations (Table 6). Modern glaciers are outlined in bold line. Map location shown on Figure 3.

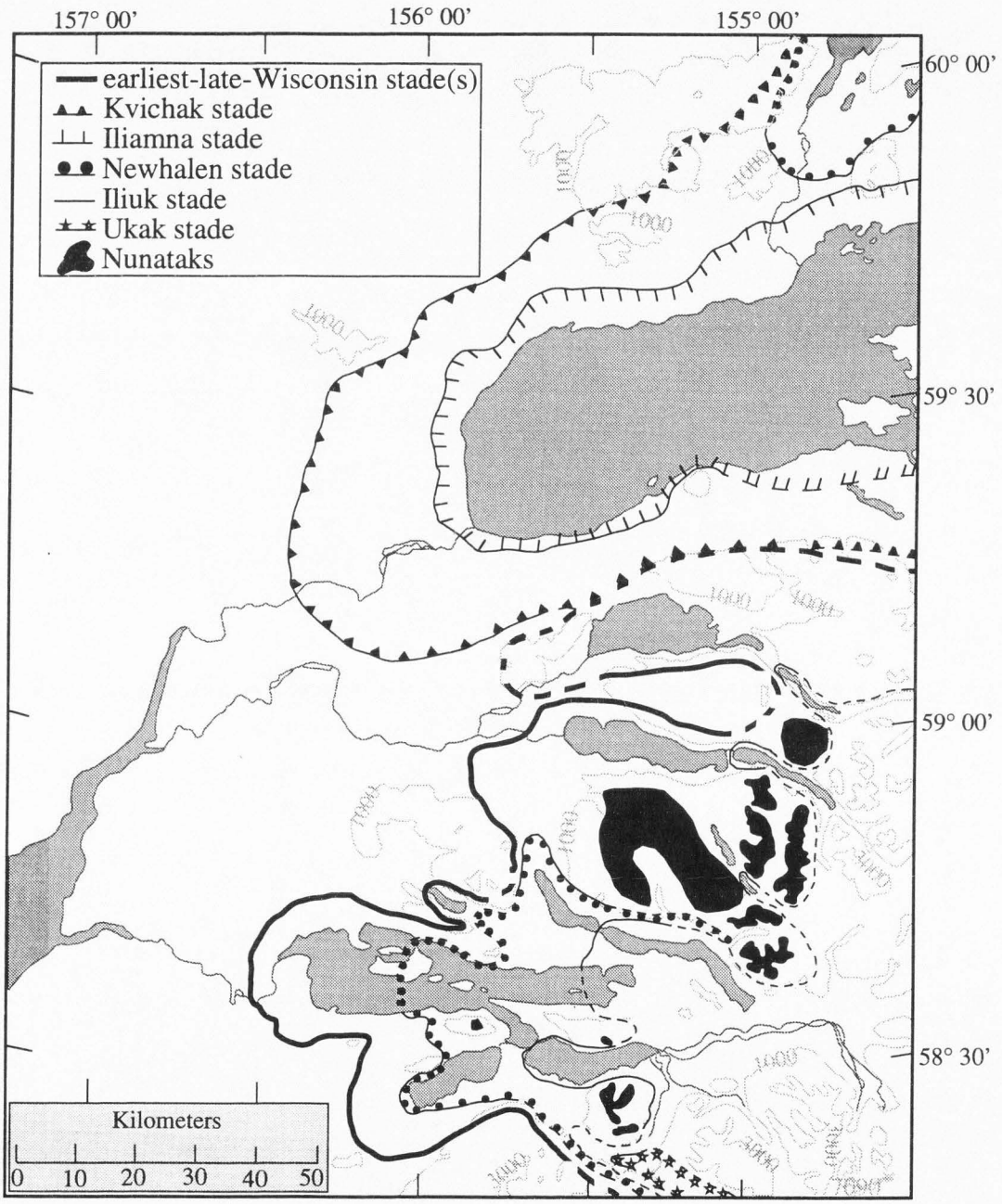

Figure 7. Late-Wisconsin ice limits for each stade of the Brooks Lake glaciation in the Iliamna/Naknek/Brooks Lake study area, including correlations with type localities.

1. The type Mak Hill moraine is reassigned to a pre-late-Wisconsin deposit.

2. The moraine damming Naknek Lake, termed the *Naknek moraine* (Mann and Peteet, 1994), may represent a single early-late-Wisconsin advance corresponding to either the Kvichak or Iliamna stade. Alternatively, the Naknek moraine may be a composite feature formed during both the Kvichak and Iliamna stades. Regardless, this moraine is broadly interpreted to be an early-late-Wisconsin deposit and it clearly records the position of the maximum late-Wisconsin advance.

3. Early-late-Wisconsin moraines correlative with the Naknek moraine enclose Idavain, Kukaklek, and Nonvianuk lakes to the north of the Naknek Lake valley.

4. Two moraines in the study area correlate with the Newhalen stade, the moraine enclosing Lake Brooks, termed the *Lake Brooks moraine*, and the moraine enclosing Lake Colville, termed the *Lake Colville moraine*.

5. Moraines that separate subbasins of lakes from the main lake basin are generally correlative with the Iliuk stade, as originally suggested by Muller (1952).

6. A lack of stratigraphic and chronologic evidence fails to distinguish the Iliuk and Newhalen stades, but Iliuk moraines are retained as morpho-stratigraphic features that separate subbasins of lakes from main-lake basins.

7. No moraines correlative with the Ukak stade were identified in the study area.

Early-Late-Wisconsin Type Localities and Advances

Kvichak Stade. The westernmost extension of the Cordilleran Ice Sheet, including ice streams that flowed westward from the Kenai and Chugach mountains, occupied Cook Inlet during the late Wisconsin (Fig. 1) (Mann and Peteet, 1994). Early during the Brooks Lake glaciation, an outlet lobe draining the Cordilleran Ice Sheet

advanced westward from Cook Inlet across a low topographic divide into the Iliamna Lake valley depositing the type Kvichak moraine (Fig. 3). The Kvichak-stade glacier is estimated to have been between 210 and 230 km long (Detterman and Reed, 1973). Trunk glaciers descending from the north and the south into the Iliamna Lake valley added a small amount of mass to the outlet lobe that entirely filled the valley. This reconstruction differs from Mann and Peteet (1994), who suggested that the late-Wisconsin ice divide coincided with the present-day topographic divide, and did not allow sufficient source area to feed the massive ice lobe that occupied the Iliamna Lake valley.

The Kvichak stade, the oldest of the Brooks Lake glaciation, is named for an approximately 30-km-broad prominent end moraine dissected by the Kvichak River 37 km downstream of Iliamna Lake (Fig. 3, site 5; Fig. 8) (Detterman and Reed, 1973). At the type locality, the moraine's morphology is extremely complex and hummocky, suggesting that the moraine was ice-cored at the time of deposition. Abundant subround kettle lakes, having moderately smooth margins, occupy depressions, and discontinuous ridges can be traced for short distances (Fig. 9). Parent material in soil pits on the type Kvichak moraine is typical of ice-contact stratified drift: well-sorted and lacking fines. Surface boulders display a patchy distribution about the moraine surface, indicating that drift was reworked and dumped by stagnating ice. Topography of the type Kvichak moraine suggests that the termination of the Kvichak stade was abrupt. The climate warmed quickly and ice was left to waste away on the landscape, rather than pulling back steadily.

Slopes on the type Kvichak moraine are relatively gentle and crest widths are relatively broad (Table 3; Appendix 1). Proximal and distal flanking slope angles range from 14-16° and 11-15°, and average 15° and 12°, respectively. The average crest width for the type Kvichak moraine is 31 m. Oxidation thicknesses are highly variable ranging from

16-39 cm and averaging 30 cm (Table 3; Appendix 1). Surface clasts dominantly display grain-size relief with coarse-grained and fine-grained weathering indices averaging 2.21 and 2.05, respectively (Table 3; Appendix 1).

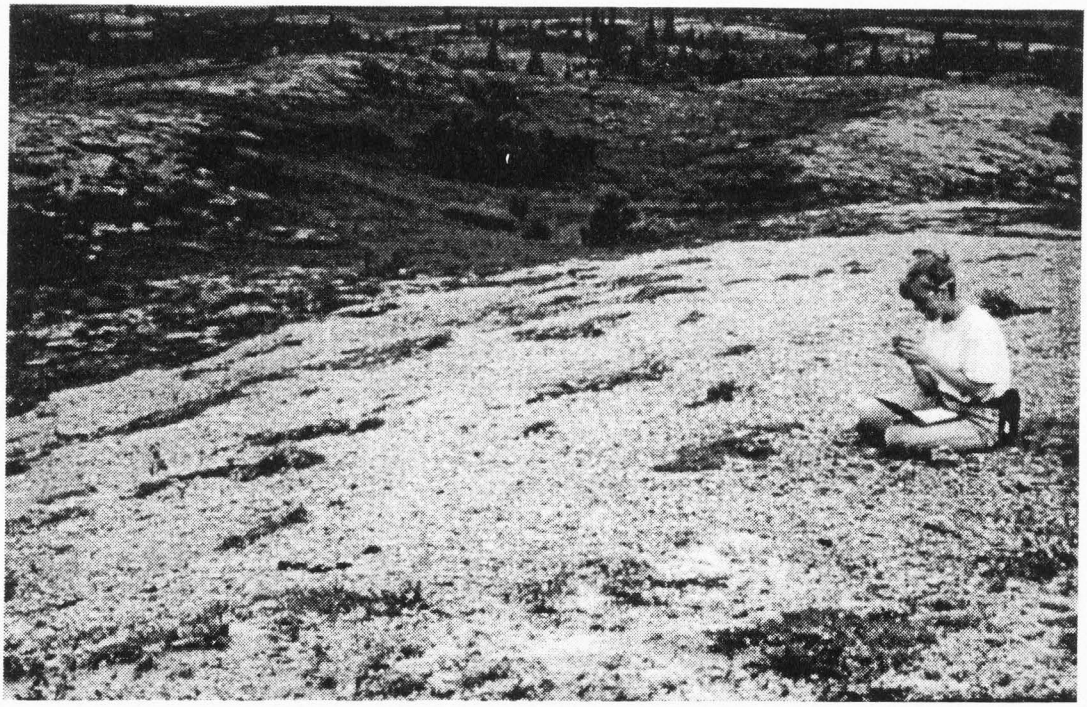

Figure 8. Type Kvichak moraine. Photograph taken approximately 5 km south of the Kvichak River. Note closed depressions and patchy distribution of surface clasts on unvegetated knolls.

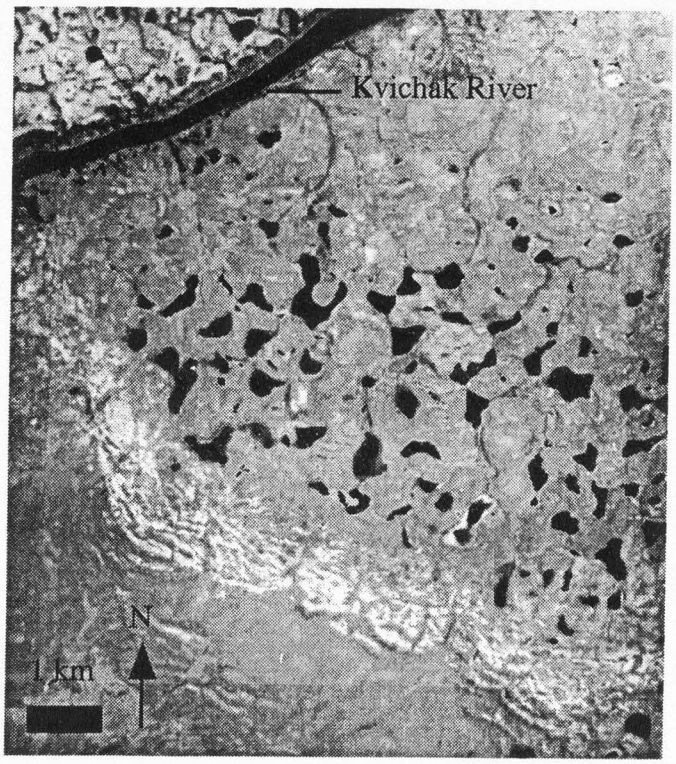

Figure 9. Aerial photograph of the type Kvichak moraine. Note the size and shape of kettle ponds on up-glacier side of the moraine, and discontinuous ridges mentioned in text.

Iliamna Stade. The same outlet lobe of the Cordilleran Ice Sheet that deposited the type Kvichak moraine occupied the Iliamna Lake valley during the Iliamna stade. The Iliamna-stade glacier was approximately 200 km long (Detterman and Reed, 1973). Nunataks, absent during the earlier Kvichak stade, existed above approximately 300 masl during the Iliamna stade.

Morainal hills near the northwest corner of Iliamna Lake, about 24 km north of the head of Kvichak River are the type locality for drift of the Iliamna stade (Fig. 3, site 6) (Detterman and Reed, 1973). Iliamna drift encircles Iliamna Lake and covers more of the region surrounding Iliamna Lake than drift of any other stade of the Brooks Lake glaciation. Despite its younger age, the type Iliamna moraine is less complex, less

TABLE 3. RELATIVE-AGE DATA SUMMARY

Site (Fig. 3)	Stade	Proximal slope Length (m)	Proximal slope Angle (°)	Distal slope Length (m)	Distal slope Angle (°)	Crest width (m)
1	Ukak	17 ± 5 (2)	20 ± 0 (2)	12 ± 1 (2)	19 ± 2 (2)	18 ± 1 (2)
2	Iliuk	36 ± 13 (3)	19 ± 1 (3)	28 ± 12 (3)	18 ± 3 (3)	25 ± 1 (2)
3	Newhalen	24 ± 1 (2)	22 ± 8 (2)	23 ± 4 (2)	17 ± 3 (2)	25 ± 4 (2)
4	Kvichak/Iliamna	17 ± 4 (4)	13 ± 3 (4)	28 ± 15 (4)	13 ± 1 (4)	25 ± 3 (4)
5	Kvichak	17 ± 6 (3)	15 ± 1 (3)	26 ± 2 (3)	12 ± 2 (3)	31 ± 6 (3)
6	Iliamna	34 ± 22 (2)	11 ± 7 (2)	17 ± 0 (2)	11 ± 1 (2)	24 ± 0 (2)
7	Iliamna	17 ± 11 (3)	11 ± 2 (3)	16 ± 11 (3)	11 ± 1 (3)	25 ± 3 (3)
8	Newhalen	20 ± 3 (3)	19 ± 2 (3)	26 ± 4 (3)	18 ± 4 (3)	19 ± 2 (3)

Site (Fig. 3)	Stade	Oxidation thickness (cm)	Weathering indices Coarse-grained	Weathering indices Fine-grained
1	Ukak	11 ± 4 (2)		
2	Iliuk	55 ± 17 (3)		
3	Newhalen	25 ± 12 (2)		
4	Kvichak/Iliamna	12 ± 5 (4)	2.50 ± 0.18 (4)	2.57 ± 0.84 (3)
5	Kvichak	30 ± 12 (3)	2.21 ± 0.22 (3)	2.05 ± 0.1. (3)
6	Iliamna	26 ± 3 (2)	1.67 ± 0.00 (1)	1.64 ± 0.00 (1)
7	Iliamna	13 ± 8 (3)	2.14 ± 0.10 (2)	1.89 ± 0.41 (2)
8	Newhalen	25 ± 10 (3)	1.95 ± 0.44 (3)	1.58 ± 0.52 (3)

Means and standard deviations of all criteria measured.
Number in parentheses is the number of stations used for mean values. See Figure 3 for locations of moraines.

hummocky, and 60 to 120 m lower than the type Kvichak moraine (Fig. 10). Parent material in soil pits on the type Iliamna moraine is matrix supported, poorly sorted, and contains abundant silt and fine sand, indicating that the drift was not water-worked. Slumped channels, a lack of continuous crests, and infilled depressions characterize the topography of the moraine.

Flanking slope angles on the type Iliamna moraine and the Iliamna lateral moraine (Fig. 3, site 7) are somewhat less steep than flanking slope angles on the type Kvichak moraine (average proximal and distal slope angles for Iliamna moraines = 11°; Table 3; Appendix 1). Average crest width varies from 23-28 m, averaging 24 m for the type Iliamna moraine, and 25 m for the correlative Iliamna lateral moraine. Oxidation thicknesses, which range from 24-28 cm, are not as variable on the type Iliamna

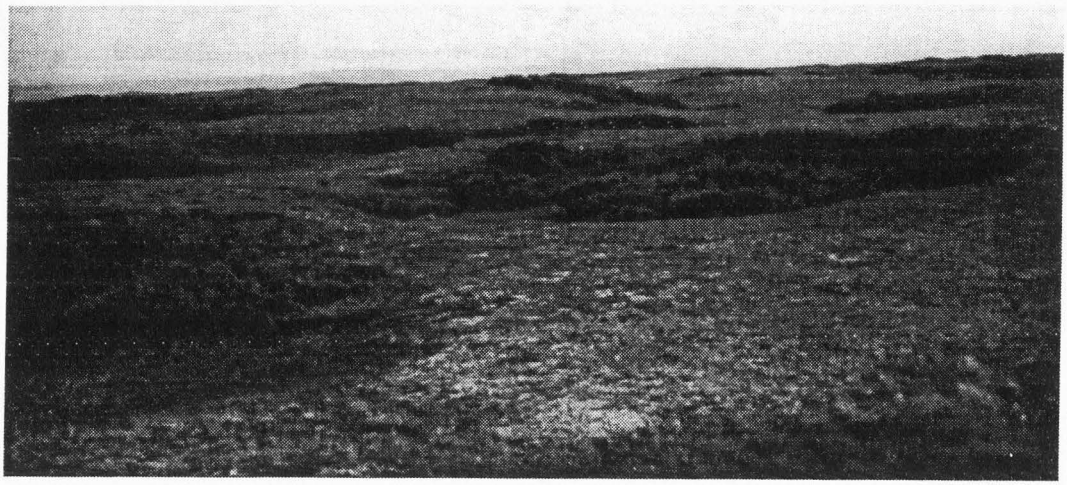

Figure 10. Type Iliamna moraine approximately 1.5 km inland of the northwestern corner of Iliamna Lake, above 40 m (above lake level) stand of the lake (Chapter 2). Note the subdued morphology of the moraine.

moraine as on the type Kvichak moraine (Table 3; Appendix 1). However, oxidation thicknesses on the Iliamna lateral moraine range from 7-22 cm. Surface clasts on both Iliamna moraines have grain-size relief (Table 3; Appendix 1). Average coarse-grained and fine-grained weathering indices on the type Iliamna moraine are 2.14 and 1.89, respectively, and 1.89 and 1.64 on the Iliamna lateral moraine.

Stratigraphic Record. Iliamna Lake, presently dammed by the type Iliamna moraine, is a remnant of a former proglacial lake previously dammed by the type Kvichak moraine. Detterman and Reed (1973) suggested that the lake attained a maximum height of 45 m above modern lake level based upon strandlines with a light vegetation, which are distinguishable on aerial photographs (Chapter 3). The landscape, once inundated by this proglacial lake between the two moraines, is relatively flat with numerous small kettle ponds. Two sites in the study area expose glacial-lacustrine sediments deposited in this lake.

At the west end of Iliamna Lake (Fig. 11, site 1; Fig. 12), well-exposed glacial-lacustrine sediments suggest two ice advances occurred during early-late-Wisconsin time, the Kvichak and Iliamna stades. The stratigraphic section rises from beach level up to the surface of an ancient lake terrace (about 30 m above lake level), and records a succession of glacial and postglacial environments following retreat of the Kvichak-stade glacier. The section can be subdivided into five main units (Figs. 12 and 13): (unit 1) 9 m of bedded and deformed sand and silt, (unit 2) 5 m of gravel, (unit 3) 8.5 m of bedded and deformed sand and silt, (unit 4) 2 m of compact diamicton, capped by (unit 5) 7 m of sand with organic-rich silt and peat at its base.

Unit 1 (0-9.0 m) shows large- and small-scale deformation, and is traceable for several kilometers along the northwestern shore of Iliamna Lake. Broad-scale warping is apparent over tens of meters, whereas individual beds are convoluted, and the entire unit appears to dip westward into the bluff. The unit is composed of well-sorted silt forming thin layers (usually 2-15 cm) interbedded with thicker fine to very-fine sand layers (usually 50-150 cm). Contacts are sharp and beds are laterally continuous. Sand layers, which are extremely well sorted, are either massive (S_m) or exhibit trough-cross bedding (S_t), and silt layers are either massive (F_m), deformed (F_d), or laminated (F_l). This alternating succession of sand and silt is cautiously interpreted as broad-scale rhythmic deposition in a proglacial lake. Intense pulses of glacial meltwater into ancestral glacial Iliamna Lake generated thicker sand layers, whereas weakened meltwater input enabled fine silt to settle out, which occurred in some sort of a cyclic manner. The cyclicity may be annual, whereby active summer meltwater inflow spawned underflows that deposited the thick sand beds and quieter weakened winter currents enabled settling of suspended silt to form the thinner silt beds.

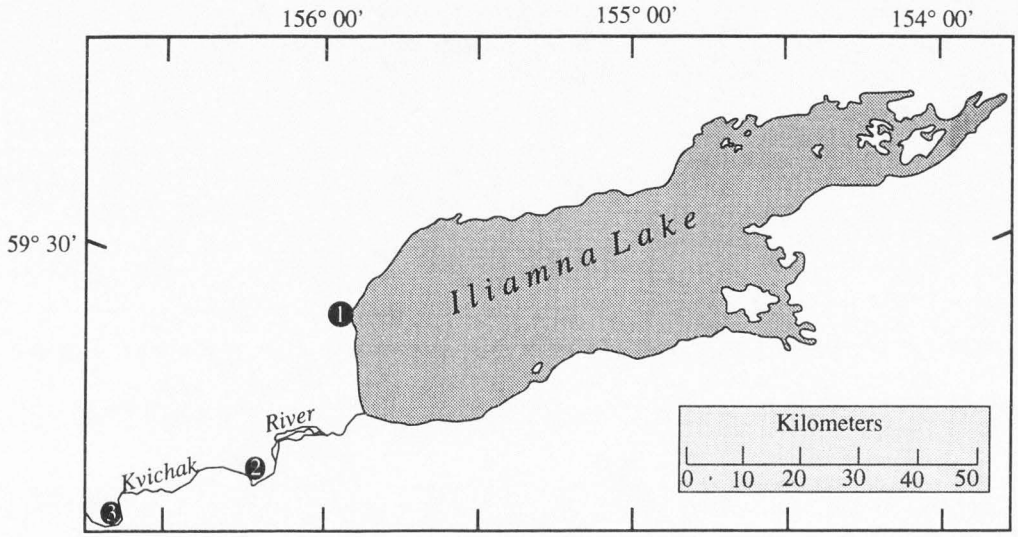

Figure 11. Iliamna Lake region showing location of: (1) deformed strata (Fig. 12), (2) laminated clay (Fig. 14), and (3) dated organic matter underlying outwash associated with the type Kvichak moraine (Figs. 24 and 25). Map location shown on Figure 3.

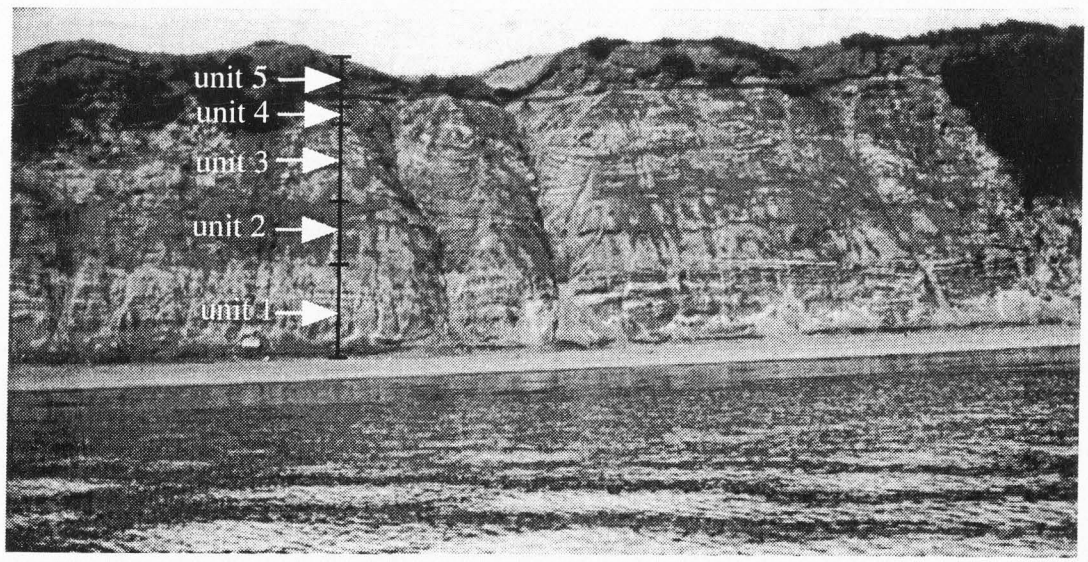

Figure 12. Deformed strata exposed at west end of Iliamna Lake showing five-fold division of units (see Figure 11 for location).

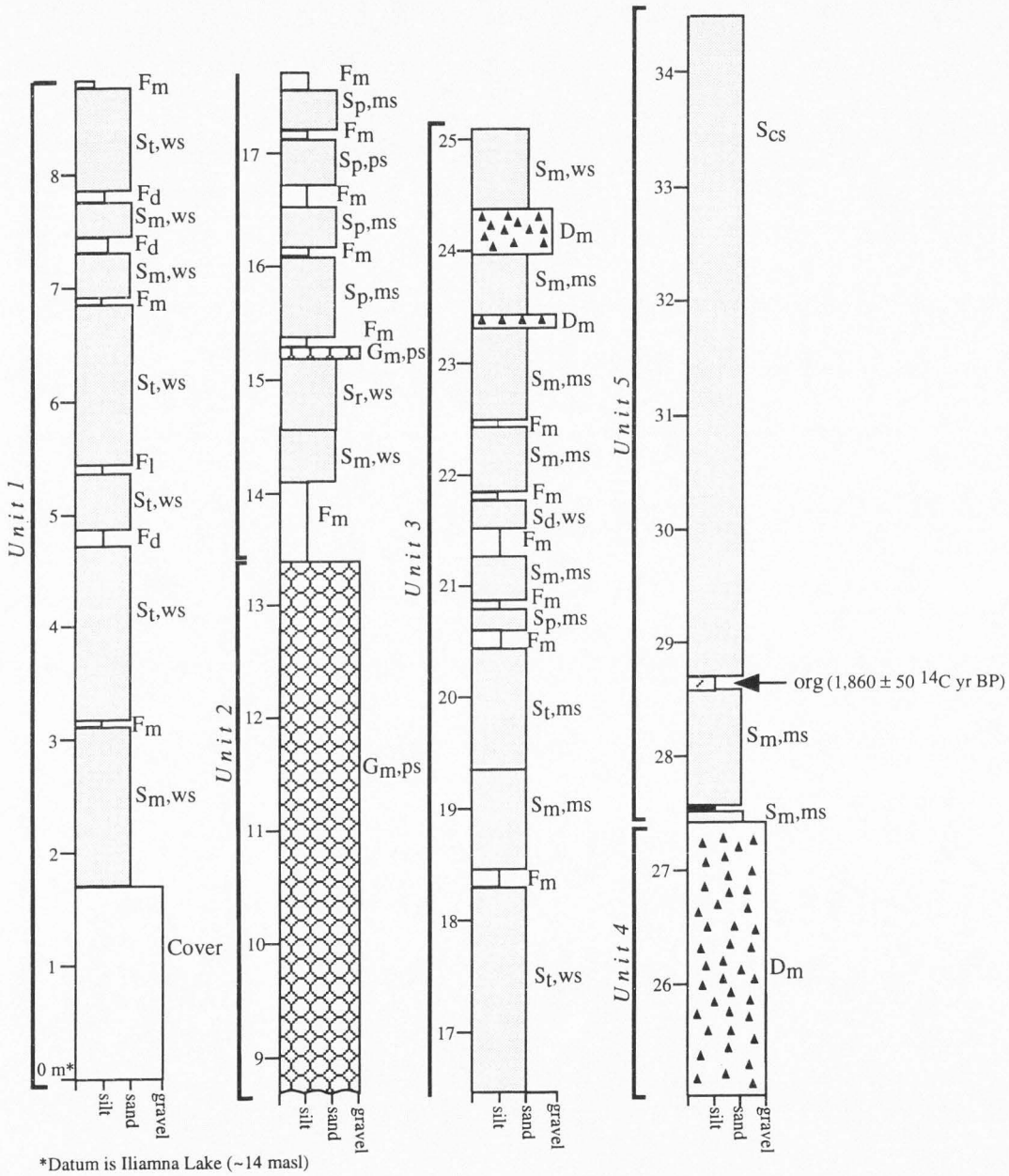

Figure 13. Stratigraphy of deformed strata at west end of Iliamna Lake (see Figure 11 for location). Explanation on p. 32.

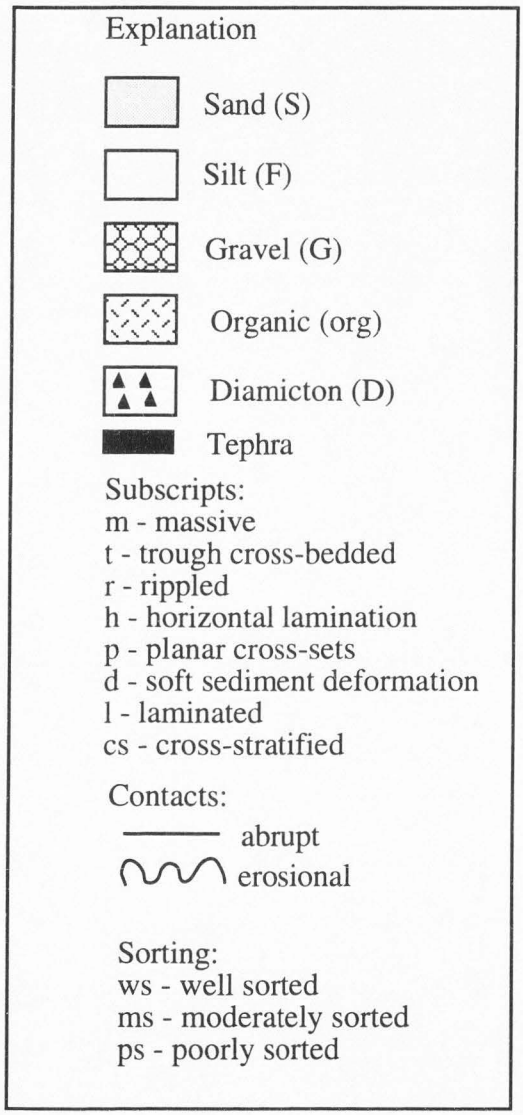

Figure 13 (continued)

Because deposition at this site probably took place in relatively shallow, nearshore water (tens of meters deep), the cyclicity of alternating sand and silt layers may represent storm surges at the down-wind end of glacial Iliamna Lake. Trough-cross bedded sand is associated with current reworking in a high energy nearshore environment of a lake where deposits are scoured into trough-like structures and subsequently filled (Ashley and others, 1985).

Regardless of the mechanism that generated rhythmic deposition, the presence of well-sorted, very-fine to fine sand reflects lacustrine processes. Bottom or littoral currents sorted the sand layers. The lateral continuity of beds and their sharp contacts are also consistent with lacustrine deposition. Overall, the stratigraphy, lateral continuity of beds, abrupt nature of contacts, and sedimentary structures suggest deposition within glacial Iliamna Lake. The deformation records overriding by the Iliamna-stade glacier (see below).

Unit 2 (9.0-13.5 m) is composed of massive gravel (G_m) that is structureless and too massive to record deformation. Cobble-sized clasts are subround and poorly sorted, and the unit has an erosional base. The gravel unit is traceable over several kilometers in bluffs exposed along the northwest portion of Iliamna Lake.

A high-energy environment is necessary to transport large cobbles. This unit may represent a beach environment as lake level fluctuated, or it may represent coarse outwash deposited by meltwater streams of the advancing Iliamna-stade glacier. If the gravel represents a beach, then it may record a shoreline regression, followed by an ice advance supplying gravel that infilled the distal portion of the lake basin. If the gravel is a glacial-fluvial deposit, then a more complex story unfolds. An advance, corresponding to ice-proximal conditions, would have occurred to deposit the gravel, followed by a retreat to

deposit the overlying sand and silt unit (unit 3), representing the distal portion of a sandur, followed by another readvance to deposit the diamicton (unit 4). The lateral continuity of the gravel and a lack of cut-and-fill beds support a beach interpretation.

Unit 3 (13.5-25.0 m) is dominated by alternating sand with subordinate silt layers. Sedimentary structures found in sand layers include: ripple laminations (S_r), planar cross-sets (S_p), and trough-cross beds (S_t), whereas silt layers are structureless (F_m). Sand units are dominantly moderately well-sorted and comprised of fine to medium sand. Beds appear to be discontinuous, but this may be due to the deformation, and contacts are dominantly gradational. Thin (typically 10-40 cm) discontinuous layers of diamicton at approximately 23.5 m and 24 .0 m are matrix supported and contain angular clasts up to roughly 10-15 cm in diameter.

The discontinuous beds, gradational contacts, coarser sand grains, and moderate sorting of unit 3 point to a glacial-fluvial origin as opposed to a lacustrine origin, such as that represented by unit 1. Glacial-fluvial deposits typically encompass a wide range of variation (Ashley and others, 1985). In this environment, ripple laminations are thought to record multidirectional paleocurrents, whereas planar cross-sets may represent channel-bar deposition. Trough-cross beds indicate abandonment and subsequent filling of channels due to rapid shifting. Sand layers probably represent the distal portion of the sandur prior to the advance of the Iliamna-stade glacier. Braided streams are not as effective at sorting as a lake, thus explaining the moderate sorting of this unit. Silt layers are thought to represent abandoned-channel fills on the sandur. Diamicton layers may represent debris flows off the front of the advancing Iliamna-stade glacier, as supported by the overlying diamicton interpreted as till (see below), or dumps from icebergs laden with debris that

were carried by streams onto the sandur, as supported by the discontinuous nature of the layers.

Unit 4 (25.0-27.5 m) is massive diamicton with a sandy matrix; angular, poorly sorted clasts (2-15 cm in diameter); and a sharp basal contact. The unit is laterally traceable for several kilometers. This diamicton is interpreted as till on the basis of its compactness, angularity of clasts, and stratigraphic position (that is, overlying braided stream deposits supplied by an advancing glacier, and its proximity to the surface of the Iliamna moraine).

Unit 5 (27.5-34.5 m) includes massive sand, pink-orange tephra that is 1-3 cm thick (Chapter 4), a buried Holocene soil (approximately 10 cm thick) containing plant macrofossils dated at 1860 ± 50 ^{14}C yr BP (Table 4), and about 6 m of cross-stratified sand forming a bluff-head dune, fed by sand of the exposed face (see Chapter 3 for a further discussion of unit 5). The thin (10 cm), lowermost sand, atop the diamicton, is thought to represent either lacustrine deposition, glacial-fluvial deposition as the Iliamna-stade glacier retreated, or eolian deposition fed by the outwash plain in front of the retreating Iliamna-stade glacier. The components of unit 5, with the exception of the lowermost sand layer, represent a postglacial environment.

To summarize, early during the Brooks Lake glaciation, the Kvichak-stade glacier advanced to deposit the type Kvichak moraine, the original moraine dam that held in ancestral glacial Iliamna Lake. Silt and sand comprising unit 1 were deposited following the retreat of the Kvichak-stade glacier from the bluff site; it was deposited in a proglacial lake dammed by the type Kvichak moraine following the Kvichak stade. A shoreline regression probably allowed gravel (unit 2) to infill the distal portion of the lake basin. Meltwater originating from advancing ice of the Iliamna-stade glacier formed an outwash plain, and deposited the overlying complex sand and silt unit (unit 3). These three units

TABLE 4. RADIOCARBON AGES REFERRED TO IN TEXT

Radiocarbon date (yr BP)	Lab ID	Material dated	Stratigraphic position	Location (Fig. 3)	Reference
26,155 ± 285	AA-15092	Plant macrofossils	Underlies outwash associated with the type Kvichak moraine	1	This paper
>41,650	AA-15095	Charcoal	Incorporated within outwash of the type Iliuk moraine	2	This paper
1860 ± 50	AA-15096	Plant macrofossils	Overlies till deposited by the Iliamna-stade glacier	3	This paper
26,570 ± 320	Beta-39578	Peat	Underlies outwash graded to the Naknek moraine	4	Mann and Peteet, 1994
39,400 ± 1000	Beta-40590	Peat	Overlies laminated clay deposited within a lake dammed by the Mak Hill moraine	4	Mann and Peteet, 1994
12,640 ± 100	Beta-33666	Organic silt	Underlies Katolinat till	5	Pinney and Begét, 1991a; Pinney, 1993
10,200 ± 100	Beta-33665	Organic silt	Underlies Katolinat till	5	Pinney and Begét, 1991a; Pinney, 1993

were then deformed as the Iliamna-stade glacier overrode the sediments and deposited its till (unit 4). Glacial-lacustrine sediments, formed in a lake behind the Kvichak-moraine dam and overlain by till that forms the type Iliamna moraine, provide strong stratigraphic evidence that ice readvanced following its retreat from the Kvichak moraine. Following deglaciation, a late-Wisconsin tephra, a Holocene soil, and Holocene eolian sand capped the stratigraphic section (unit 5).

A second site, approximately 30 km southwest, exposes well-laminated silt and clay at river level along the Kvichak River (Fig. 11, site 2). Each layer is thin (approximately 1 cm), well sorted, contains fine laminae, with sharp basal and upper contacts (Fig. 14). These characteristics are consistent with rhythmites deposited in a lake by overflow and interflow (Ashley and others, 1985). The silt and clay couplets (varves) probably represent seasonal alteration between the amount and grain size of sediment transported to the depositional site. Additionally, the laminated silt and clay is laterally

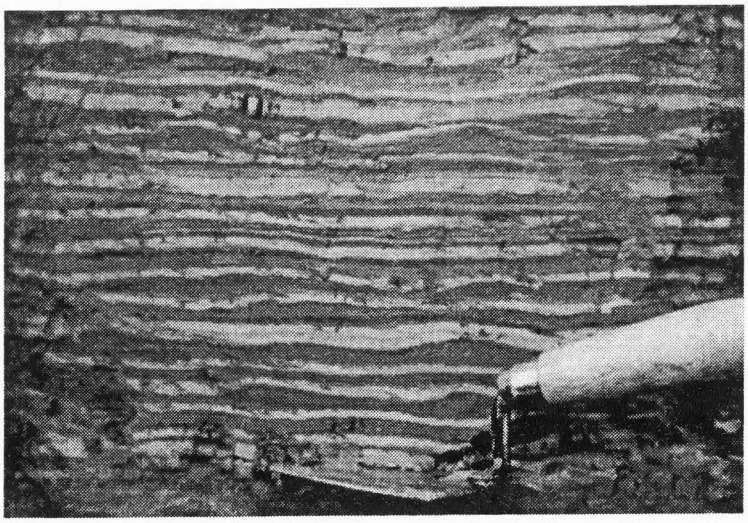

Figure 14. Laminated silt and clay found at river level along the Kvichak River (see Figure 11 for location).

traceable for approximately 5-10 kilometers between the type Iliamna and type Kvichak moraines. These lake beds lend support to the interpretation of unit 1 at site 1 as glacial-lacustrine sediments, and further confirm the conclusion that ancestral glacial Iliamna Lake was held in by the type Kvichak moraine following retreat of the Kvichak-stade glacier.

Late-Glacial Type Localities and Advances

Newhalen Stade. Mountains to the northeast of Lake Clark formed a topographic barrier that diverted the Cordilleran Ice Sheet, but supported a confluent system of local-mountain glaciers. Valley glaciers draining the ice mass upvalley of Lake Clark and Tazimina Lake coalesced roughly 2 km southeast of Pickerel Lake to occupy the Newhalen River valley and deposit the type Newhalen moraine (Fig. 3) (Detterman and Reed, 1973). The Newhalen-stade glacier extended 30-50 km southward, and nunataks were present above 250-300 masl.

An end moraine crossing the Newhalen River 9.6 km north of the village of Iliamna is the type locality for drift of the Newhalen stade (Fig. 3, site 8) (Detterman and Reed, 1973). At the type locality, its morphology is extremely irregular and hummocky, lacking laterally continuous ridges (Fig. 15). Rounded clasts, a lack of fines, and a clast-supported matrix characterize the parent material in soil pits, indicating extensive water reworking by meltwater associated with stagnating ice.

Distal and proximal slope angles on the type Newhalen moraine are significantly steeper than those on both the type Kvichak and type Iliamna moraines, and crest widths are sharper (Table 3; Appendix 1). The average proximal and distal slope angles are 19° and 18°, respectively. Crest widths average 18-21 m. Oxidation thickness averages 25 cm, and ranges from 17-36 cm (Table 3; Appendix 1). Coarse-grained and fine-grained

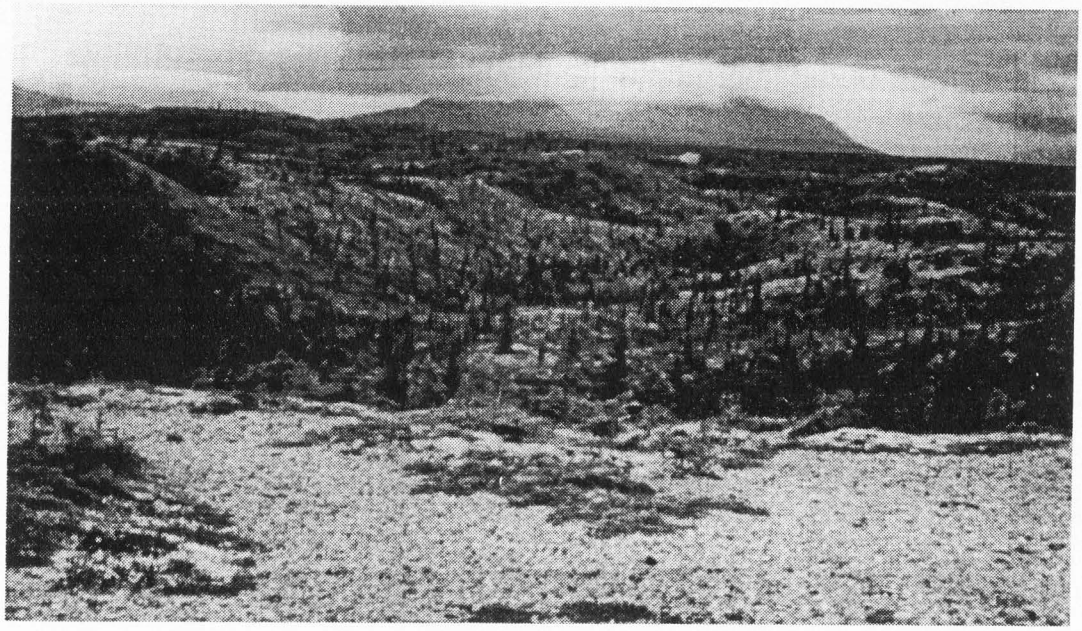

Figure 15. Type Newhalen moraine on the eastern side of the Newhalen River. Trees in valley bottom are approximately 3 m tall. Note the extremely hummocky and irregular morphology.

weathering indices are similar to one another, averaging 1.95 and 1.58, respectively (Table 3; Appendix 1).

Iliuk Stade. High mountains, up to 2300 masl, southeast of Naknek Lake, supported a confluent system of local-mountain glaciers during the Iliuk stade. The present-day ice cap, approximately 50 km long and 10 km wide, southeast of Naknek Lake (Fig. 6), which was presumably higher and more extensive during the Iliuk stade, was the major source area for the Iliuk-stade glacier. Outlet glaciers descended westward into the Naknek Lake valley through several troughs whose rivers feed present-day Naknek Lake.

The southernmost tongue of the Iliuk glacier occupied the Valley of Ten Thousand Smokes. It diverged around Mt. Katolinat, and extended approximately 5 km down Margot Creek valley, while filling the Ukak River valley down to the easternmost end of Iliuk Arm (Fig. 3). A second ice tongue squeezed down Ikagluik Creek valley; however, the largest Iliuk-stade glacier flowed westward through the Rainbow and Savonoski River valleys (Fig. 3). Small alpine valley glaciers originating in numerous cirques coalesced to nourish the westward-flowing valley glaciers from the north and the south. For example, present-day glaciers occupying Mt. Griggs (Fig. 6) presumably fed valley glaciers flowing down the major river valleys. Highlands separating Iliuk Arm from Lake Grosvenor split the Iliuk glacier. The southern branch occupied the trough now filled by Iliuk Arm of Naknek Lake, depositing the type Iliuk moraine (Muller, 1952), whereas the northern branch filled the Lake Grosvenor basin.

The Iliuk-stade glacier extended 60-70 km beyond the summit of the present-day ice cap. Lateral moraines along the northern edge of Mt. Katolinat (Fig. 3) suggest that the Iliuk-stade glacier was no higher than 150-170 masl.

The Iliuk stade is named for the moraine partially separating Iliuk Arm of Naknek Lake from Lake Brooks (Fig. 3, site 2) (Muller, 1952). At its type locality, the Iliuk moraine has been slightly modified by postdepositional weathering. It forms a laterally continuous, sharp, arcuate end moraine (Figs. 16 and 17). Two soil pits were dug on the type Iliuk moraine and one in Iliuk drift near the Valley of Ten Thousand Smokes. Parent material was not accessible at the type locality because frozen ground prevented digging deeper than 1.5 m, yet in neither case was diamicton reached. An exposure through the moraine at the outlet of Iliuk Arm showed well-sorted sand and bouldery, rounded gravel, suggesting that the Iliuk-stade glacier incorporated its proglacial outwash into its drift,

and/or that the moraine may have been deposited subaqueously. Parent material in Iliuk drift upvalley, however, was reached at a depth of 90 cm, where it comprised a clast-supported diamicton with a coarse-sandy matrix that lacked fines.

Average Iliuk moraine slope angles and crest widths are comparable to those on the type Newhalen moraine: 19° and 18°, respectively (Table 3; Appendix 1). Crest widths average 25 m. Oxidation thicknesses vary from 39-73 cm (Appendix 1), and average 55 cm (Table 3). A lack of surface clasts on the Iliuk moraine prevented the use of surface-clast pitting as a relative-age measurement. Also, the type Iliuk moraine has been terraced by lake shorelines below 30 masl.

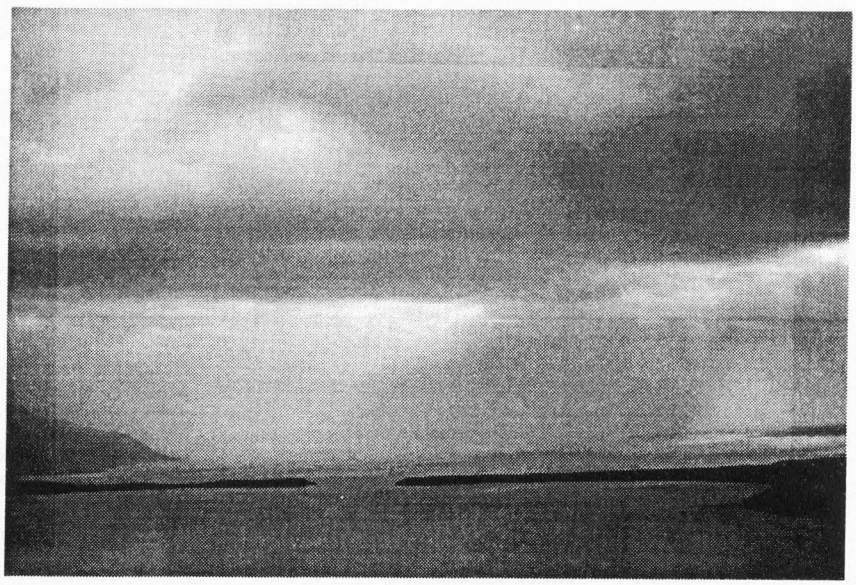

Figure 16. Type Iliuk moraine looking east to Iliuk Arm. Photograph taken from the top of Dumpling Mountain (Fig. 3).

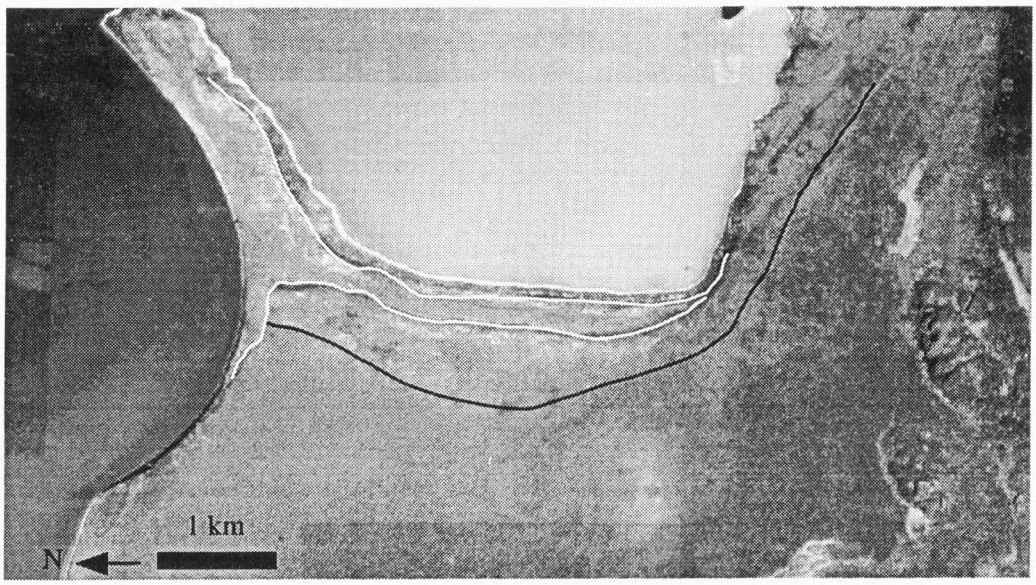

Figure 17. Aerial photograph of the type Iliuk moraine. Note shorelines (highlighted by white lines) that have terraced the moraine, and that glacier flowed from top to bottom of photograph. Black line designates western edge of the moraine.

Correlative Iliuk moraines elsewhere in the Iliamna/Naknek/Brooks Lake area separate upper "arms" of lakes from main-lake basins (Muller, 1952): Lake Grosvenor from Lake Colville; Murray Lake from Hammersly Lake; Kulik Lake from Nonvianuk Lake; and Battle Lake from Kukaklek Lake (Fig. 7). This criterion, however, unravels in Detterman and Reed's (1973) interpretation of glacial deposits in the Iliamna Lake valley, where Iliuk moraines do not extend beyond high-mountain tributary valleys. The discrepancy between the position of Iliuk moraines in the Naknek Lake valley and the Iliamna Lake valley led Lea (1989) to suggest that Muller's (1952) Iliuk moraines were correlative with Detterman and Reed's (1973) Newhalen moraines. The absence of

stratigraphic evidence in the study area to distinguish Newhalen and Iliuk stades suggests that the Iliuk stade and its associated moraines may represent a stabilization point for retreating Newhalen-stade glaciers. Nevertheless, Iliuk moraines are retained as morpho-stratigraphic features that separate subbasins from main lake basins.

Ukak Stade. I consider the Ukak stade a minor readvance of the Brooks Lake glaciation based upon the stratigraphic evidence for a readvance and ^{14}C evidence for a latest-Wisconsin age presented by Pinney and Begét (1991a) and Pinney (1993). Lethe volcaniclastic deposits, which are thought to have been erupted during ice-free conditions, are overlain by and incorporated into Ukak drift demonstrating that the type Ukak moraine represents a readvance.

Glaciers advanced approximately 25 km northwest beyond the present-day Knife Creek glaciers (Fig. 6) during the Ukak stade (Pinney, 1993). En route to its terminus 3-5 km west of the Valley of Ten Thousand Smokes, the Ukak-stade glacier coalesced with a smaller valley glacier descending northward from Mt. Mageik (Fig. 6, site 5) .

The type Ukak moraine is fresh, little modified, and hummocky (Fig. 3, site 1; Fig. 18) (Pinney and Begét, 1991a; Pinney, 1993); its irregular character is attributed to its deposition by stagnating ice. Marshes and swamps occupy depressions, and parent material in soil pits is clast supported and lacks fines.

Type Ukak moraine's crest widths are sharp, and proximal and distal slope angles are similar to those on the type Newhalen and type Iliuk moraines (mean proximal and distal slope angles = 20° and 19 °, respectively; Table 3; Appendix 1). Average crest widths, which range from 17-19 m, are sharper on the type Ukak moraine than any other type locality of the Brooks Lake glaciation. Oxidation thickness averages 11 cm (Table 3; Appendix 1). A lack of surface clasts on the type Ukak moraine precluded the use of

Figure 18. Type Ukak moraine at the western end of the Valley of Ten Thousand Smokes. Note the moraines's proximity to the mountain front and its fresh, hummocky morphology.

surface-clast pitting as a relative-age measurement. Although it was not possible to correlate other moraines in the study area with the Ukak stade, it is difficult to discern a readvance without the benefit of stratigraphic evidence such as that used by Pinney and Begét (1991a).

Relative-Age Data

Dating of mountain-glacier drift located in harsh environments, where there is little organic matter for radiocarbon dating, is hampered by a lack of absolute-age control, and

the Brooks Lake glacial sequence is no exception. Relative dating of deposits affords temporal information about the relative length of time separating deposits, and it is useful for correlating moraines with the type localities of a glaciation. Most relative-age studies focus on differentiating glacial deposits of different glaciations, which are separated by tens of thousands of years. Differentiating stades within a single glaciation, separated by thousands of years, is inherently more difficult. An insufficient length of time elapses between stades, and the variability in the weathering parameters is too small to resolve such high-frequency events.

Nonetheless, of the relative-age data used in this study, moraine morphologic measurements appear to separate the type localities of the Brooks Lake glaciation. Soil development is hampered by a lack of consistent parent material, differential loess input, textural variability, and vegetational differences across the study area. Analysis of soil properties consisted of relatively simple measures; thus, more detailed analyses might reveal soil-development trends. Surface-clast pitting is hampered by lithologic variability among clasts, insufficient time necessary to develop weathering pits, and a lack of surface clasts on the type Iliuk and Ukak moraines.

Morphology. Slope angles separate the type localities of late-Wisconsin moraines into two groups (Fig. 19a). The type Kvichak and type Iliamna moraines are less steep (averages range from 11-15°) than the type Newhalen, type Iliuk, and type Ukak moraines (averages range from 18-20°). The grand mean and standard deviation for the less steep Kvichak and Iliamna moraines is 12 ± 3, and 19 ± 1 for steeper Iliuk, Newhalen, and Ukak moraines. The group means do not overlap at one standard deviation, indicating that they are distinct. Colman and Pierce (1986) demonstrated that higher scarps in central Idaho had steeper slope angles than lower scarps of similar age, showing that slope angle is a

function of slope height. Slope angles in the study area, however, do not appear to be a function of slope lengths. The lack of correlation between the two (r values range from 0.066 for the type Iliuk moraine to 0.463 for the type Newhalen moraine) indicates that slope angles alone are a viable measure of moraine degradation.

Although no major time breaks are distinguishable from crest-width data, crest widths on the type-locality moraines generally broaden with age, with the exception of the type Iliuk moraine, whose crest is broader than anticipated by the observed trend in crest widths (Fig. 19b). Eastern and northern portions of the type Iliuk moraine were under water during high stands of Naknek Lake, terracing the moraine (Fig. 17). Data were collected from below the high terrace of Naknek Lake, suggesting the broader crest width is a result of wave action in the lake. Excluding this data point separates the remaining four type localities into two groups. The type Kvichak and Iliamna moraines have broader crest widths (grand mean and standard deviation = 28 ± 5 m), whereas the type Newhalen and type Ukak moraines have sharper crest widths (grand mean and standard deviation = 19 ± 1 m). Of all type localities, the type Ukak moraine has the narrowest crest width (18 m), whereas the type Kvichak moraine has the broadest crest width (31 m).

A prevalent pitfall affecting morphologic relative-age data revolves around the assumption that the initial form of the moraine is comparable for all moraines in the study area. However, the type Kvichak moraine, for instance, has a much more hummocky morphology than the younger type Iliamna moraine. This suggests that the type Iliamna moraine was initially less hummocky than the stagnant-ice influenced Kvichak moraine, violating the assumption.

Similarly, the type Kvichak moraine, deposited by stagnating ice, is morphologically dissimilar to the type Iliuk moraine, a simple, arcuate ridge deposited at

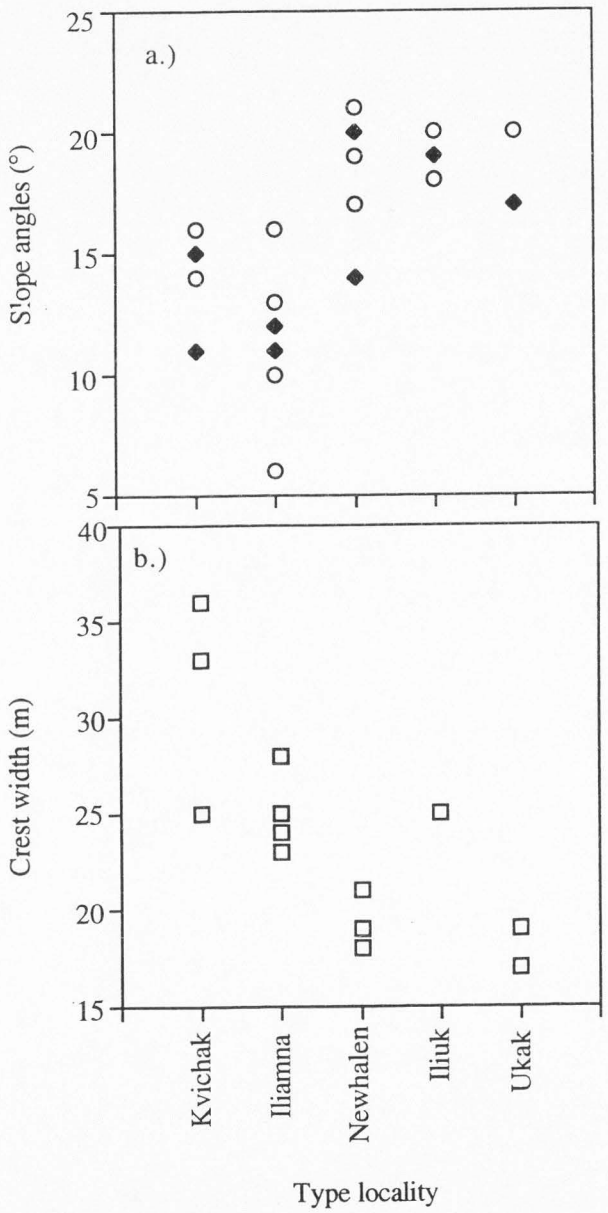

Figure 19. Morphometric relative-age data from the five type-locality moraines of the Brooks Lake glaciation. (a) Slope angles measured on distal (diamond) and proximal (circle) moraine slopes. (b) Crest widths.

an active ice margin. Nevertheless, slope angles appear to be steeper on late glacial moraines than on early-late-Wisconsin moraines of the Brooks Lake glaciation, suggesting that slope-degradational processes are a dominant control on the morphology of moraines.

The distinction between early-late-Wisconsin Kvichak and Iliamna moraines from the late glacial Newhalen, Iliuk, and Ukak moraines, based upon morphometric data, suggests that the Iliamna and Newhalen stades were separated by a substantial interval of time. This conclusion agrees with that of Detterman and Reed (1973), who suggested that a considerable time interval separated the Newhalen stade from the earlier Iliamna stade.

Soil Development. Oxidation thicknesses do not differentiate between moraines at the five type locality moraines (Fig. 20). The variation in oxidation thickness between three pits on a single moraine exceeds the variation between moraines (for example, thicknesses on the type Kvichak moraine range from 16-39 cm, and 39-73 on the type Iliuk moraine; Appendix 1). Muncell colors dominantly vary within the narrow range of a 10 Y/R hue; thus, they are not useful for differentiating moraines (Appendix 1). Loess thickness is generally insignificant. Some soil B horizons were divisible into a B_t (textural) and a B_{ox} (oxidized) zone, either a reflection of pedogenic processes or loess input, whereas other horizons lacked a B_t zone. Nevertheless, the presence of B_t horizons does not show a trend.

Several possibilities might explain the widespread variation in soil properties between and among moraines. Portions of the type Iliuk moraine, for instance, have been submerged beneath Naknek Lake during higher stands of the lake (Chapter 3), enabling sandy beach deposits to accumulate on top of the drift. Consequently, soils have been formed into beach deposits rather than till. Second, the texture of parent material

comprising each moraine varied, which significantly affected soil development. Third, some sites had received a minor amount (about 2-8 cm) of loess input, which probably accelerated soil development, whereas others had not. Fourth, the crest surfaces where soil pits were dug may have been subject to wind deflation. Fifth, soil pits on the type Iliuk and type Iliamna moraines were dug on vegetated surfaces consisting of upland tundra, moss with open to full stands of spruce, and low birch shrubs. Such vegetation differences would also affect soil development. Combined, these factors have obscured any potential temporal patterns in soil development.

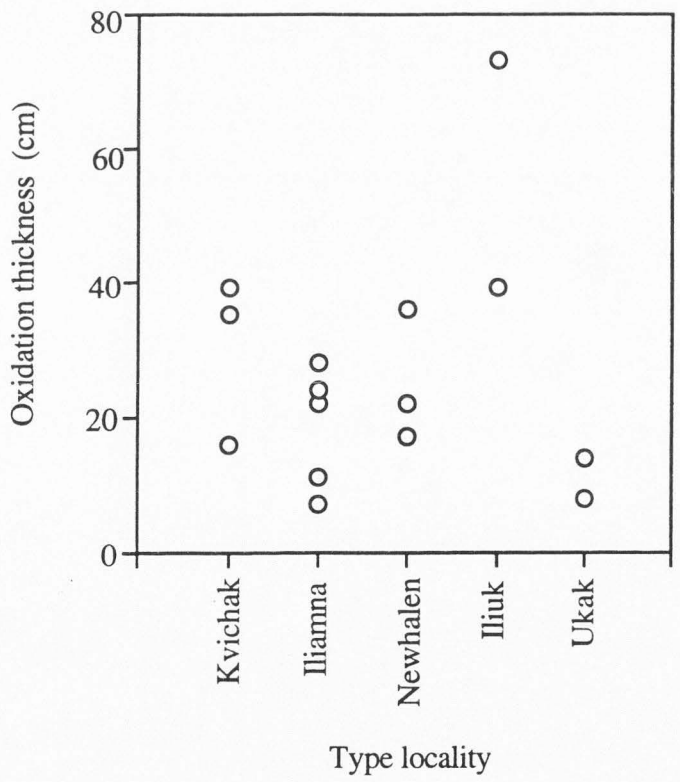

Figure 20. Oxidation thickness measured in soil pits dug into moraines of each type locality of the Brooks Lake glaciation.

Surface-Clast Pitting. Surface-clast pitting fails to distinguish moraines (Fig. 21). On any one moraine, some surface clasts had cavernous pits (pitting class = 4), whereas other clasts on the same moraine were unweathered (pitting class = 1). Because pits require tens of thousands of years to develop, this criterion is not appropriate for differentiating moraines separated by thousands of years. Coarse-grained indices are slightly higher overall (mean = 2.62) than fine-grained (mean = 1.79) and this is the expected trend.

Other factors may have affected pit development. First, the larger the diameter of a clast exposed at the surface, the more apt it is to show large pits (that is, large pits cannot form in small clasts). Second, subtle compositional and textural variations may influence pit development. Third, a sample size of 25 clasts may have been insufficient to detect trends in such a variable system. Finally, the pitting classification scheme was not fully developed when studying the type Newhalen moraine.

Fine-grained clast pitting may be somewhat more useful than coarse-grained clast pitting. Two out of three weathering indices for clasts on the type Newhalen moraine appear higher than expected. If these values are excluded, because the pitting scheme was not adequately defined when those measurements were taken, then pit development increases from the type Iliamna to the type Kvichak moraine. The coarse-grained data do not conform to an expected pattern of increasing pit development with increasing age, thus are not useful for differentiating moraines.

Additionally, measurement of the thickness of weathering rinds of basalt pebbles from the B horizon was attempted. Weathering rinds were dominantly nonexistent, and the technique did not bode useful.

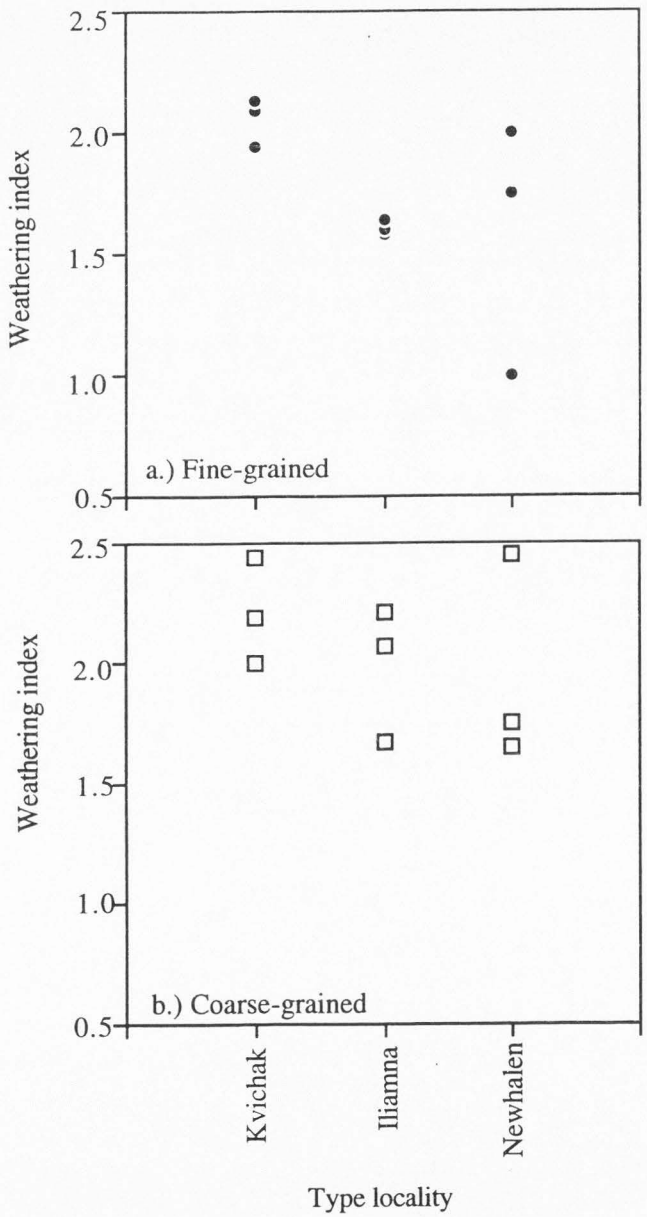

Figure 21. Weathering index (see text for equation) calculated for (a) fine-grained, and (b) coarse-grained rocks measured on surfaces of three type-locality moraines of the Brooks Lake glaciation.

Other Moraines and Correlations

Naknek Moraine. High volcanic peaks formed a topographic barrier east of the Naknek Lake valley during early-late-Wisconsin time. This barrier deflected the Cordilleran Ice Sheet while supporting a confluent system of local-mountain glaciers that deposited the Naknek moraine (Fig. 3, site 4). Assuming that the source area headed at the present-day topographic divide, the Naknek glacier was approximately 130 km long. Flowing westward from mountains of the Aleutian Range, the Naknek glacier consisted of numerous tributaries and distributary lobes. The Savonoski River valley contained the largest tributary. Subsidiary tributaries included the Rainbow River valley and the Valley of Ten Thousand Smokes. Smaller valley glaciers fed main valley glaciers from both the north and the south.

A granitic erratic, found on Dumpling Mountain (Fig. 3) at an elevation of 300 masl, affords a minimum estimate of the glacier's height, approximately 40 km east of the terminus. The upper elevation of glacial deposits mapped from aerial photographs indicates that the peaks of Mt. Katolinat, Dumpling Mountain, and Mt. La Gorce above approximately 350-400 masl were ice free, but lower elevations were glaciated extensively.

The Naknek glacier had a tri-lobate terminus, and its southernmost lobe was deflected southwestward by Mt. Katolinat into the Lake Brooks basin (Fig. 7). It extended 14 km beyond the west end of Lake Brooks. The central and most massive lobe of the Naknek glacier, which entirely filled the Naknek Lake basin, advanced 3-8 km beyond the western end of Naknek Lake. Above Naknek Lake, a small ice tongue pushed northwestward to fill the Idavain Lake basin. North of Idavain Lake, the Naknek glacier coalesced with ice occupying the Lake Grosvenor-Colville basin, where ice advanced northward towards the Alagnak River, joining with ice that had descended westward into

the Nonvianuk-Kulik Lake basin.

The Naknek moraine is dissected by the Naknek River approximately 10 km from the mouth of Naknek Lake (Fig. 3, site 4). Its morphology is hummocky with numerous kettle ponds and few moderately continuous ridges (Figs. 22 and 23). Parent material in soil pits contains lenses of fine sand, and the diamicton is predominantly matrix-supported. Additionally, surface boulders display a patchy distribution, suggesting that drift was reworked and dumped by stagnating ice, while the rest of the debris was carried away by meltwater. Like the type Kvichak moraine, these features suggest that the Naknek moraine was also deposited by stagnating ice, following a rapid climate warming.

Compared to moraines upvalley, the Naknek moraine appears to be an older, more subdued landform (Table 3; Appendix 1). Slope angles are consistent with early-late-Wisconsin Kvichak and Iliamna moraines in the study area (average for both proximal and distal slope angles = 13°). Average crest width is 25 m. Oxidation thicknesses average 12 cm, and coarse-grained and fine-grained weathering indices average 2.50 and 2.57, respectively (Table 3).

According to Riehle and Detterman (1993), there are two distinct early-late-Wisconsin moraines in the Naknek Lake valley: the Mak Hill moraine, which they ascribed to the Kvichak stade, and the Naknek moraine, which they assigned to the Iliamna stade. However, the type Mak Hill moraine is reassigned to a pre-late-Wisconsin advance (for reasons to be discussed in the Geochronology section of this chapter), and the Naknek moraine is considered the only early-late-Wisconsin moraine in the valley. Moraines upvalley are ascribed to younger alpine valley late glacial advances.

Although there is strong stratigraphic evidence for two discrete early-late-Wisconsin glacial advances in the Iliamna Lake valley, such evidence is lacking in the Naknek Lake

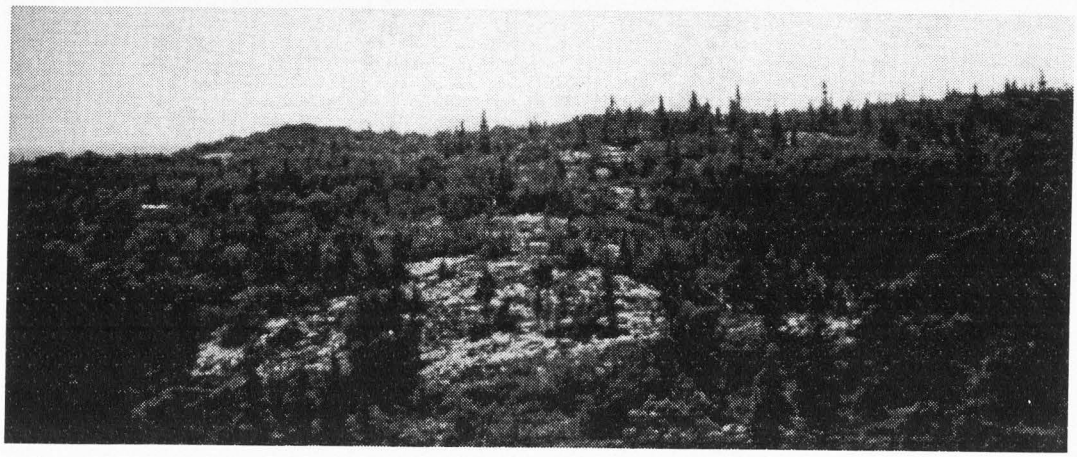

Figure 22. The Naknek moraine approximately 10 km north of the Naknek River. Note the moraine's relatively subdued hummocky morphology, similar to the type Kvichak moraine.

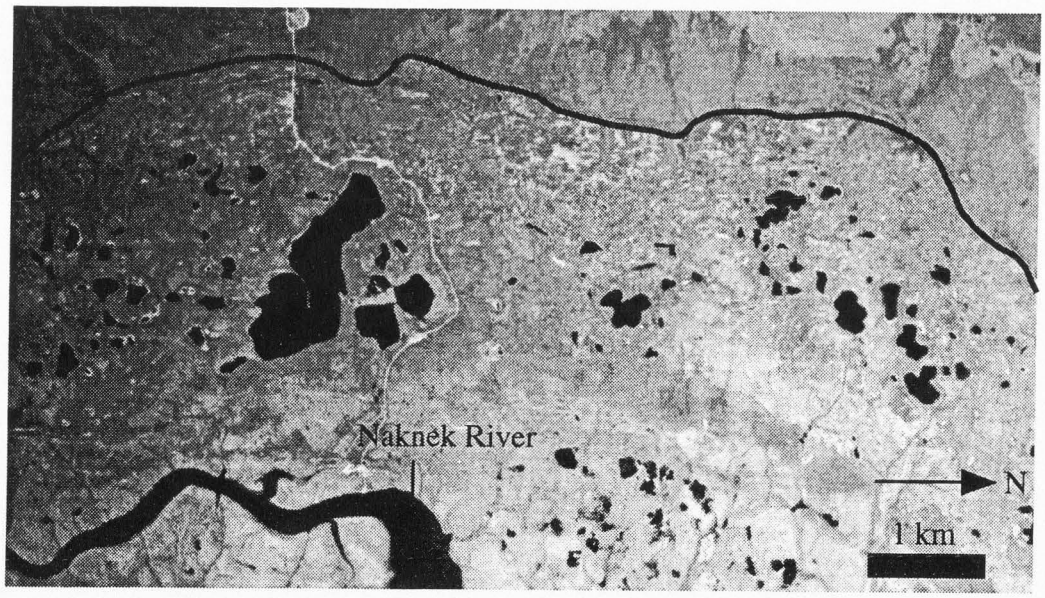

Figure 23. Aerial photograph of the Naknek moraine. Note abundant kettle ponds and discontinuous ridges. Outer limit of moraine is highlighted in black, and the glacier flowed from the bottom to the top of the page.

valley. Thus, the Naknek moraine is considered correlative with either the Kvichak or Iliamna stades, or both. Feasibly, a single early-late-Wisconsin advance may have deposited the Naknek moraine, or two distinct advances may have terminated near the same position making the individual moraines indistinguishable. The lack of a two-fold, Kvichak/Iliamna glacial sequence in the Naknek Lake valley suggests that the glacial system here responded differently than the glacial system in Iliamna Lake valley to climate change or glacier-bed dynamics as a result of differing ice sources and glacier configurations. Moraines correlative with the Naknek moraine can be traced from the Naknek Lake valley, north to the Kukaklek Lake valley, where glaciers were also fed by a local-mountain ice source (Fig. 7).

Lake Brooks Moraine. The Lake Brooks glacier was substantially smaller than the maximum late-Wisconsin Naknek glacier, but its source area and flow direction were similar (Fig. 7). A southern tongue of the glacier, which terminated at the west end of Lake Brooks approximately 20 km beyond the position of the type Iliuk moraine, deposited the Lake Brooks moraine that presently dams the lake. Meltwater drained to the southwest, but at present there is no outlet at the southwest end of Lake Brooks. Rather, Brooks River drains Lake Brooks to the northeast into the Naknek Lake basin. A more northerly tongue of the glacier probably terminated in Naknek Lake at this time. The glacier overrode a low topographic divide north of Naknek Lake to fill the Grosvenor-Colville lake basin. Areas above approximately 200 masl were ice-free during this advance.

The Lake Brooks moraine is a narrow (approximately 40-50 m), 5-km-broad, laterally continuous, arcuate ridge deposited at an active ice margin (Fig. 3, site 3). Parent material in soil pits is compact diamicton, consisting of angular clasts in a silt and fine-sand matrix. Proximal and distal slope angles are steep, similar to slope angles on late glacial

moraines (average proximal slope = 22°, distal slope = 17°; Table 3; Appendix 1). Average crest width is 25 m. Oxidation thicknesses average 25 cm (Table 3). Surface clasts >15 cm were absent on the moraine.

Flanking slope angles on the Lake Brooks moraine overlap with those on the type Newhalen moraine, and younger type Iliuk and Ukak moraines. Based upon its position in the moraine sequence, the Lake Brooks moraine is of pre-Iliuk age. The Lake Brooks moraine is younger than the Iliamna stade based upon steeper slopes than those on the type Iliamna moraine, indicating that it is older than the early-late Wisconsin moraines. Thus, the Lake Brooks moraine is correlative with the Newhalen stade.

The glacier that deposited the Lake Brooks moraine was part of a multi-lobate glacier that deposited moraines at the eastern end of Idavain Lake and the northern end of Lake Colville (Fig. 7). However, correlative moraines in Kukaklek and Nonvianuk lake valleys are apparently absent. This suggests that local-mountain glaciers upvalley of Kukaklek and Nonvianuk lakes responded differently to climate change, probably due to differing valley hypsometries. The Naknek Lake valley is mostly flat for approximately 100 km (that is, the toe of the type Iliuk moraine is 51 masl, whereas the toe of the Naknek moraine, ~20 km downvalley, is 45 masl); therefore, small vertical changes in equilibrium-line altitudes would have triggered large changes in glacier mass balance. In contrast, valleys to the north are steeper, and require greater changes in equilibrium-line altitudes for glaciers to advance downvalley.

Although slope angles and crest widths on the Lake Brooks moraine are similar to those on the type Newhalen moraine, the genesis of the two moraines appears different. The hummocky morphology of the type Newhalen moraine suggests that it was deposited by stagnating ice. In contrast, the regular morphology of Lake Brooks moraine indicates

that it was deposited at an active ice margin, suggesting that climate steadily warmed, enabling the glacier to retreat at an even pace. Two temporally equivalent glaciers appear to have responded differently to climate change. This suggests that either: (1) climate change varied significantly over small regional scales in mountainous areas, (2) glaciers respond differently because of different source areas, geometries, debris cover, or glacier/bed dynamics, or (3) a combination of both (1) and (2). Alternatively, the Newhalen-stade glacier, which occupied a narrow valley, could have received greater rock-fall debris from proximal valley walls than the Lake Brooks glacier that occupied a broader valley; the extensive debris cover would have contributed to stagnant-ice formation.

Geochronology--Radiocarbon Control

Mak Hill Glaciation. Drift of the Mak Hill glaciation, originally thought to be early Wisconsin age (Muller, 1952), is found on upland surfaces east of the Bristol Bay lowlands (Detterman and Reed, 1973; Riehle and Detterman, 1993). The type locality for the Mak Hill glaciation is a knoll approximately 12.8 km east of Naknek Lake (Fig. 3) (Muller, 1952). Contrary to Riehle and Detterman (1993), the type Mak Hill moraine is hereby reassigned to a pre-late-Wisconsin deposit. This conclusion is based upon a minimum-limiting ^{14}C age of approximately 39 ka (Table 4) on peat from the Naknek Lake valley that apparently postdates the Mak Hill moraine (Mann and Peteet, 1994), and on the presence of a thick (about 2 m) eolian unit, presumably late Wisconsin, that mantles Mak Hill drift, but is absent from younger deposits (Thompson and others, 1994b).

Early-Late-Wisconsin Advances. Dated organic matter from the base of a river bluff approximately 20 km downstream of the type Kvichak moraine (Fig. 11, site 3) provides a new maximum-limiting age on the type Kvichak moraine. The 10-m

stratigraphic section is subdivided into three units (Fig. 24): (unit 1) 1.7 m of dark-brown peat and dense organic silt, capped by 50 cm of reduced fine sand; (unit 2) approximately 8.5 m of fine to medium sand containing large-scale planar-cross sets; and (unit 3) a 0.5-m-thick modern soil and organic mat.

Plant macrofossils collected from a peaty, organic-rich layer 35 cm below the top of unit 1 were dated at 26,155 ± 285 ^{14}C yr BP (Table 4; Figs. 24 and 25). This organic-rich silt and peat is correlated to the nonglacial late-Pleistocene Etolin complex of Lea and others (1991), interpreted as wetland sediments deposited within shallow ponds and lakes. The Etolin complex is a prominent stratigraphic unit found throughout the southern Nushagak lowland (Fig. 2). It is composed of dark-brown, organic-rich silt, and detrital peat that ranges from 0.3-4.0 m thick, and is typically capped by a thin, discontinuous white tephra. Radiocarbon ages combined with paleoecological data suggest that the Etolin complex in the Nushagak lowland predates 30,000 ^{14}C yr BP, but is most likely >40,000 ^{14}C yr BP (based upon a series of nonfinite ages), and correlates with the middle Wisconsin (Lea, 1989; Lea and others, 1991). The present correlation of unit 1 at the Kvichak River site with the Etolin complex is based upon its similar stratigraphic position below late-Wisconsin-age deposits (see below) and its similar composition. No white tephra was found at the site, however.

This new age of 26,155 ± 285 ^{14}C yr BP provides the youngest reported age for the Etolin complex, and is the farthest northeast that the unit has been found. The age is indistinguishable from a recently reported age of 26,570 ± 320 ^{14}C yr BP on peat in the Naknek River valley underlying outwash graded to the Naknek moraine (Table 4; Fig. 3) (Mann and Peteet, 1994). The peat caps a 3-m-thick succession of organic-rich silt and

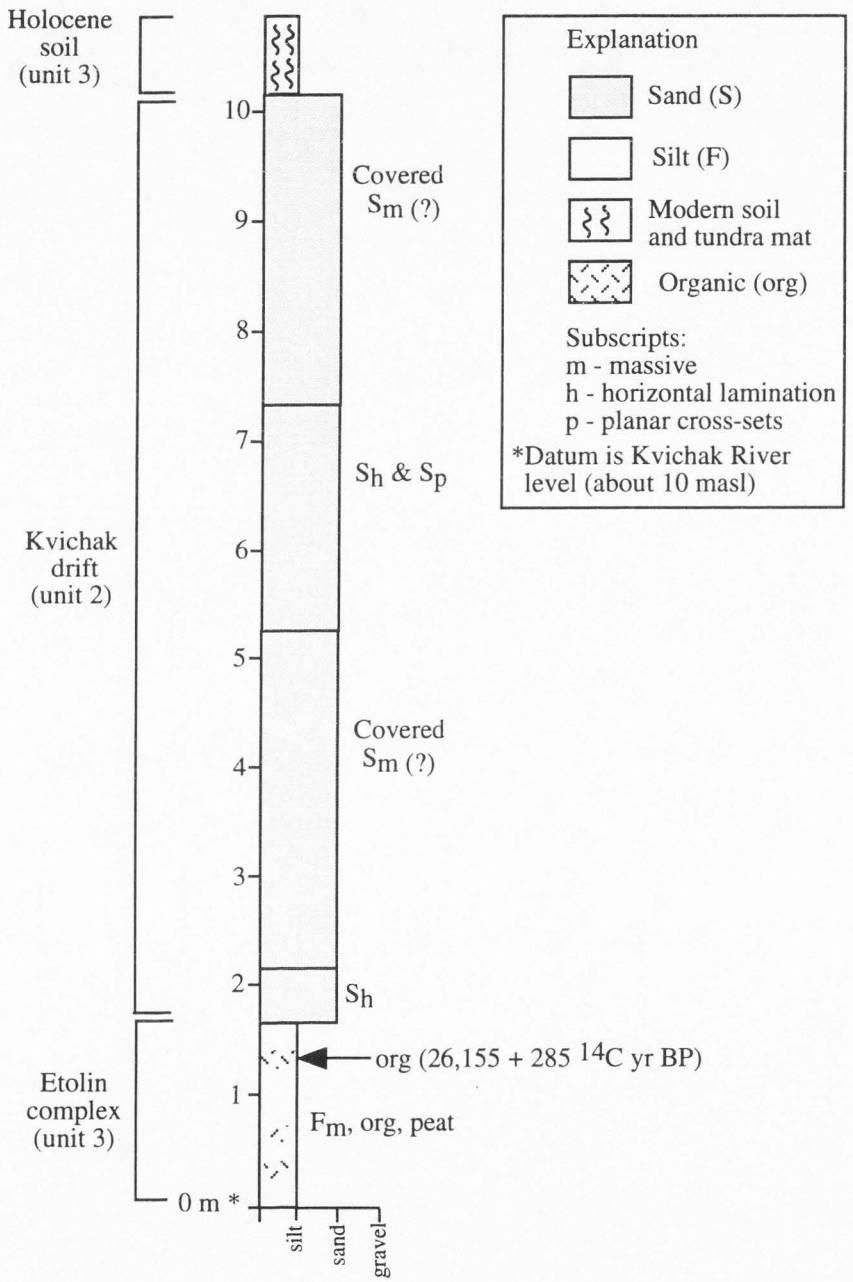

Figure 24. Stratigraphic section of river-bluff exposure located approximately 10 km downstream of the type Kvichak moraine. Section includes the Etolin complex, overlain by outwash associated with the type Kvichak moraine, and modern soil.

peat, which Peter Lea (personal communication, 1994) and I also interpret as the Etolin complex based upon its stratigraphic position, white capping tephra, thickness, and composition.

The two radiocarbon ages from the top of the Etolin complex, found on the Kvichak Bay side of Bristol Bay, are younger than a >30 ka age assigned to the Etolin complex by Lea (1989) and Lea and others (1991). The younger age, however, is not inconsistent with the timing of the transition to full-glacial climates in Alaska (Lea, 1989).

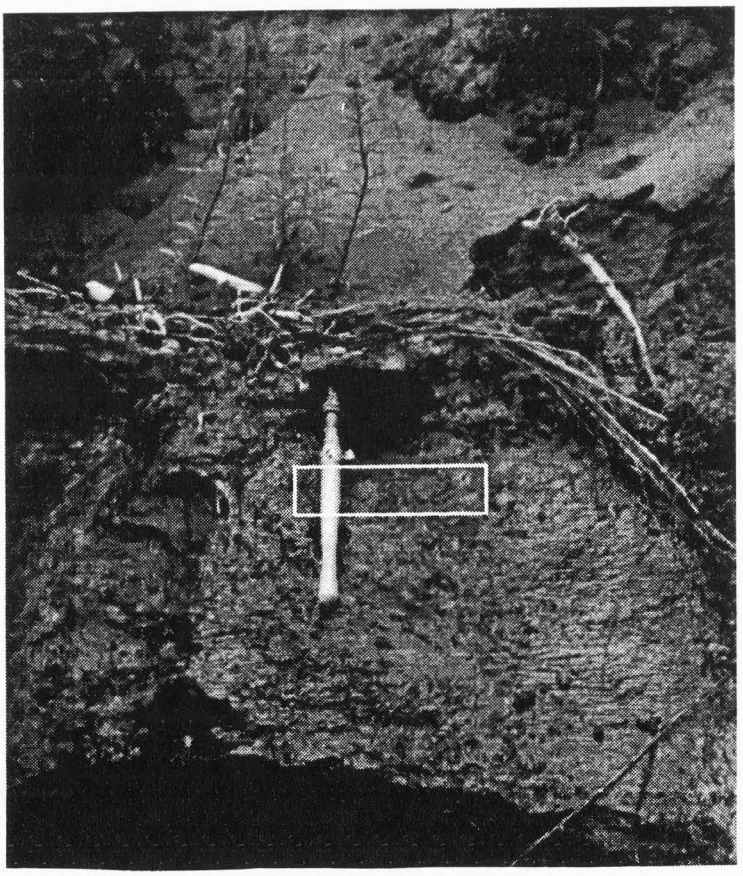

Figure 25. Organic-rich silt and peat unit (Etolin complex), including the location of dated sample (box).

Also, the ages reported by Lea (1989) and Lea and others (1991) may have come from organic units lower in the Etolin complex. Furthermore, the Etolin complex may be a time-transgressive unit, younger in the Kvichak Bay region than in the Nushagak lowland.

Sedimentary structures within unit 2 (Fig. 24) include horizontal laminations (S_h), suggesting shallow, fast-water flow, typical of a braided stream, and planar-cross sets (Sp), characteristic of channel-bar deposits (Ashley and others, 1985). These structures imply that unit 2 represents braided stream deposits that were deposited on the outwash plain supplied by the Kvichak-stade glacier. Also, the surface of unit 2 is graded to the type Kvichak moraine front. Braided stream deposits interpreted as outwash and containing horizontal laminations, planar-cross beds, ripple laminations, and trough cross-beds, overlie the Etolin complex in the Naknek River valley as well (Mann and Peteet, 1994). Eolian deposits of the Igushik Formation (Lea, 1989), which typically overlie the Etolin complex in areas beyond the limit of late-Wisconsin ice in the Nushagak lowland, are apparently missing at both sites, or the uppermost covered sand unit atop glacial-fluvial deposits at the Kvichak River site may comprise the Igushik Formation.

Late Glacial Advances. Charcoal collected from near the surface at the type locality of the Iliuk stade was dated at >41,650 ^{14}C yr BP (Table 4). Because this is a non-finite maximum age, it cannot be used to constrain the age of the moraine.

It was not possible to obtain new finite ages for late glacial advances of the Brooks Lake glaciation. Age control on Iliuk and Ukak glacial deposits, however, is presented by Pinney and Begét (1991a) and Pinney (1993), and is reviewed below. Lethe volcaniclastic deposits, whose source, chemistry, and distribution are discussed fully in Chapter 4, were laid down during ice-free conditions, providing an important late Wisconsin stratigraphic

horizon within the study area. Airfall Lethe pumice and ash overlie Iliuk drift and Iliuk glaciolacustrine deposits, and are also overlain by and incorporated into Ukak drift near the Valley of Ten Thousand Smokes.

Silt and clay containing dropstones are thought to record a small lake, called Glacial Lake Overlook, dammed by the Ukak glacier (Pinney, 1993). Two distinct layers of organic-rich silt within these lake deposits were dated at 10,200 ± 100 ^{14}C yr BP and 12,640 ± 100 ^{14}C yr BP (Table 4; Fig. 3). The younger silt directly underlies a diamicton thought to have been deposited by the Holocene Katolinat glacial advance, whereas the older silt lies approximately 50 cm below this diamicton, and is wholly contained Glacial Lake Overlook deposits.

Lethe volcaniclastics combined with ^{14}C dating provide a minimum-limiting age of 12,640 ± 100 ^{14}C yr BP on the Iliuk stade, and therefore, the older Newhalen stade. Stratigraphic evidence indicates that Ukak drift postdates the eruption of Lethe tephra. Radiocarbon ages of 12,640 ± 100 ^{14}C yr BP and 10,200 ± 100 ^{14}C yr BP, obtained from glacial-lacustrine deposits associated with the Ukak advance, afford a maximum age on the Ukak moraine by dating the presence of glacial Lake Overlook, and provide a minimum-limiting age on the Ukak advance, respectively.

Interpretation of the chronology of the Ukak advance is weakened by the lack of Ukak diamicton at the dated site. Radiocarbon ages on the Ukak advance rely on the interpretation that these glacial-lacustrine sediments correspond with the Ukak advance. The evidence is equivocal, however. Although the organic silt underlying Katolinat till clearly provides a valid minimum age on the Ukak stade, the interpretation of the lowermost silt as a maximum age is less secure because it dates the deposition of lake

sediments rather than the Ukak moraine. The age of the Lethe volcaniclastics (>12,640 ± 100 ^{14}C yr BP) provides a more secure maximum age for the Ukak moraine.

Pinney and Begét (1991a) and Pinney (1993) suggested that the Ukak stade is correlative with the European Younger Dryas interval (dated at 11,000-10,000 ^{14}C yr BP). However, age control supportive of this hypothesis is not convincing. The maximum age of Ukak drift is more than 1000 yr older than the beginning of the Younger Dryas, and given the potential contamination of old carbon in the dated organic silt, the uncertainty in its age is too great. Multiple dates are necessary to pinpoint the precise timing of the advance before it can be safely correlated with Younger Dryas.

Geochronology--Relative-Age Control

Moraine slope angles afford the only other temporal information for the Brooks Lake glaciation. Steeper slope angles on moraine deposited during the late-glacial stades suggest a considerable length of time elapsed between these stades and early-late-Wisconsin stades. This time-stratigraphic marker subdivides the Brooks Lake glaciation into an early and late phase, which constitutes the basis for correlation with other glacial sequences in Alaska that have been divided similarly (see below).

Correlations

Glacial Records. Ideally, the chronology for the Brooks Lake glaciation would include more closely limiting maximum and minimum ages on each stade; nevertheless, broad correlations can be drawn between the Brooks Lake glaciation and other late-Wisconsin glacial sequences in Alaska. Late-Wisconsin glacial sequences in Alaska have been studied in the Brooks Range, Seward Peninsula, Kuskokwim Mountains, Wrangell-St. Elias Mountains, Yukon-Tanana Upland, Bristol Bay, Glacier Bay, upper Cook Inlet,

and Glacier Bay (Fig. 1) (Hamilton, 1994). Most of these sequences have not been subdivided to the extent of the Brooks Lake glaciation, and they lack firm chronologic control.

Deposits of the Tolstoi Lake glaciation in the Kuskokwim Mountains, for example, have been assigned to the late Wisconsin based primarily upon topographic freshness, slight weathering of surface boulders, weak soil development, and unmodified cirques (Kline and Bundtzen, 1986). This glaciation is correlated with the Brooks Lake glaciation (Table 5). Similarly, deposits of the Salcha glacial episode found in the Yukon-Tanana Upland have been assigned a late-Wisconsin age (Weber, 1986). Four glacial advances are represented in most valleys, but have not been subdivided, and the glaciation is broadly correlative with the Brooks Lake glaciation (Table 5).

Glaciers originating in the Kigluaik Mountains deposited drift ascribed to the Mount Osborn glaciation that postdates the Salmon Lake glaciation (>40 ka) (Kaufman and Hopkins, 1986). Deglaciation was complete by 11.5 ka based upon a ^{14}C age from a cirque (Peck and others, 1990). These ages indicate that drift of Mount Osborn age is correlative with drift of the Brooks Lake glaciation (Table 5). Likewise, ^{14}C ages suggest that glaciers of the Macauley glaciation in the Wrangrell-St. Elias Mountains advanced after 29 ka and major valleys and valley heads in front of modern glaciers were ice-free by 11.3 ka (Denton, 1974); the Macauley glaciation is correlated with the Brooks Lake glaciation (Table 5). Finally, late-Wisconsin glaciation in the northwest Alaska Range, ascribed to the Farewell 2 phase, consisted of four major advances, but the deposits lack chronologic control and are generally correlated with deposits of the Brooks Lake glaciation (Table 5) (Kline and Bundtzen, 1986).

TABLE 5. PROVISIONAL CORRELATIONS BETWEEN THE BROOKS LAKE GLACIATION AND OTHER LATE-WISCONSIN GLACIAL SEQUENCES IN ALASKA

Bristol Bay	North-central Alaska Range	Brooks Range	Upper Cook Inlet	Glacier Bay	Wood River Range	Northwestern Alaska Range	Wrangrell-St. Elias Mountains	Yukon-Tanana Upland	Kuskokwim Mountains	Seward Peninsula
Brooks Lake glaciation	McKinley Park glaciation (1)	Itkillik II (2)	(3)	(4)	(5)	(6)	(7)	(8)	(9)	(10)
(10,200 ± 100) Ukak	Phases 3 and 4 (12.8-11.5 ka)	Itkillik II Late Phase (13-11.5 ka)	Elmendorf moraine (13.7-11.7 ka)	Eurhythmic readvance (12,430 ± 100)		Farewell 2 glaciation	Macauley glaciation (29-11.3 ka)	Salcha glaciation	Tolstoi Lake glaciation	Mt. Osborn glaciation (<40ka) (>12 ka)
(12,640 ± 100) Iliuk Newhalen										
Iliamna Kvichak (26,155 ± 285)	Phase 2 (15-14.1 ka) Phase 1 (26-17 ka)	Itkillik II Main Phase (24-13 ka)	Naptowne glaciation	Raven House	Alegnagik Okstukuk					

All dates are radiocarbon yr BP

References:

(1) Tenbrink and Waythomas, 1985; Werner, 1995
(2) Hamilton and Porter, 1975
(3) Schmoll and others, 1972
(4) Mann, 1986
(5) Lea, 1989
(6) Kline and Bundtzen, 1986
(7) Denton, 1974
(8) Weber, 1986
(9) Kline and Bundtzen, 1986
(10) Kaufman and Hopkins, 1986

Some Alaskan late-Wisconsin glacial advances are characterized by a two-fold subdivision, consisting of an early/main phase and a late phase. Wisconsin glaciation in the Brooks Range, termed the Itkillik glaciation (Detterman and others, 1958), is subdivided into Itkillik I and II (Hamilton and Porter, 1975). Itkillik II (24-11.5 ka) is divisible into a Main Phase (24-13 ka) and a Late Phase (13-11.5 ka) (Hamilton, 1982, 1986). Allowing for uncertainties in age control, and some asynchroneity between the two mountain ranges, the Kvichak and Iliamna stades are tentatively correlated with the Itkillik II Main phase, and Newhalen, Iliuk, and Ukak stades with the Itkillik II Late Phase (Table 5).

End moraines of Raven House drift from Glacier Bay are thought to be of late Wisconsin age (Mann, 1986). Maximum-limiting age estimates are based upon the age of

an associated terrace using calculated rates of uplift and tilting. The terrace formed during middle-Wisconsin time and Raven House drift overlies the terrace. A widespread marine transgression accompanied deglaciation before 13,000-14,000 ^{14}C yr BP (Mann, 1986). Till of the Eurhythmic readvance contains wood dated at 12.4 ka. Drift of Raven House age is considered equivalent to early-phase drift of the Brooks Lake glaciation, and drift of the Eurhythmic readvance is considered correlative with late-phase deposits of the Brooks Lake glaciation (Table 5).

During the Naptowne glaciation of Karlstrom (1964), which may have consisted of both an early- and late-Wisconsin advance, glaciers entered upper Cook Inlet. The Elmendorf moraine was deposited between 13.7 and 11.7 ka (Schmoll and others, 1972). The late-Wisconsin, pre-Elmendorf deposits are correlated with early-phase deposits of the Brooks Lake glaciation, and the advance that deposited the Elmendorf moraine is correlated with the Late Phase of the Brooks Lake glaciation (Table 5).

Lea (1989) correlated Okstukuk and Alegnagik moraines, originating from the Wood River Range, southwestern Alaska, with Kvichak and Iliamna stades of the Brooks Lake glaciation, respectively (Table 6). Moraine morphology of Aleknagik and Okstukuk moraines suggests a pre-Holocene age for both moraines (Lea, 1989). The absence of a thick loess cover, present on older deposits, precludes a pre-late-Wisconsin age assignment (Thompson and others, 1994b).

Only one glacial record, deposits of the north-central Alaska Range late-Wisconsin glaciation (McKinley Park), shows evidence of four late-Wisconsin advances: phase 1 (26-17 ka), phase 2 (15.0-14.1 ka), phase 3 (12.8-11.8 ka), and phase 4 (10.5-9.5 ka), based upon the present age control (TenBrink and Waythomas, 1985; Werner, 1995). In this case, phase 1 is correlated with the Kvichak stade, phase 2 with the Iliamna stade (see

eolian record below), and phases 3 and 4 with the Newhalen, Iliuk, and Ukak stades (Table 5).

Applying this subdivision to the Brooks Lake glaciation lumps early-late-Wisconsin Kvichak and Iliamna stades into an early phase, and the Newhalen, Iliuk, and Ukak stades into a late phase. The age estimate for the interval separating these phases from Alaskan glacial sequences suggests that the break between the early and late phases of the Brooks Lake glaciation occurred at approximately 13-14 ka (see below). The five recognized stades of the Brooks Lake glaciation exceeds any other late-Wisconsin glacial sequence in Alaska. Perhaps the threshold required to trigger an advance or retreat was significantly easier to cross for glaciers on the upper Alaska Peninsula, possibly a result of the relatively flat hypsometry of valleys occupied by glaciers, and also a result of warmer temperatures. Glaciers in interior Alaska occupied steeper valleys and were situated in a cold and dry environment. These factors made glaciers on the Alaska Peninsula more sensitive to climate change than interior glaciers.

Eolian Record. The Igushik Formation comprises a widespread blanket of late-Wisconsin eolian sand and silt (Lea, 1989; Lea and others, 1991). The thickness of the Igushik Formation varies regionally from 1-15 m. A 0.3-3.0-m-thick, massive to faintly laminated purplish-gray silt bed, termed the Tunuing silt, interrupts sand-sheet deposits and is associated with ice-wedge casts near the base of the Igushik Formation. Radiocarbon ages on sparsely distributed organic macrofossils within the silt bed suggest it was deposited between approximately 22-17 ka. Its deposition is believed to coincide with a slackening in eolian activity as a result of either ice pullback into lake basins or a shutdown in meltwater production. Similarly, the occurrence of ice-wedge casts within the Tunuing silt indicates that the decrease in eolian activity was accompanied by continuous permafrost,

and a thin winter snow cover. The bulk of the Igushik Formation was laid down by reinvigorated sand-sheet eolian deposition, following the deposition of the Tunuing silt. A later slackening of eolian activity is represented by a fine-grained zone deposited at 14.3 ka (Lea, 1989).

If ice pullback is the correct climatic interpretation for the Tunuing silt, I propose, as did Lea (1989), that it was deposited during the interstadial separating the Kvichak and Iliamna stades, and is correlative with glacial-lacustrine deposits (unit 1) at the west end of Iliamna Lake. The upper fine-grained zone dated at 14.3 ka appears to correlate with the major interstadial separating early and late phases of glacial advances in Alaska, and correlates with the interstadial separating the Iliamna and Newhalen stades.

Equilibrium-Line-Altitude Estimates

The position of the present-day snowline, determined from the lowest elevation of firn on 1:63,360-scale topographic maps and aerial photographs, is summarized by Detterman (1986) (Fig. 26). Equal snowline elevations are aligned northeast-southwest, parallel to the coast. Snowline is lowest, 900 masl, along the east side of the Alaska Peninsula, and rises westward by approximately 100 m over 20 km. Modern snowline rises northward a short distance from Naknek Lake to Kukaklek Lake, where it takes an approximately 50-km jog westward at the eastern tip of Naknek Lake (Detterman, 1986). The mean present-day ELA, an estimate of snowline, calculated for cirque glaciers occupying Mt. Griggs is 1490 ± 30 masl, and 1090 ± 150 masl calculated for the ice cap southeast of Naknek Lake (Table 6).

Late-Glacial Advances. The average ELA during the Iliuk stade was 840 ± 40 masl calculated using the THAR method for the type Iliuk-stade reconstructed glacier, and

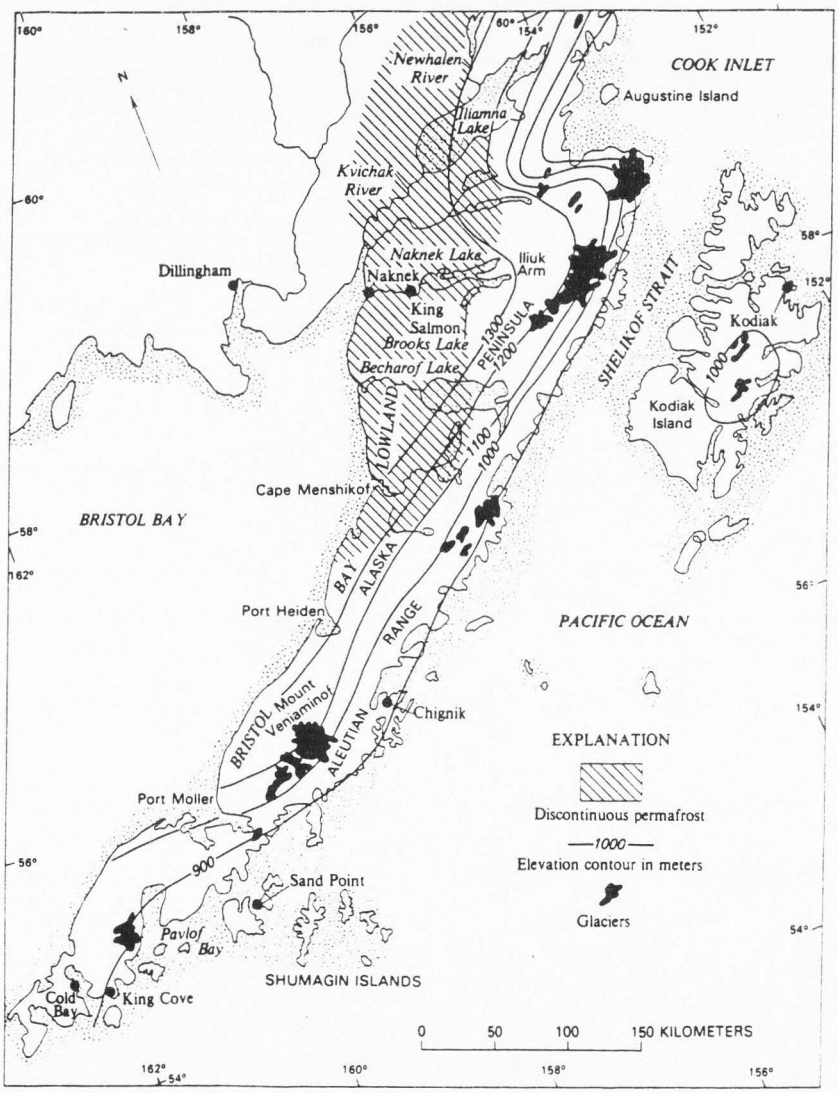

Figure 26. Modern snowline along the Alaska Peninsula (from Detterman, 1986).

TABLE 6. DATA USED FOR EQUILIBRIUM-LINE-ALTITUDE RECONSTRUCTIONS AND MODERN EQUILIBRIUM-LINE-ALTITUDE ESTIMATES. HEADWALL SITES ARE SHOWN IN FIGURE 6

Source	Location (Fig. 6)	Headwall (ft)	Toe (ft)	ELA (m)
Iliuk-stade reconstructed glacier at type locality				
Kukak Volcano	1	6400	170	799
Mt. Denison	2	6400	170	799
Snowy Mt.	3	7000	170	871
Knife Creek	4	6700	170	835
Mt. Mageik	5	7000	170	871
			Average:	**835**
			Stdev:	36
Lake Brooks reconstructed glacier				
Kukak Volcano	1	6400	150	795
Mt. Denison	2	6400	150	795
Snowy Mt.	3	7000	150	867
Knife Creek	4	6700	150	831
Mt. Mageik	5	7000	150	867
			Average:	**831**
			Stdev:	36
Iliuk-stade reconstructed glacier at Lake Grosvenor				
Kukak Volcano	1	6600	200	828
Mt. Denison	2	6400	200	804
Snowy Mt.	3	7000	200	876
			Average:	**836**
			Stdev:	37
Lake Colville reconstructed glacier at Lake Grosvenor				
Kukak Volcano	1	6600	175	824
Mt. Denison	2	6400	175	800
Snowy Mt.	3	7000	175	872
			Average:	**832**
			Stdev:	37
Modern glaciers				
Kukak Volcano	1	6600	1000	972
Mt. Denison	2	6400	1000	948
Snowy Mt.	3	7000	1200	1056
Knife Creek	4	6700	2300	1218
Mt. Mageik	5	7000	2400	1272
			Average:	**1093**
			Stdev:	146
Modern glaciers				
Mt. Griggs	6	7400	3200	1464
	6	6600	3900	1494
	6	6000	4500	1530
	6	7500	3200	1476
			Average:	**1491**
			Stdev:	29

840 ± 40 masl, calculated for the Iliuk-stade glacier that terminated at the west end of Lake Grosvenor (Table 6). The ELA, therefore, was lowered between 250 and 650 m below the present during the Iliuk stade. Likewise, average ELA for the Lake Brooks reconstructed glacier was 830 ± 40 masl, and 830 ± 40 masl for the Lake Colville reconstructed glacier.

Cirque-floor altitudes were also used to estimate paleo-ELA for glaciers that deposited Iliuk-stade moraines damming Murray, Kulik, and Battle lakes north of Naknek Lake (Fig. 3). These estimates range from approximately 900-950 masl, slightly higher than ELA for the Iliuk reconstructed glacier in the Naknek Lake valley, reflecting either: (1) cirque-floor altitudes that overestimate ELA relative to the THAR method (for example, Meierding, 1982) or (2) a minor northward rise in ELA, consistent with the present-day trend in snowline (Detterman, 1986).

Early-Late-Wisconsin Advances. Early-late-Wisconsin, full-glacial ELA cannot be determined accurately. The Kvichak-stade and Iliamna-stade glaciers were the western outlet extensions of the Cordilleran Ice Sheet; therefore, their source-area elevations are difficult to determine. The elevation of the highest late-Wisconsin lateral moraine deposited by the Naknek glacier provides a minimum estimate of approximately 670 masl for the ELA of the Naknek glacier (Mann and Peteet, 1994), suggesting that full-glacial ELA was no lower than 420-820 m below present. For comparison, late-Wisconsin ELA lowering was about 200-400 m in the western part of Alaska, in such places as the Kigluaik Mountains of northwestern Alaska (Kaufman and Hopkins, 1986) and the Ahklun Mountains of southwestern Alaska (Lea, 1984), and 450-600 m in eastern portions of Alaska (Péwé, 1975).

Discussion. The Naknek Lake basin is relatively flat over 100 km. Toes of the Iliuk (51 masl), Lake Brooks (45 masl), and Naknek moraines (45 masl) are at roughly

equal elevations. The valley's hypsometry suggests that once glaciers occupied the valley floor, only a minimal change in ELA was required to significantly advance or retreat the late-Wisconsin glaciers. The full-glacial ELA may, therefore, have been only a few tens of meters below the Iliuk-stade ELA, 250-650 lower than present and consistent with ELA lowering measured in other parts of Alaska. In addition, because ELA intersects a broad, flat valley, the glaciers there were ultrasensitive to climate change. This helps to explain the inconsistency in the number and spacing of late Wisconsin moraines in the Naknek Lake valley as compared to other valleys.

SUMMARY AND CONCLUSION

The five stades of the Brooks Lake glaciation comprise more studied events than any late-Wisconsin glacial record yet described in Alaska. The westernmost extension of the Cordilleran Ice Sheet overtopped a low topographic divide at the southern end of the Alaska Range, where it spilled into the Iliamna Lake valley and deposited the type Kvichak and Iliamna moraines. The type Kvichak moraine forms an extensive, hummocky, highly irregular landform, which dammed ancestral glacial Iliamna Lake. The type Iliamna moraine is a topographically lower, more subdued landform that presently encloses Iliamna Lake.

Mountains upvalley of Naknek Lake formed a topographic barrier that diverted the Cordilleran Ice Sheet, while supporting a confluent system of local-mountain glaciers that deposited the Naknek moraine. The moraine is the obvious limit of late-Wisconsin ice in the Naknek Lake valley located beyond the thick loess sequence that caps pre-late-Wisconsin moraines.

Morphologically, the Naknek moraine is similar to the type Kvichak moraine, but

based on slope angles and crest widths, it is also similar to younger Iliamna moraines. Flanking slope angles on the type Kvichak, type Iliamna, and Naknek moraines (about 11-15°) are similar, and imply that these landforms are similar in age, and that they are older than late glacial Newhalen, Iliuk, Ukak, and Lake Brooks moraines.

Bluff stratigraphy of two exposures in the Iliamna Lake valley provides temporal evidence for a two-fold, early-late-Wisconsin glacial advance; however, evidence for a two-fold, early-late-Wisconsin glacial advance is lacking in the Naknek Lake valley. Consequently, the Naknek moraine is deemed an undifferentiated early-late-Wisconsin deposit correlative to either: (1) the type Kvichak moraine, (2) the type Iliamna moraine, or (3) both.

Plant macrofossils underlying outwash associated with the type Kvichak moraine afford a new maximum-limiting age of 26,155 ± 285 ^{14}C yr BP on the moraine. This age agrees with a recently reported maximum-limiting age of 26,570 ± 320 ^{14}C yr BP for peat underlying outwash graded to the Naknek moraine (Mann and Peteet, 1994).

During the later part of the Brooks Lake glaciation, local-mountain valley glaciers advanced to deposit the type Newhalen, Iliuk, and Ukak moraines. Glaciers in the Lake Clark drainage deposited the type Newhalen moraine, whose morphology is extremely hummocky and irregular. The type Iliuk moraine forms a simple, arcuate ridge at the western edge of Iliuk Arm, whereas the type Ukak moraine represents the most minor readvance. Morphology of the type Ukak moraine is fresh, hummocky, and little modified.

Slope angles on the late-glacial moraines are steeper (about 18-20°) than slope angles on early-late-Wisconsin moraines, suggesting that late glacial advances were

separated from the early advances by a substantial length of time. The Lake Brooks moraine is believed to be correlative with the type Newhalen moraine based upon comparable slope angles, and position in the valley-moraine sequence. It is older than the type Iliuk moraine, but younger than early-late-Wisconsin moraines. Even though stratigraphic or geochronologic evidence fails to distinguish the Newhalen and Iliuk stades, Iliuk moraines are retained as morpho-stratigraphic features that separate subbasins of lakes from main lake basins.

Lethe volcaniclastics (>12,640 ± 100 ^{14}C yr BP), which overlie Iliuk drift and are overlain by and incorporated into Ukak drift, provide a minimum-limiting age on the Iliuk stade and a maximum age on the type Ukak moraine (Pinney and Begét, 1991a). Organic-rich silt dated at 10,200 ± 100 ^{14}C yr BP directly underlying Holocene Katolinat till affords a minimum-limiting age on the Ukak moraine (Pinney and Begét, 1991a).

Correlations between stades of the Brooks Lake glaciation and other late-Wisconsin glacial sequences in Alaska are impeded by a lack of absolute-age control. Where glacial sequences in Alaska are undivided, the glaciation is correlated with the Brooks Lake glaciation. Where other some Alaskan sequences have been subdivided into an early/main phase, and a late phase, the early/main phase is correlated with the Kvichak and Iliamna stades, and the late phase with the Newhalen, Iliuk, and Ukak stades. Correlation of the time break between early/main and late phases suggests that the interstadial separating the Iliamna and Newhalen stades took place at approximately 13-14 ka. Only one glacial sequence, that ascribed to the McKinley Park glaciation (MP) in the north-central Alaska Range, has been divided into four phases based upon the current age control. Tentative correlations assign the Kvichak stade to MP phase 1, the Iliamna stade to MP phase 2, and

the Newhalen, Iliuk, and Ukak stades to MP phases 3 and 4.

Lea (1989) has documented the distribution, stratigraphy, and age of the Igushik Formation. The Tunuing silt (about 22-17 ka) represents a slackening in eolian activity thought to record ice pullback into lake basins. This interval is thought to be correlative with the interstadial separating the Kvichak and Iliamna stades. The uppermost fine-grained zone in the Igushik Formation, dated at 14.3 ka, may correspond to the interstadial separating the Iliamna and Newhalen stades.

From a global perspective, the Alaska Peninsula glacial record is correlative with marine oxygen-isotope stage 2. Around the globe, stage 2 was an interval of pronounced and variable climate change. African lakes were dry during this time, whereas lakes in the southwestern United States were at a maximum. The Laurentide Ice Sheet, which was high enough to divert the jet stream southward, was centered over Canada. All mountainous areas of the globe record evidence for glacial advances during stage 2 (for example, the western U.S., New Zealand, Europe, and South America). The Brooks Lake glaciation, in southwestern Alaska, not only represents regional climate change in Alaska during this time, but also reflects a global climate cooling associated with oxygen-isotope stage 2.

Recently, there has been mounting evidence for abrupt and extreme climate changes during the late Pleistocene [for example, the Greenland Ice Core (Dansgaard and others, 1993; Grootes and others, 1993)], with several significant changes within the late Wisconsin. Increasing evidence suggests that these rapid climate changes are felt globally (for example, the Younger Dryas cold climate oscillation).

Dansgaard-Oeschger cycles (high frequency climate fluctuations) were identified in the Greenland Ice Core, whereas *Heinrich events*, which occur at the close and typically the

coldest portion of a Dansgaard-Oeschger cycle, and are followed by a warming, were identified in marine cores from the North Atlantic Ocean.

Heinrich event 2, dated at 21 ka, appears correlative with the Tunuing silt within the Igushik Formation; therefore, it is correlative with the interstadial separating the Kvichak and Iliamna stades. Heinrich event 1 (14.3 ka) is correlative with the Alaska-wide interstadial separating early and late phases of a glaciation, and is thereby correlative with the interstadial separating the Iliamna and Newhalen stades. Heinrich event 0 is dated at 10.5 ka, and correlative with the Younger Dryas, and possibly the Ukak stade as Pinney and Begét (1991a) suggested; however, additional age control is essential to document such a correlation.

Because high latitudes are affected the most by global climate changes, one would expect high-latitude mountain glaciers to also respond to dramatic global climate changes [for example, Broecker (1994) challenged glacial geologists to identify *Dansgaard-Oeschger cycles* , thought to be global events, in high-latitude mountain-glacier sequences]. The Alaska Peninsula glacial sequence appears to be one such high-frequency, high-resolution climate record.

CHAPTER 3
EMERGENT POSTGLACIAL SHORELINES OF NAKNEK AND ILIAMNA LAKES, SOUTHWESTERN ALASKA

ABSTRACT

Following late-Wisconsin deglaciation of the Iliamna and Naknek lake basins, lake levels lowered, creating a flight of beach ridges and wave-cut terraces rimming the lakes. A horizontal, or nearly horizontal, terrace at ~40 m above Iliamna Lake indicates that the terrace is not tilted over 70 km northeast to southwest as a result of glacial-isostatic rebound or regional tectonism. Likewise, the common elevation of a 15-m terrace at five sites across 50 km, and a 30-m terrace identified at three sites across 45 km around Naknek Lake suggests that these shorelines are also horizontal. The most prominent terraces above both lakes lie about halfway between the highest terrace and the present-day lake level (24 m above Iliamna Lake and 15 m above Naknek Lake). If these terraces are correlative, then this indicates some climate control on lake-level fluctuations. On the other hand, Iliamna Lake shows six terraces and Naknek Lake only three, suggesting that other factors, including different histories of outlet erosion, played a role in lake-level changes at the two lakes.

The ages of the 24-m terrace and higher terraces at Iliamna Lake, and all three terraces at Naknek Lake are constrained to latest-Wisconsin/early-Holocene time, a time of significant climate transition. The ~40-m terrace at Iliamna Lake was probably cut during the Newhalen stade (~14 ka). The lower ~30-m terrace, and thereby higher ones as well, is older than a pink-orange tephra with a correlated age of 12.6 ka, and the 24-m terrace and

higher ones are older than 8.3 ka. At Naknek Lake all three terraces are older than 7.4 ka, and younger than the Iliuk stade (~13 ka).

INTRODUCTION

Closed basins develop from a limited number of geologic processes including glacial erosion. Lakes that fill these basins fluctuate in response to a suite of causes: climate change, downcutting of thresholds, tectonism, diversion of inflows, or glacial-isostatic rebound. Shorelines preserved on the landscape typically record the most recent fluctuations of a lake.

Lakes along the upper Alaska Peninsula, southwestern Alaska, occupy glacial troughs sculpted by ice flowing from east to west, and are dammed by terminal moraines of late-Wisconsin age (Fig. 27) (Chapter 2). Iliamna Lake, which is 125 km long by 30 km wide, is the largest lake in the United States outside of the Great Lakes, and during its highest stand (59 masl) was about 20% larger (Fig. 28) (Detterman and Reed, 1973). Naknek Lake is approximately 60 km long by 15 km wide, and attained a maximum length and width of roughly 65-70 km by 20 km at its highest level (40 masl).

Following deglaciation of the lake basins, lake levels fluctuated, creating a flight of wave-cut terraces and beach ridges rimming Iliamna and Naknek lakes. Terraces are especially well preserved, and are laterally traceable for tens of kilometers in places (Figs. 29 and 30). These features record lake-level stabilization for extended intervals followed by relatively rapid lowering. Some terraces might have formed following a lake-level rise. No stratigraphic or geomorphic evidence such as submerged beaches was found, however, to evaluate this possibility.

If lake-level fluctuations of Iliamna and Naknek lakes were climatically induced,

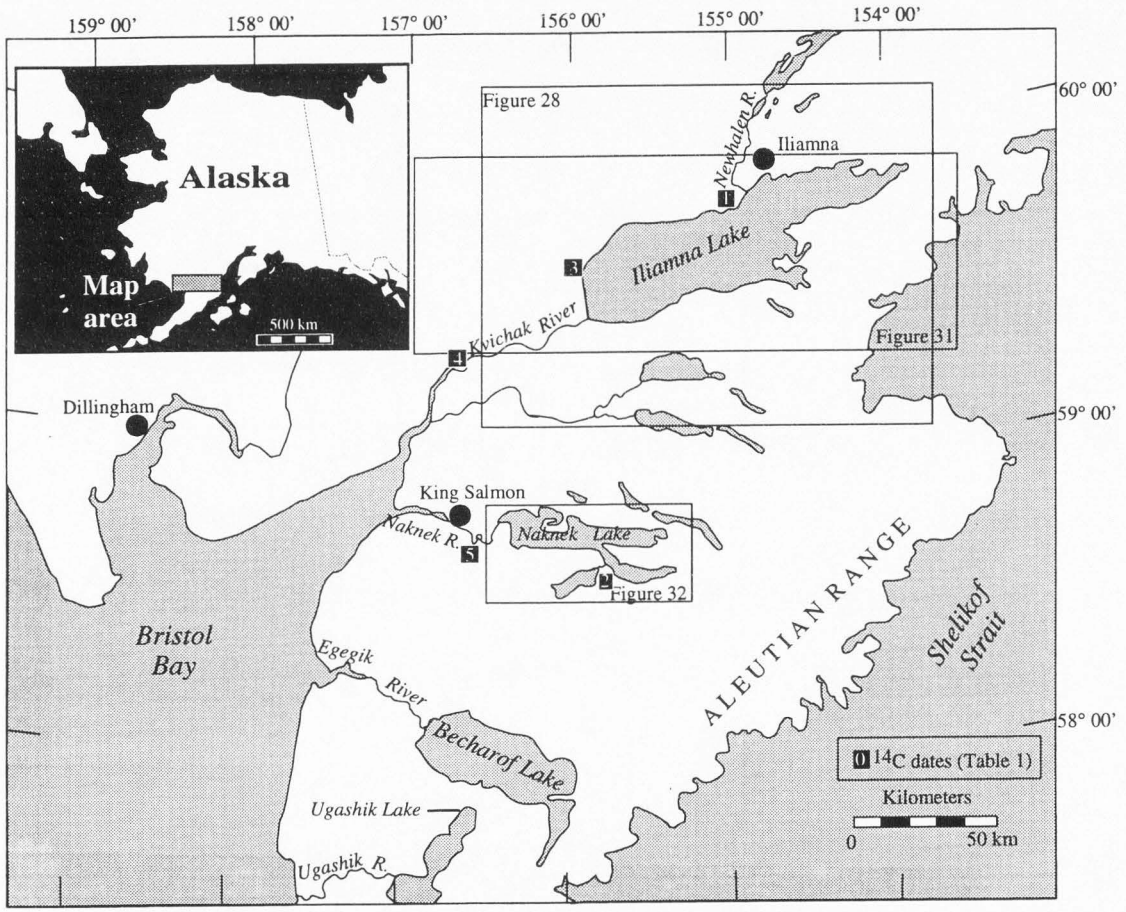

Figure 27. Upper Alaska Peninsula showing sites referred to in Table 7 and locations of Figures 28, 31, and 32.

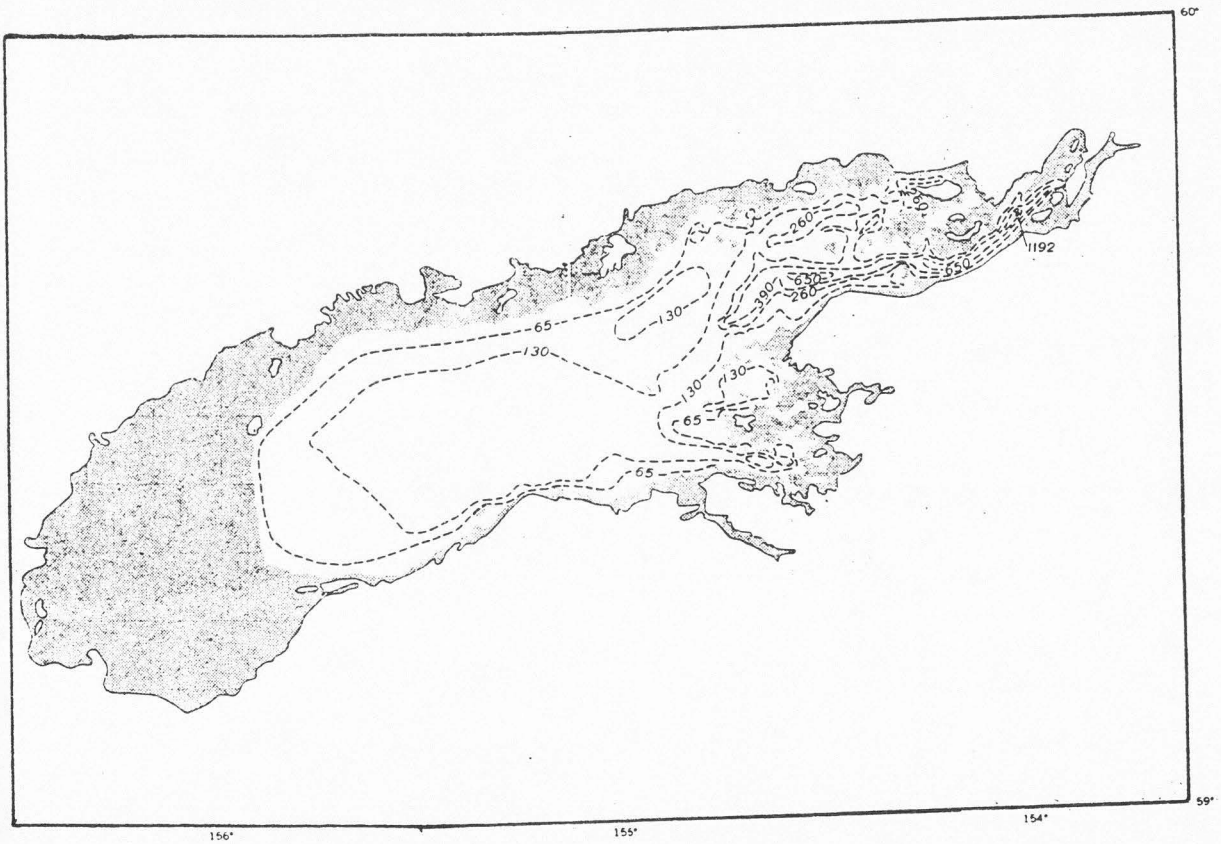

Figure 28. Area covered at maximum stand (~45 m above present-day lake level; shaded) and bathymetry (contours in feet) of Iliamna Lake (from Detterman and Reed, 1973).

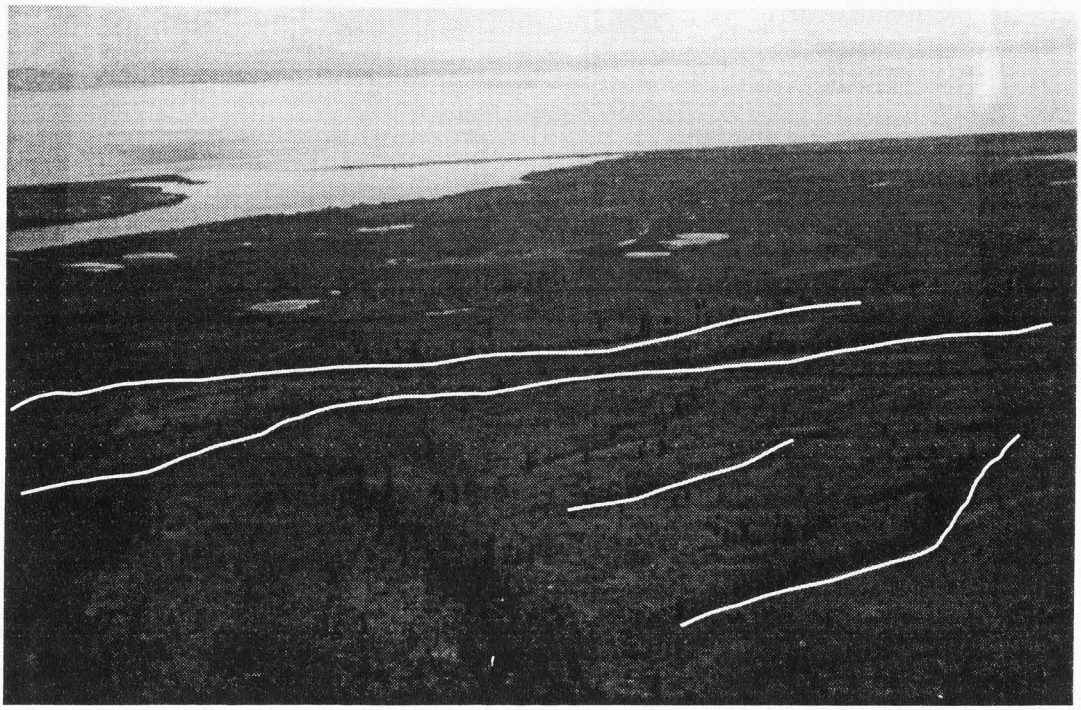

Figure 29. Lake terraces preserved on the west side of the Newhalen River, north of Iliamna Lake. Shoreline angles highlighted by white line.

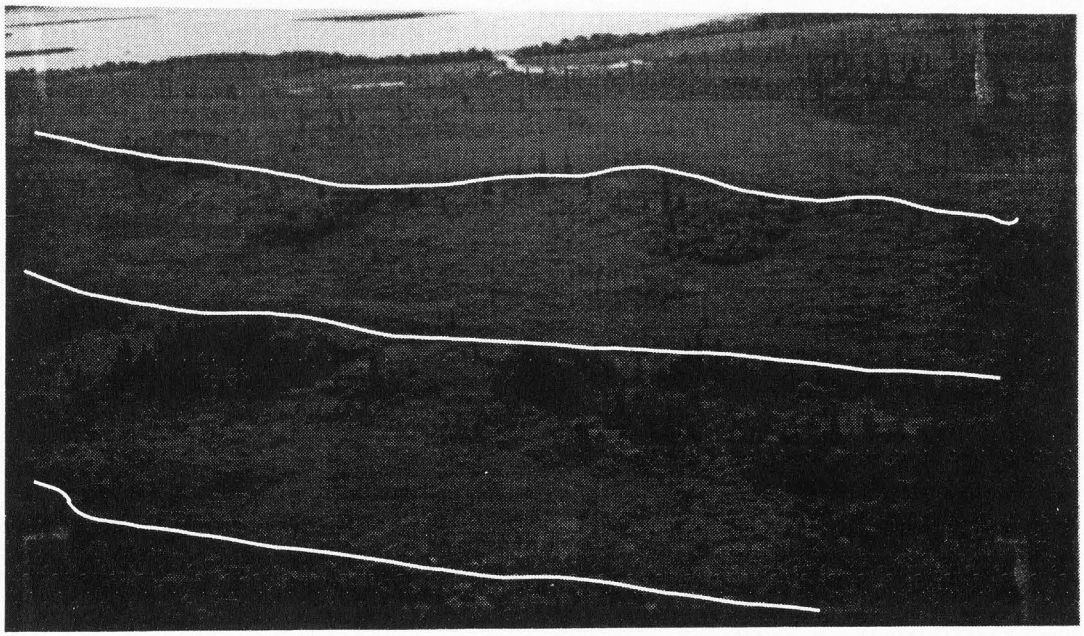

Figure 30. Lake terraces preserved at the western end of Naknek Lake, north of the Naknek River. Shoreline angles highlighted by white line.

then both should have behaved synchronously, with perhaps similar amplitudes of change. The construction of shorelines would coincide temporally at the two lakes. Likewise, if climate stabilized for an extended duration, then terraces formed during that interval would be broader and better defined than terraces formed during shorter lake-level stabilization. If Iliamna and Naknek lakes lowered in response to downcutting their moraine dams, then their lake-level fluctuations would not be expected to be in phase. Although this study may not resolve whether or not lake levels fluctuated in response to climate or outlet incision, it will provide a reference for future studies aimed at evaluating such changes along the Alaska Peninsula.

In either case, the abandoned shorelines provide an invaluable datum that can be used to assess the magnitude and direction of postglacial basin tilting. Such tilting may have been in response to tectonic forces proximal to the Aleutian trench, or to postglacial isostatic rebound proximal to ice loading from the east where ice was thickest. Because glaciers flowed westward into the lake basins (Chapter 2), glacial-isostatic depression would have been oriented east to west; therefore, tilting in this direction should be most pronounced.

The objectives of this research are to: (1) measure the height of terraces at Iliamna and Naknek lakes, (2) determine the amount and direction that shorelines at both lakes have been warped or tilted, and (3) assess the possible causes and ages of lake-level fluctuations and associated shorelines. This study improves previous work in the area, which primarily documented the existence of shorelines and established their elevations at one to two sites around the lakes.

PREVIOUS WORK

Iliamna Lake

Lake level at Iliamna Lake was apparently highest following deglaciation of the lake basin. Detterman and Reed (1973) identified a series of terraces above present-day lake level [14 masl (47 ft)]. Four major terrace levels are most prominent, and are best preserved on the west side of the Newhalen River near its mouth (Fig. 29; Fig. 31, site 1): 12 m, 24 m, 30 m, and 39 m, whereas less extensive terraces are developed at 17 m and 36 m (values are heights above present-day lake level), and are considered by Detterman and Reed (1973) accurate to within ± 1 m. The 12 m and 24 m terraces are the broadest and most continuous, typically 300-900 m wide. Terraces generally slope 5° lakeward, and are terminated by a wave-cut scarp behind a lower terrace. Iliamna Lake attained a maximum height of 45 m above present-day lake level (Fig. 28). The highest shoreline is distinguishable on aerial photographs by its light vegetation cover, presumably a result of substrate variations.

Detterman and Reed (1973) suggested that Iliamna Lake terraces may be tilted down to the southwest due to isostatic adjustment following deglaciation of the basin. They presented no data, however, to assess this assertion. Nor did they indicate the exact locations or number of measurements taken on terraces.

Naknek Lake

Lake Brooks is 9 m above Naknek Lake, which is 10 masl. The two lakes are presently connected by the 2-km-long Brooks River (Fig. 32), whereas previously, they were joined. At its highest stand of 30 m above present-day lake level, Naknek Lake was connected with Lake Brooks. Once the level dropped below 9 m above present-day lake

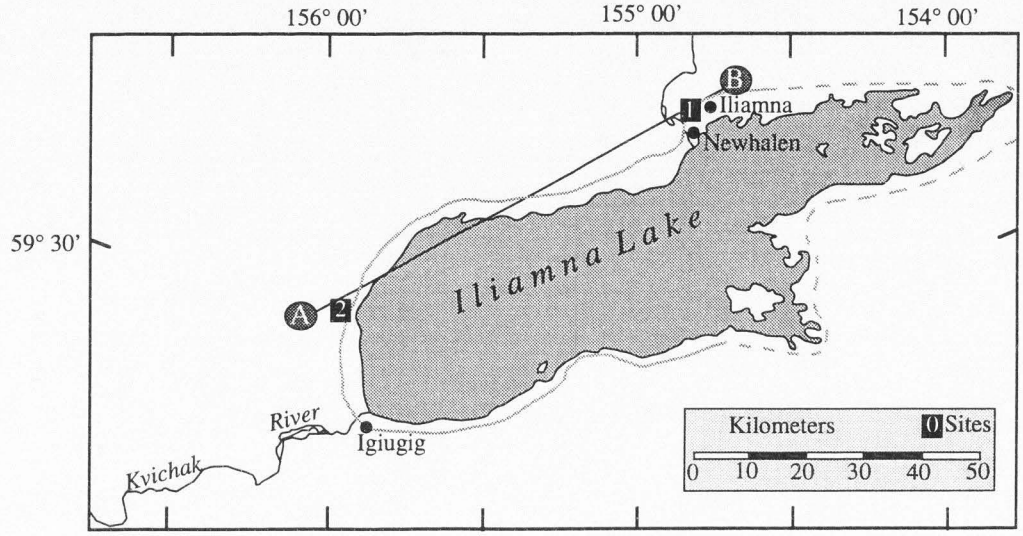

Figure 31. Iliamna Lake showing location of shoreline-measurement sites, and transect A-B (Fig. 34). The ~40 m terrace is sketched in gray.

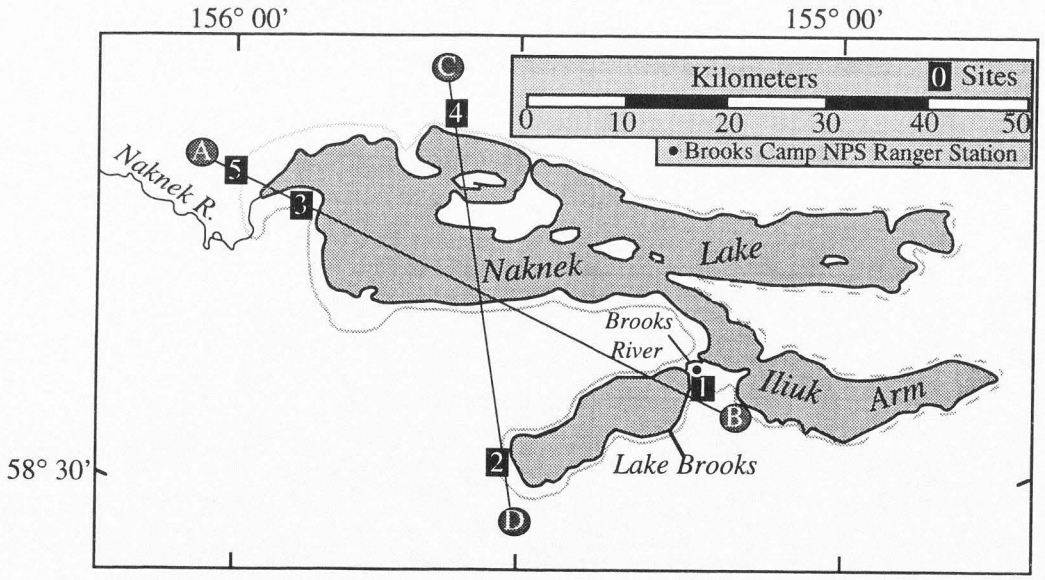

Figure 32. Naknek Lake showing location of shoreline-measurement sites, and transects A-B and C-D (Fig. 35). The highest (~30) m terrace is sketched in gray.

level, the two lakes became separated. Archaeological sites on the south side of Brooks River, between Lake Brooks and Iliuk Arm, indicate that the lakes must have been separated by the time of human occupation. Charcoal collected from beach deposits and dated at 7360 ± 250 ^{14}C yr BP affords a minimum-limiting age on the separation of the two lakes, and is the oldest age that constrains the lowering of the lake below this level (Table 7) (Dumond, 1981).

TABLE 7. RADIOCARBON AGES BEARING ON THE AGES OF ILIAMNA AND NAKNEK LAKE TERRACES

Date (yr BP)	Lab ID	Material	Stratigraphic position	Location (Fig. 27)	Reference
8250 ± 350	W-1479	Organic matter	24 m terrace; 3.4 m below ground surface	1	Detterman and others, 1965
7360 ± 250	I-1160	Charcoal	On surface, 500 m east of Lake Brooks	2	Dumond, 1981
1860 ± 50	AA-15096	Plant macrofossils	Exposure at northwest corner of Iliamna Lake; 28.5 m above lake level	3	This paper
26,155 ± 285	AA-15092	Plant macrofossils	Underlies outwash associated with the type Kvichak moraine	4	This paper
26,570 ± 320	Beta-39578	Peat	Underlies outwash graded to the Naknek moraine	5	Mann and Peteet, 1994

Riehle and Detterman (1993) used a hand level to measure three evenly spaced lake terraces at one site (58° 44' N, 156° 06' W) up to 30 m above present-day Naknek Lake level: 5 m, 15 m, and 30 m. They did not anticipate exact correspondence of terrace levels between Naknek Lake and other lakes along the Alaska Peninsula due to regional differences in tectonic and isostatic uplift, and local differences in the rate and timing of outlet incision. Because they measured terraces at only one location, their data are insufficient to address basin tilting and warping.

METHODS

Lake terraces were delineated on 1:63,360-scale aerial photographs, and accessible sites were located. In the field, spot elevations were measured at the back of lake terraces using a digital altimeter manufactured by Lietz and precise to ± 0.1 m. Measurements were tied to lake-level elevation, accounting for barometric changes throughout the measurement interval, and corrected elevations were calculated by linear interpolation between calibration points.

The accuracy of measurements are a function of: (1) the number of readings taken on any given terrace, (2) the rate of change of barometric pressure, and (3) the length of time between measurements and calibrations. On 14 out of 17 terraces measured, repeat readings on each terrace have a standard deviation of 0 or 1 m (Tables 8 and 9). On the remaining three terraces, the standard deviation is 2-3 m. The standard deviation apparently increases with the number of days over which readings were taken. Note that eight repeat readings taken at site 1 on terrace NL2 over two days range by 5 m, and only five are within ±1 m, although the standard deviation of these measurements is 2 m. There

TABLE 8. TERRACE ELEVATIONS MEASURED ABOVE ILIAMNA LAKE

Location (Fig. 31)	Iliamna Lake terraces (meters above lake level)				
Site 1	*IL1 (1)*	*IL2 (1)*			*IL3 (1)*
	12	27			38
	12	27			38
	12 ± 0	**27 ± 0**			41
					39 ± 2
Site 2	*IL4 (1)*	*IL5 (1)*	*IL6 (1)*	*IL7 (1)*	*IL8 (1)*
	8	24	31	35	40
	8	24	31	35	42
	8 ± 0	25	**31 ± 0**	**35 ± 0**	**41 ± 1**
		24 ± 1			

was no attempt to assign each terrace elevation an error estimate because of the varying factors that influence their accuracy. Instead, an overall error estimate of ±1 m for all terraces is used. This estimate is consistent with the standard deviation of repeated readings in 14 out of 17 cases.

Shoreline elevations above Iliamna Lake were measured at two localities: (1) those accessible by dirt roads on the east side of the Newhalen River near the towns of Iliamna and Newhalen (Fig. 31, site 1) and (2) at the northwest corner of Iliamna Lake (Fig. 31, site 2), where a topographic profile was also measured. Shorelines above Naknek Lake were measured at five sites: (1) the eastern end of Lake Brooks (Fig. 32, site 1), (2) the western end of Lake Brooks (Fig. 32, site 2), (3) the north side of Naknek Lake (Fig. 32, site 3), (4) the west-central end of Naknek Lake (Fig. 32, site 4), and (5) the north side of

TABLE 9. TERRACE ELEVATIONS MEASURED ABOVE NAKNEK LAKE

Location (Fig. 32)	Naknek Lake terraces (meters above lake level)		
Site 1	*NL1 (1)*	*NL2 (2)*	*NL3 (2)*
	5	11	33
	6	12	33
	6± 1	12	28
		14	27
		16	**30 ± 3**
		14	
		14	
		15	
		14 ± 2	
Site 2		*NL4 (1)*	
		16	
		14	
		15 ± 1	
Site 3		*NL5 (1)*	*NL6 (1)*
		14	29
		14	29
		14 ± 0	**29 ± 0**
Site 4		*NL7 (1)*	*NL8 (1)*
		15	31
		15	31
		15 ± 0	**31 ± 0**
Site 5		*NL9 (1)*	
		16	
		15	
		15	
		15 ± 1	

the Naknek River (Fig. 32, site 5). Sites 2, 3, and 4 were accessed by boat; site 1 by foot from Brooks Camp National Park Service Ranger Station, and site 5 by vehicle along the dirt road from King Salmon to the head of the Naknek River.

An exposure at the northwest corner of Iliamna Lake provides geochronologic control on lake-level fluctuations (Fig. 31, site 2; Chapter 2). Elevations within the section were measured by locating vertical distances (eye-heights) against the bluff face using a hand-held level, and are probably accurate to within ±10%.

RESULTS AND DISCUSSION

Physiography of Terraces

Iliamna Lake. Three prominent terraces are distinguishable around the villages of Iliamna and Newhalen, designated here as terraces IL1, IL2, and IL3 (Fig. 31, site 1; Table 8). The lowest terrace (IL1) is 12 m above the lake, the second at 27 m (IL2), and the highest at 39 m (IL3). Five terraces are present at the northwest corner of Iliamna Lake at elevations of 8 m (IL4), 24 m (IL5), 31 m (IL6), 35 m (IL 7), and 41 m (IL8) above Iliamna Lake (Fig. 31, site 2; Table 8). Of the eight measured terraces, six overlap with Detterman and Reed's (1973) terrace elevations, and two are at significantly different elevations (Table 8). The elevation of the IL3 and IL8 terraces at site 1 and site 2, respectively, overlap at about 40 m. Terrace IL5 (site 2), at 24 m, is approximately 120 m wide, and forms the broadest terrace above Iliamna Lake, whereas an 8 m terrace (IL4), recognized at site 2, is the second widest (75 m) terrace (Fig. 33).

Naknek Lake. Three distinct terrace levels are present above Naknek Lake: 6 m, 15 m, and 31 m, and terrace elevations overlap with those reported by Riehle and Detterman (1993) (Table 9). Elevations of the highest ~30-m terrace measured at three sites

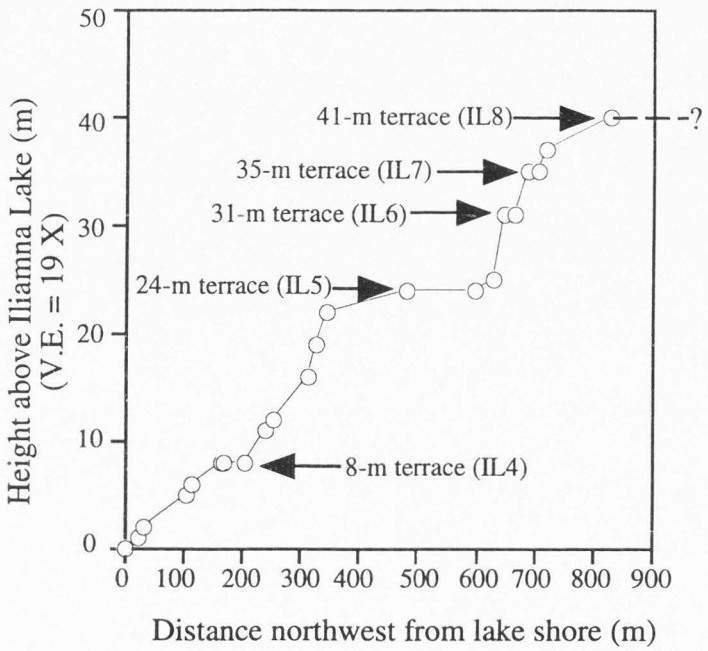

Figure 33. Topographic profile of terraces above Iliamna Lake at site 2 (Fig. 31). Uncertainty in measurements is contained within the plot symbol.

are indistinguishable from one another given the 1-m accuracy. The lowest terrace at 6 m (NL1) (Table 9) was only found at the western end of Iliuk Arm (Fig. 32, site 1). At all sites, a 14-15 m terrace was identified (Table 9). The greater width of this terrace, observable on aerial photographs, coupled with its widespread distribution demonstrates that it is the most prominent of the three terraces.

Correlations

Iliamna Lake. There are two different interpretations to the Iliamna Lake data set. The first interpretation (*horizontal interpretation*) suggests that the 39-m terrace at site 1 is correlative with the 41-m terrace at site 2, and the 27-m terrace at site 1 with the 24-m terrace at site 2 (see below), suggesting that they are horizontal. The remaining four

terraces have no correlatives. An alternative interpretation (*tilted interpretation*) correlates terraces at different elevations from site 1 to site 2, and implies that they are tilted northeast to southwest by approximately 3-4 m.

Horizontal Interpretation. The elevations of terraces IL3 and IL8 are indistinguishable, suggesting that the terrace is horizontal over 70 km northeast-southwest, or tilted by less than the 1-m accuracy (Fig. 34). Implicit in this conclusion is that lower,

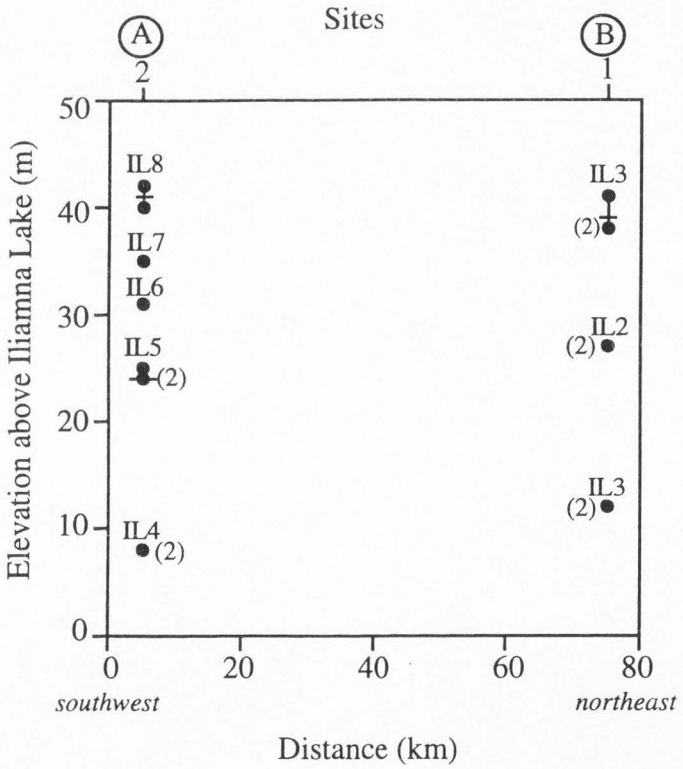

Figure 34. Iliamna Lake terraces measured at sites 1 and 2 along transect A-B (Fig. 31). Elevation of the ~40 m terrace overlaps at two sites spaced 70 km apart in a northeast to southwest direction. Circles represent individual readings; horizontal lines are averages of repeat readings on a terrace (where horizontal lines are absent, circle represents the average of repeat readings on that terrace); vertical lines span range of readings on a terrace; number in parentheses indicates number of overlapping readings at a particular elevation.

younger terraces, including the newly recognized 8 m terrace at site 2, are horizontal as well.

At site 1 on the east side of the Newhalen River, I correlate Detterman and Reed's (1973) 12-m terrace with terrace IL1; however, their 24-m and 30-m terraces were not identified here. The apparent absence of these two terraces can be explained in the context of the 27-m (IL2) terrace. I found only a single terrace between 12 m and 39 m at site 1. Its elevation at 27 m falls halfway between the 24- and 30-m terraces of Detterman and Reed (1973), implying that one of the two terraces is missing. While measuring this terrace, the barometric pressure fluctuated extremely, with apparent elevation changing in place by up to 12 m in approximately 10 minutes. The two readings of 27 m (Table 8) were made after barometric pressure stabilized, and the paucity of tie-ins to lake level during this interval hampered accurate interpolation of the altimeter readings. The 27-m measurement is probably associated with a broader error than is indicated by the standard deviation alone, and should probably have measured 24 m, a supposition supported by the breadth of the terrace. Therefore, the 30-m terrace has presumably been eroded away by eastward migration of the Newhalen River. Detterman and Reed (1973) used a helicopter to access the west side of the river, where a more complete suite of terraces is preserved (Fig. 29).

Tilted Interpretation. The alternative explanation that the terraces are tilted essentially hinges on the true elevation of the poorly constrained 27-m terrace. If 27 m is indeed the true elevation of the terrace at site 1, and if it is correlative with the 24-m terrace at site 2, then this implies that the terrace is tilted northeast to southwest by about 3 m. In turn, the 39-m terrace at site 1 may be correlative with the 35-m terrace at site 2, suggesting that this terrace is tilted by about 4 m. Likewise, the 12-m terrace at site 1 may correlate

with the 8-m terrace at site 2, implying that it too is tilted by about 4 m. And finally, the 41-m terrace at site 2 may correspond to the 45-m shoreline identified by Detterman and Reed (1973). Overall, this interpretation suggests about 4 m of tilting over 70 km for all terraces.

Naknek Lake. Altimeter readings of terrace elevations around Naknek Lake are highly precise because of barometric stability and frequent repeat readings. Correlation of terraces NL2 (14 m), NL4 (15 m), NL5 (15 m), NL7 (15 m), and NL9 (15 m), which average 15 m, suggests that the terrace is not tilted in a north-south direction over 35 km, nor in an east-west direction over nearly 50 km (Fig. 35). Likewise, correlation of the higher terraces NL3 (30 m), NL6 (29 m), and NL8 (31 m), which average 30 m, imply that the shoreline is not tilted in a northwest-southeast direction over 40 km, nor in an east-west direction over 45 km (Fig. 35). The horizontal form of terraces at Naknek Lake lends support to the horizontal interpretation of Iliamna Lake terraces; however, the possibility that the latter are tilted by ~4 m cannot be excluded given the data set at hand.

Climatic Implications

The prominent 24-m and 15-m terraces both lie about halfway between the highest terrace and present-day lake level at Iliamna and Naknek lakes, respectively. Alone, each terrace simply implies that there was sufficient water to fill the basin to its threshold causing prolonged stabilization at the outlet that enabled a prominent terrace to form. However, because both lakes have a prominent terrace that lies halfway between the highest terrace and present-day lake level, they may be correlative. This indicates a climate control; that is, climate stabilized for an extended duration allowing broader and better defined terraces to form. This conclusion is not unreasonable given the known dramatic climate changes that

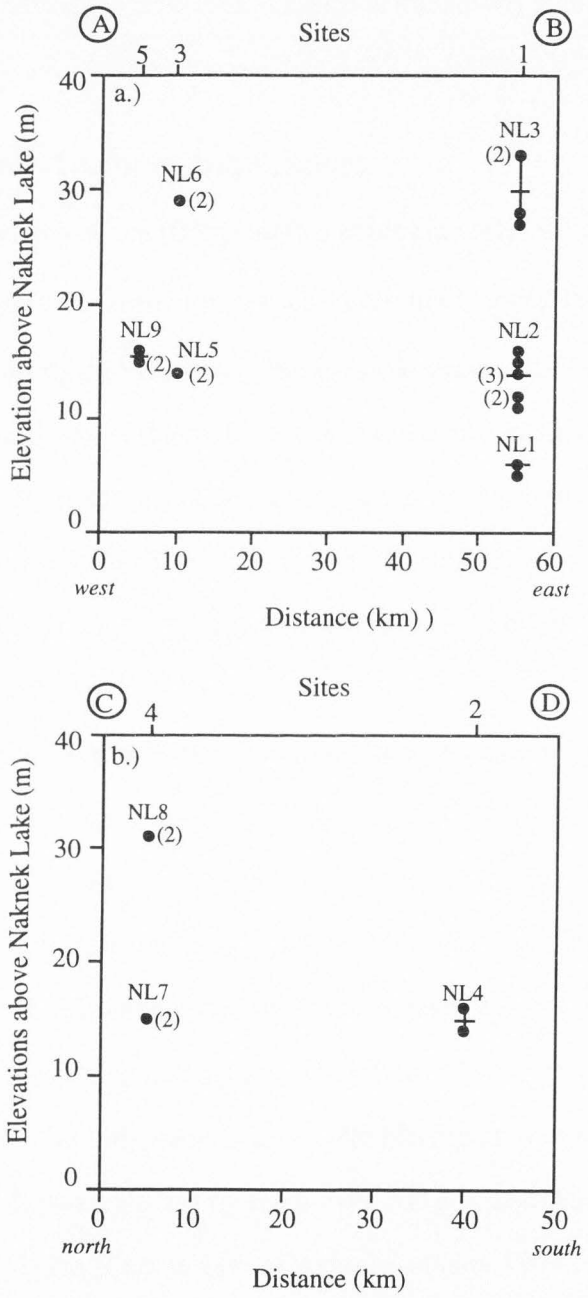

Figure 35. Terraces measured above Naknek Lake at sites 1-5 along transects A-B and C-D (Fig. 32). Elevations measured in both (a) east-west (transect A-B; Fig. 32) and (b) north-south (transect C-D; Fig. 32) directions. Symbols same as for Figure 34.

took place during the period (~Pleistocene-Holocene transition) recorded by the terraces (see below).

Glacial-Isostatic and Tectonic Implications

Because the density of ice (0.9 g/cm^3) is approximately one third the density of the earth's mantle (~3.3 g/cm^3), depression caused by ice loading can be estimated as one third the ice thickness, assuming equilibrium conditions (Andrews, 1975; Dawson, 1992). Ice that filled the central portions of the Iliamna and Naknek lake basins was approximately 600 m thick (Mann and Peteet, 1994); however, both basins are now occupied by water, and this mass causes present-day isostatic loading. Therefore, ice should have depressed the central part of the basins by ~200 m, but because water now occupies the basins, expected rebound should only be ~190 m.

The difference in ice load between the eastern and western ends of each basin leads to postglacial basin tilting. Ice at the eastern ends of Iliamna and Naknek lake basins was approximately 900 m thick, and 300 m thick at the western ends (Mann and Peteet, 1994). Therefore, the expected postglacial tilting should have been about 200 m over 80 km. The tilt between sites 1 and 2 at Iliamna Lake should have been about 130 m, and about 100 m between sites 1 and 5 at Naknek Lake (Figs. 31 and 32). These values are somewhat higher, but consistent with tilting measured at Lake Michigan. For example, Glenwood shorelines at Lake Michigan are tilted by 60 m over 300 km, and Algonquin shorelines are tilted by 100 m over 170 km [Larsen 1987; Clark and others, 1994 (originally from Taylor (1990)].

Clearly, data of the present study do not display this 100-130 m of anticipated tilting. At most, 4 m of tilting is recognized at Iliamna Lake. The lack of tilting in both

basins suggests that glacial-isostatic rebound was complete before the highest terraces were cut. More specifically, the lack of tilting in these basins might be explained by four ways: (1) *Restrained rebound* (elastic isostatic recovery that occurred while the area was still glaciated, but under a diminishing ice load) that allowed the basin to rebound before shorelines were cut. (2) Isostatic recovery was extremely rapid, perhaps taking place during the restrained rebound phase. (3) Ice advances to the western ends of the lake basins were too rapid to establish full isostatic depression. Finally, (4) the recovery was more horizontal than expected.

The horizontal, or nearly horizontal, terraces also indicate limited tectonic effects in the region, which is surprising given the basins' proximity to the active Aleutian trench.

On the other hand, Kaufman and others (1994) found last interglacial deposits (about 125 ka) at ~6 masl near South Naknek village located near the mouth of the Naknek River, suggesting limited tectonic effect during the late Quaternary.

Geochronology

The ages of terraces surrounding Iliamna and Naknek lakes are well constrained by ^{14}C ages, stratigraphic relationships, and tephra (Fig. 36). This chronology restricts the formation of most terraces to latest Wisconsin and early Holocene time.

Iliamna Lake. Chronologic data for the 24-m terrace and higher terraces demonstrates that they formed sometime between late-Wisconsin time and early-Holocene time. Presented here is additional chronologic control that more tightly constrains the age of the terraces within this interval. Because drift of the Iliamna stade is notched by the 39-m terrace, this shoreline and lower shorelines are of post-Iliamna age. Based on a new ^{14}C age on peat below late-Wisconsin outwash on the Kvichak River (Chapter 2), the terraces

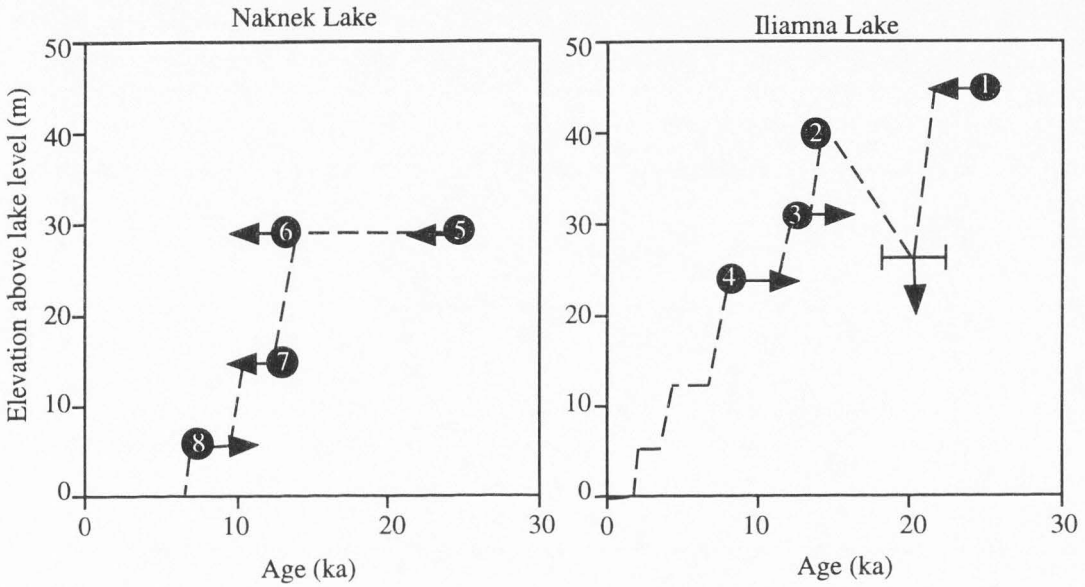

Figure 36. Hydrograph summarizing the elevation and ages of terraces at Iliamna and Naknek lakes. Left-pointing arrows indicate maximum ages; right-pointing arrows indicate minimum ages; error bar and down-pointing arrow indicate lake-level fall during the Iliamna stade (Chapter 1). Geochronological control as follows: (1) pre-glacial organics (Chapter 1), (2) correlated age of Newhalen stade, (3) correlated age of Lethe tephra, (4) organic matter above 24-m terrace, (5) pre-glacial organics, (6) Iliuk stade, (7) Iliuk stade, and (8) charcoal from 6-m terrace. Refer to text for a further discussion of geochronological control. The 24-m (4) and 15-m (7) terraces at Iliamna and Naknek lakes, respectively are thought to be correlative based upon their prominent character, and their position halfway between the highest terrace and present-day lake level.

are younger than 26,155 ± 285 ^{14}C yr BP (Table 7). Organic matter collected 3.4 m below the surface of an exposure formed on top of the 24-m terrace affords a minimum-limiting age of 8250 ± 350 ^{14}C yr BP on this terrace, and thereby, the higher terraces (Table 7) (Detterman and others, 1965).

Based upon aerial-photograph interpretation, it appears that an outwash plain of the Newhalen-stade glacier is graded to a hanging delta 4.5 km northeast of the village of Iliamna. An ancestral drainage, traceable on 1:63,360-scale aerial photographs, flowed westward along the terminal margin of the Newhalen glacier, then turned southward, approximately 0.5 km east of the Newhalen River and drained into Iliamna Lake. The delta is graded to the 39 m terrace (IL3); thus, it dates this terrace to the Newhalen stade, which, based on arguments presented in Chapter 2, is younger than about 14 ka.

An exposure at the northwest corner of Iliamna Lake (Fig. 31, site 2; Fig. 37) affords geochronologic control that further constrains the timing of lake-level fluctuations. At ~27.3 m above beach level is the upper contact of a 2-m-thick massive diamicton interpreted as till deposited during the advance of the Iliamna-stade glacier (Chapter 2). The till is underlain by glacial-lacustrine sediments, beach gravel, and glacial-fluvial sediments, and overlain by 10 cm of massive sand, a pink-orange tephra (1-3 cm thick) that is correlated with the Lethe tephra and is older than 12.6 ka (Chapter 4). Massive sand (~1 m), a buried Holocene soil (about 10 cm thick) containing plant macrofossils dated at 1860 ± 50 ^{14}C yr BP (Table 7), and approximately 6 m of cross-stratified sand that forms a bluff-head dune overlie the tephra.

The soil found at approximately 28.5 m requires that the lake was below this level by 1860 ± 50 ^{14}C yr BP. To use the tephra at approximately 27.5 to constrain the terrace

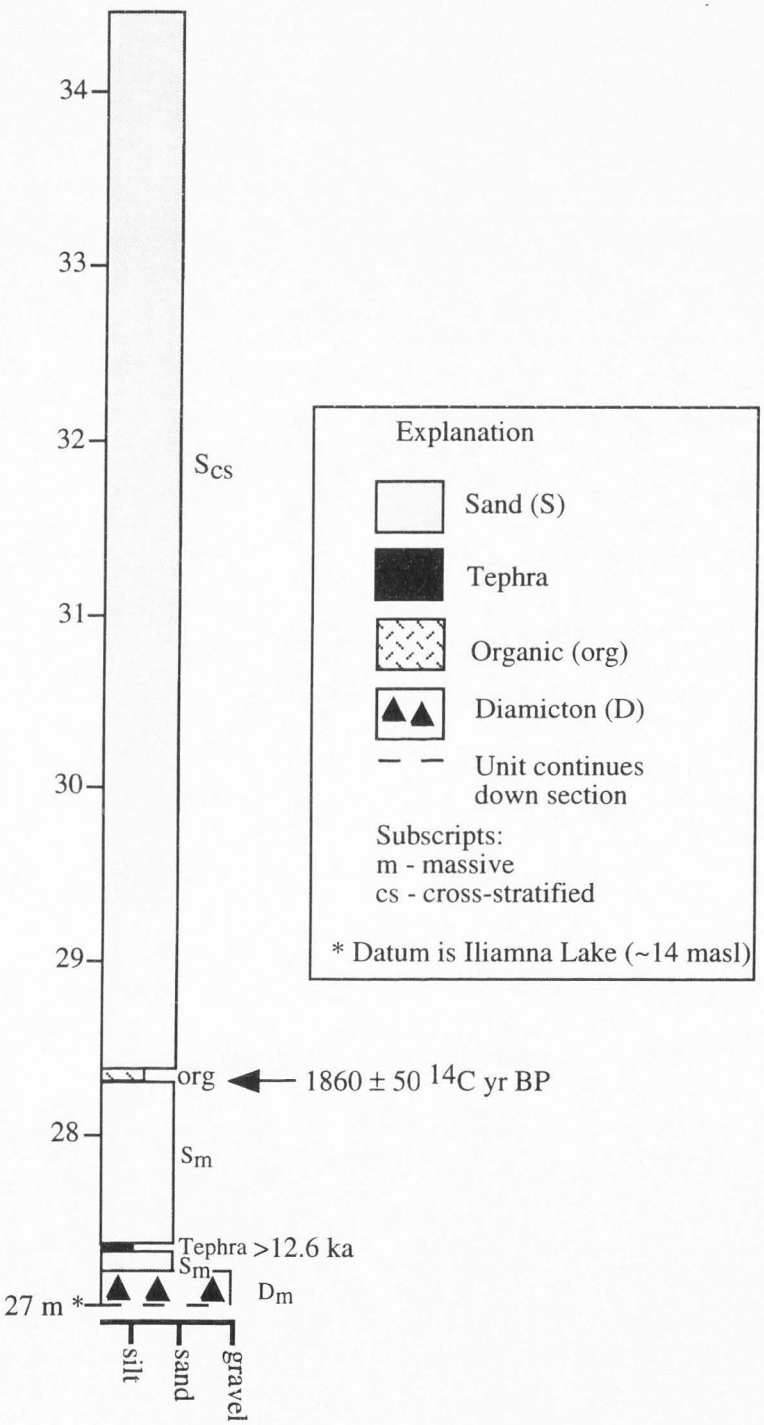

Figure 37. Upper part of stratigraphic section at northwest corner of Iliamna Lake (Fig. 31, site 2) showing position of dated organic matter and pink-orange (Lethe) tephra.

ages depends upon the interpretation of its depositional environment and elevation. It clearly is lower than the 41-m terrace (IL8), and is most likely associated with the 31-m terrace (IL6). If the sand above and below the tephra is lacustrine, then the tephra was deposited within the lake when the lake level was above the 31-m terrace. If the overlying sand is eolian, then the tephra would have fallen onto the terrace after the terrace was cut. This latter interpretation is favored in light of the purity and sharp bounding surfaces of the tephra; it is not incorporated into, nor does it incorporate the overlying or underlying sand. If the tephra had been deposited in the lake, then currents would have reworked the tephra and incorporated sand. If this is the correct interpretation, then the tephra provides a minimum-limiting age on the 31-m terrace, suggesting that it and higher terraces are older than 12.6 ka.

To summarize, at its highest stand of 45 m, Iliamna Lake was held in by the type Kvichak moraine, and glacial-lacustrine sediments were deposited. Peat that underlies outwash deposited on an outwash plain supplied by the Kvichak-stade glacier provides a maximum-limiting age of 26 ka on this stand of the lake. Lake level then fell below 31 m, enabling beach gravel to infill the distal portion of the basin. Next, outwash and diamicton were deposited by the Iliamna-stade glacier (Chapter 2). Following retreat of the Iliamna-stade glacier from the bluff site, lake level stabilized at ~40 m, during the Newhalen stade (~14 ka). After this time, yet prior to 12.6 ka, lake level fell to 31 m. Sometime after the lake fell below this elevation, the pink-orange tephra was deposited on the 31-m terrace surface.

Naknek Lake. Organic matter that underlies outwash graded to the Naknek moraine, dated at 26 ka (Mann and Peteet, 1994), affords a maximum-limiting on Naknek Lake terraces. Both the 30- and 15-m terraces notch the type Iliuk moraine, demonstrating that they are of post-Iliuk age (~13 ka) (Chapter 2). Charcoal dated at 7.4 ka (Dumond, 1981) affords a minimum-limiting age on the separation of Naknek and Brooks lakes, and thereby the 30-, 15-, and 6-m terraces.

SUMMARY AND CONCLUSION

A ~40-m terrace was found at two sites separated by 70 km northeast to southwest above Iliamna Lake, and horizontal terraces of 15 and 30 m were identified across 50 km east to west, and 35 km north to south at Naknek Lake. The horizontal, or nearly horizontal, form of these three terraces demonstrates that they are not tilted, within the ±1-m accuracy, due to glacial-isostatic rebound, nor warped due to regional tectonism. Most significantly, the lack of anticipated ~100 m of tilting suggests that isostatic recovery was complete prior to the fall of both lakes from their highest stand.

Results of this study also suggest limited deformation by regional tectonism since the retreat of glaciers, enabling shorelines around the lakes to retain a consistent shape and elevation. This is surprising given the proximity (~25-100 km) of the lake basins to the Aleutian trench. Nonetheless, it is consistent with the recent discovery of a last interglacial marine bed at ~ 6 masl near South Naknek village (Kaufman and others, 1994).

Lake-level fluctuations in the study area are thought to be in part climatically influenced. The most prominent terraces, the 24-m terrace at Iliamna Lake and the 15-m terrace at Naknek Lake, are both about half-way between the highest terrace and present-day lake level at each lake. This suggests that they may be correlative. If so, then regional

effective precipitation on the upper Alaska Peninsula was sufficient to stabilize lake levels long enough to form these prominent terraces. Correlation of terraces between Iliamna and Naknek lakes is hampered by different numbers of terraces at each lake. The presence of six terraces at Iliamna Lake and three terraces at Naknek Lake suggests that the rate and timing of outflow incision also controlled the formation of terraces.

The ~40-m terrace at Iliamna Lake probably dates to Newhalen time (~14 ka); the ~30-m terrace is older than 12.6 ka, and the 24-m terrace is older than 8.3 ka. At Naknek Lake, all terraces are younger than the Iliuk stade (~13 ka), and older than 7.4 ka. This is a period of major global climate transition; therefore, it is not unreasonable to anticipate a climate response.

CHAPTER 4

CORRELATION, AGE, AND MAJOR-ELEMENT CHEMISTRY OF LATE QUATERNARY TEPHRA IN THE ILIAMNA/NAKNEK/BROOKS LAKE AREA, SOUTHWESTERN ALASKA

ABSTRACT

Electron-microprobe analysis of individual glass shards and pumice grains separated from 16 tephra samples from the northern Alaska Peninsula allows five samples to be correlated with latest-Pleistocene Lethe tephra of Pinney and Begét (1991a,b). These correlations extend the Lethe ash plume ~125 km westward and ~150 km northwestward from its assumed source area near the Valley of Ten Thousand Smokes. Major-element chemistry of four early Holocene black tephras fails to support any correlations, suggesting that there are multiple black tephras in the area. Two new ^{14}C ages confirm that at least two have significantly different ages, separated by ~1300 yr. Finally, ash C of Dumond (1981) is tricolored, comprising gray, black, and yellow zones at several sites in the Lake Brooks area. Attempts to correlate the color zones based upon their major-element chemistries demonstrate that ash C consists of more than one chemically distinct tephra and that there is little consistency between color zones at different sites. These results indicate that caution must be used when using tephra color for stratigraphic correlations.

INTRODUCTION

Tephra layers are regionally isochronous stratigraphic markers that afford relatively instantaneous time datums and have been used in Alaska and elsewhere to correlate and date sediments for geological (Begét and others, 1991; Pinney and Begét 1991a,b; Begét

and others, 1992) and archeological studies (Nowak, 1968; Dumond, 1981). Each tephra has a unique chemical composition that is a function of the parent magma, tectonic setting of the volcanic field, and magma differentiation history (see Sarna-Wojcicki and Davis, 1991, for a review of the principles of tephrochronology). The bulk chemical composition of a tephra can vary with distance from its eruptive source as denser grains settle earlier from the eruptive plume than lighter grains. However, the volcanic glass phase of a tephra generally has a constant composition at proximal, intermediate, and distal sites. Therefore, tephra layers may be correlated where their major-element glass chemistries are similar.

Many active (within the last few hundred years) and prehistorically active Aleutian Range volcanoes in proximity to the Iliamna/Naknek/Brooks Lake study area (Fig. 38) have generated numerous tephra layers, providing a detailed record of late Quaternary volcanism. This study uses electron-microprobe analyses of individual glass shards of 16 tephra layers sampled on the upper Alaska Peninsula, southwestern Alaska, (Fig. 38) to correlate and chemically characterize tephra layers in the region. The objectives of this tephra study are to: (1) present and interpret the results of electron-microprobe analyses, (2) correlate between samples based upon their major-element glass chemistries and age constraints, and (3) reconstruct the ash plume for multiple correlative tephra layers.

Lethe Tephra

Lethe tephra, erupted during the latest Pleistocene, is an invaluable marker horizon near the Valley of Ten Thousand Smokes (Pinney and Begét 1991a,b; Pinney, 1993). An origin at the head of the valley is suggested, but not confirmed, by the presence of thick (~4 m) proximal deposits just south of the valley. Lethe volcaniclastic deposits have been identified about 20 km west of the presumed source in late-Pleistocene sediments near

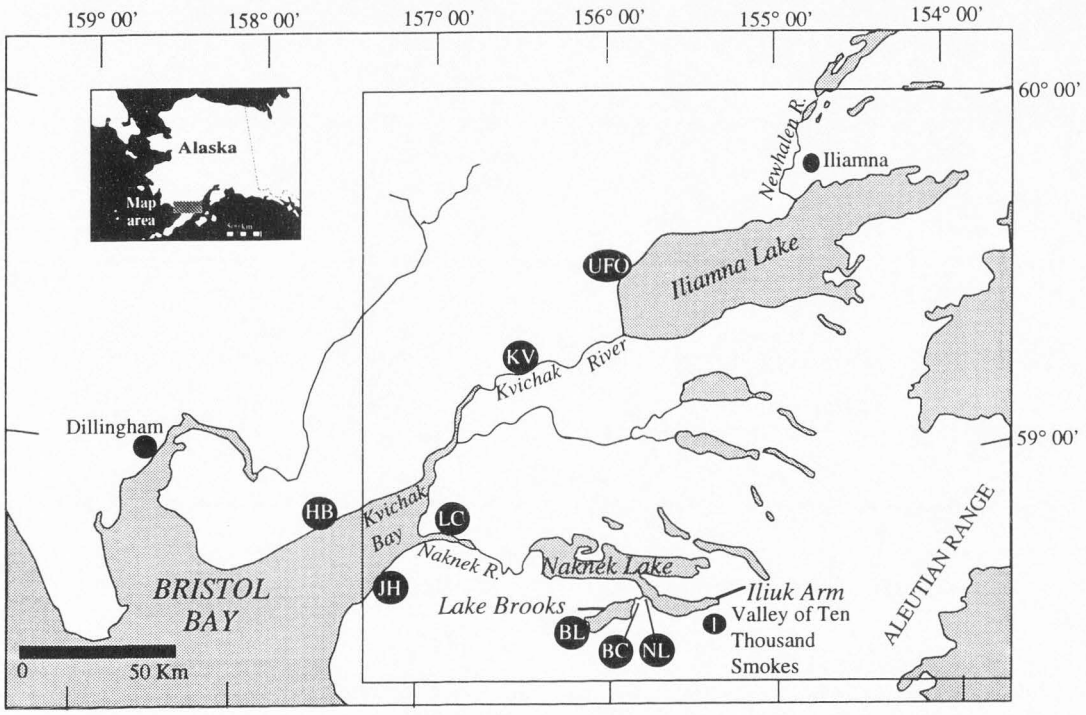

Figure 38. Northern Alaska Peninsula showing location of the Iliamna/Naknek/Brooks Lake study area, southwestern Alaska, and stratigraphic sections referred to in text. Locations of sample sites as follows: UFO = UFO bluffs; KV = Kvichak River; LC = Leader Creek; JH = Johnston Hill; HB = Halfmoon Bay; BL = Lake Brooks moraine; BC = Brooks Camp; NL = Iliuk moraine; 1 = location of Pinney and Begét's (1991a,b) ^{14}C date.

Iliuk Arm of Naknek Lake. Pinney and Begét (1991b) recognized that the known distribution of Lethe tephra is likely to expand with more tephra studies. D. Pinney and R. Reger (personal communication, 1995) recently discovered correlative tephra ~260 km northeast of the source area, along the Kenai Peninsula. Glass chemistry of Lethe tephra is homogenous across its presently known extent and throughout a variety of air-fall types, ranging from fine-grained distal ash to pumice lapilli.

The relative age of Lethe tephra is constrained by its stratigraphic position atop Iliuk drift, and below and incorporated into Ukak drift (Chapter 2). Pinney and Begét (1991a,b) argued that radiocarbon dates on organic silt underlying Holocene glacial deposits places a minimum-limiting age of 12,650 ± 100 ^{14}C yr BP upon Lethe tephra (Fig. 38; Table 10). Radiocarbon ages of 12.7 and 12.8 ka from organic matter that overlies two pink-orange tephras, which correlate with Lethe tephra, strengthen the known age control on Lethe tephra (Peter Lea, personal communication, 1994).

Black Tephra

A black tephra was consistently found approximately 0-10 cm above a pink tephra at nearly every pink-tephra collection site (for example, Fig. 39). The objective of this portion of the tephra study is to use electron-microprobe data to determine whether or not these black tephras are correlative.

Tephra Associated with Archaeological Sites

Archaeologists have identified a suite of ten volcanic ashes at archaeological sites near Naknek and Brooks lakes based upon color, thickness, and stratigraphic position (Nowak, 1968; Dumond, 1981). This local tephra sequence is labelled alphabetically from

TABLE 10. RADIOCARBON AGES REFERRED TO IN TEXT

Radiocarbon date (yr BP)	Lab ID	Material dated	Stratigraphic position	Location (Fig. 38)	Reference
9310 ± 70	AA-15093	Plant macrofossils	Exposure along Kvichak River; overlies a pink-orange and a black tephra ~1 m below surface	KV	This paper
5365 ± 55	AA-15094	Plant macrofossils	Exposure along Kvichak River; overlies organic layer AA-15093 ~80 cm below surface	KV	This paper
1860 ± 50	AA-15096	Plant macrofossils	Exposure at northwest corner of Iliamna Lake 28.5 m above lake level	UFO	This paper
8005 ± 70	AA-15097	Plant macrofossils	Exposure along Naknek River; ~1.8 m below ground surface	LC	This paper
12,650 ± 100	Beat-33666	Organic silt	Underlies Katolinat till (Chapter 1)	1	Pinney and Begét (1991a,b)

A-J, and spans a time from 38 yr BP (ash A; Mt. Katmai eruption of 1912) to 6595 yr BP (ash J) (Table 11). The ages of ashes A-J are well constrained by radiocarbon dating of organic material associated with individual ashes, and stratigraphic relationships to cultural materials. Ashes A (white), C (gray), and G (yellow) are most easily recognized in the field because of their thickness and distinctive color. However, ashes D, E, and F, are

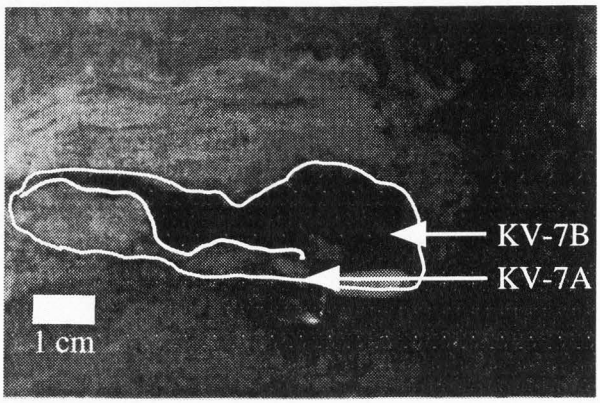

Figure 39. Pink-orange tephra (KV-7A) and black tephra (KV-7B) at Kvichak River section (KV). White lines show contact between the two tephras, base of the pink tephra, and top of the black tephra.

TABLE 11. AGES AND CHARACTERISTICS OF VOLCANIC ASH DEPOSITS A-J (MODIFIED FROM DUMOND, 1981)

Ash	Age (yr BP)	Color	Thickness
A	83	white	20
B	245	blackish grey	1-2
C	545	grey, black, yellow	10
D	1095	black, grey	1-2
E	1545	black, grey	1-2
F	2645	black	3
G	3895	yellow	3
H	4095	black, orange, yellow	1-2
I	5495	grey	1-2
J	6495	brown	3

uniformly black to dark gray, and petrographic data indicates that there may be more than three ashes present (Dumond, 1981). Attempts to characterize these ashes by petrographic characteristics, index of refraction, and neutron activation analyses have been relatively unsuccessful (Nowak, 1968; Dumond, 1981).

In a preliminary study, Riehle (undated) catalogued individual Holocene tephra layers near Lake Brooks. He suggested that using tephra layers to correlate among cultural sites in the area is hindered by their: (1) megascopic similarity, (2) thin, fine-grained nature and contamination, and (3) poor preservation. He presented new major-element glass chemistries for Holocene tephra layers in the area, but did not report them with respect to Dumond's (1981) scheme of A-J. Eighteen chemically distinct tephra deposits all younger than 4500 yr BP around Brooks Camp were identified, which is considerably more than identified by Dumond (1981).

Ash C consists of an uppermost gray horizon, a central black zone, and a lower yellow horizon termed a "weathering rind" by Donald Dumond (personal communication, 1994) (Fig. 40a). Because tephra layers typically have a distinctive color, the three different color zones of the ash suggest that ash C may comprise three ashes, rather than a single ash. This suggestion agrees with Dumond's (1981) contention that ashes D, E, and F each contain more than one ash; it also agrees with Riehle's discovery of 18 different tephra layers deposited since 4500 yr BP, the interval during which only eight ashes (ashes A-H) were recognized by Dumond (1981). The purpose of this part of the tephra study is to analyze each of the three color zones of ash C for its major-element chemistry to determine if the ash is a single discrete ash, or a collective of multiple ashes. Like the analysis of the pink and black tephras, this analysis will aid in testing the validity of color as a diagnostic characteristic for field identification of discrete tephra.

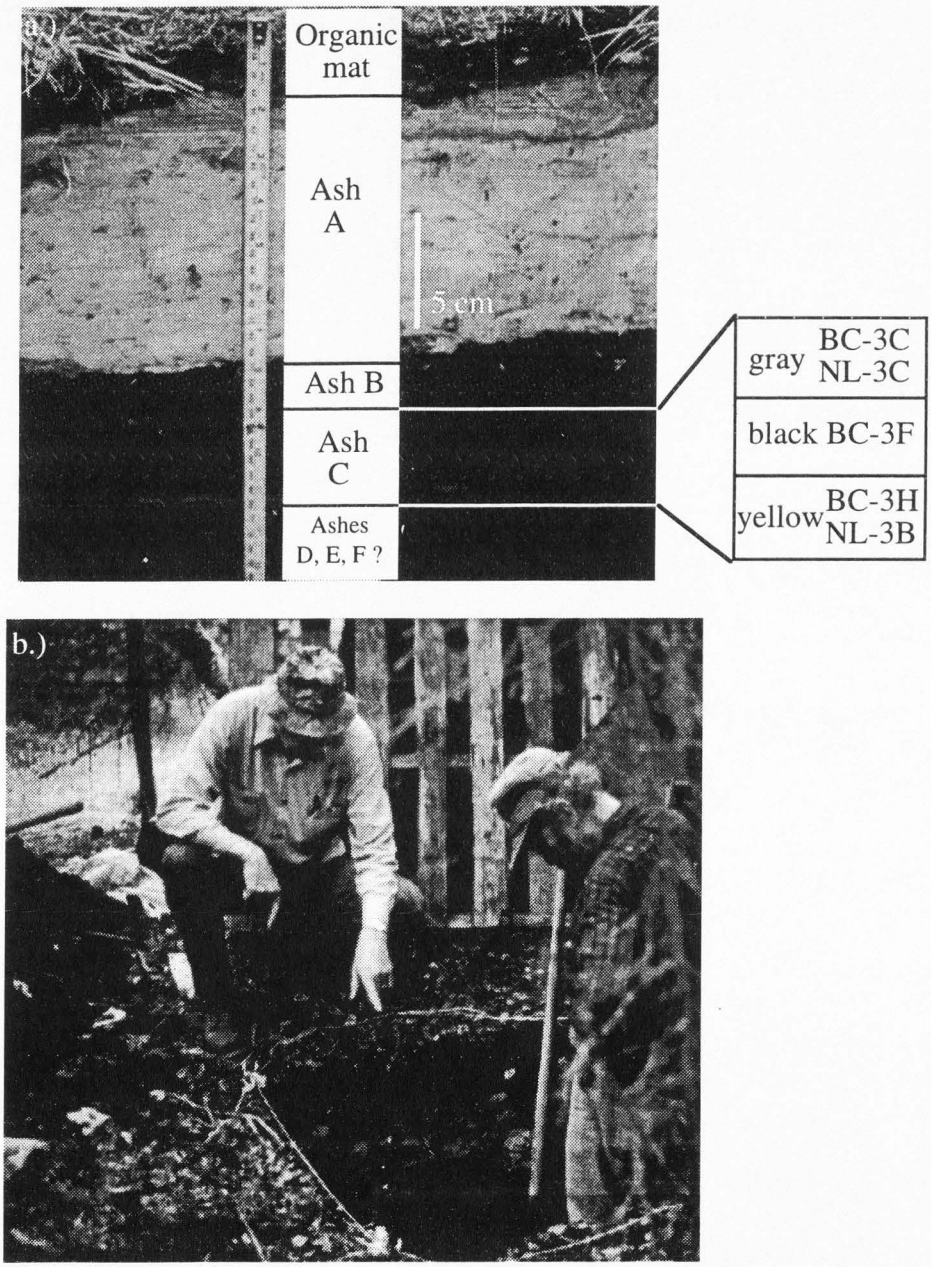

Figure 40. (a) Excavation pit showing ashes A, B, and C of Dumond (1981). Inset shows sample names and color zones. (b) Pit excavation at Brooks Camp by Donald Dumond (left) and Richard Bland (right).

METHODS

Tephra and organic samples were collected from hand-dug test pits and natural exposures, and 16 were selected for analysis.[2] Thickness, color, and texture were recorded in the field. Glass or pumice separates were prepared for major-element chemical analysis by electron microprobe. The separation procedure involved: (1) washing samples with distilled water, (2) sonicating samples 1-3 times for 30-60 seconds, (3) removing organic material by stirring tephra and water in a beaker, then quickly decanting organics, or by dissolving organics in hydrogen peroxide, (4) using the Frantz magnetic separator to separate glass and pumice shards from other grains, (5) crushing and sieving samples to between 45-90 μm, and (6) using heavy liquids (sodium polytungstate) to separate glass and pumice shards from microlites and extraneous grains. James Riehle and Charles Meyer (United States Geological Survey of Anchorage, Alaska and Menlo Park, California, respectively) analyzed shards for their major-element chemistry (~20 shards per sample) (see Appendix 2 for conditions and laboratory standard used during electron-microprobe analyses).

Each tephra was characterized by its dominant composition, or compositions for those containing multiple populations. Electron-microprobe analysis gives grain-discrete results that can be used to identify and exclude secondary populations of nonglass. I identified outliers in samples by their distinctly high or low oxide content compared to the majority of grains. Following Pinney (1993) and Riehle (1994), shards with low analysis totals were discarded. Outliers are probably either minerals, microlites, or foreign glass

---

[2] Refer to methods section of Chapter 2 for a discussion of sample preparation for ^{14}C dating.

shards. Foreign shards are derived from mixing with other tephra layers, an eruption of mixed assemblage, or from contemporaneous eruptions of different sources. Low analysis totals may indicate excessively small or thin shards that burned during analysis, had a high water content, or were vesicular (Pinney, 1993). Mean composition(s) and standard deviation(s) were calculated for each tephra, after outliers were removed and multiple modes identified (always $n \geq 2$), for correlation with other tephras (Appendix 2). Primary and secondary populations are designated as "a" or "b", respectively, at the end of the sample ID name (for example, BC-4Aa and BC-4Ab).

Similarity coefficients (S.C.), defined as the average ratio of nine major oxides of a known to an unknown sample, where the lesser value is always the numerator, were used to correlate tephras based upon their major-element chemistries (Borchardt and others, 1972). S.C. ranges between 0 and 1, where a value of 1 denotes a perfect match. Variability in S.C. results from both instrumental variability and variability of glass composition. Based on his experience with Alaskan tephra, Riehle (undated) considered, on average, S.C. values ≥ 0.95 indicative of correlative samples. Correlations based on values of 0.94-0.95 were considered uncertain, and values of <0.94 did not support a correlation. S.C. of 0.95 was used to support correlations of tephra layers in the Iliamna/Naknek/Brooks Lake study area.[3]

TEPHRA STRATIGRAPHY

Here I present detailed stratigraphic sections from which tephra samples were collected. The Results and Discussion section that interprets major-element chemistries for

---

[3] In accordance with Pinney and Begét (1991b), the oxide MnO was excluded in calculating the S.C. for the pink-orange and Lethe tephras, and the remaining oxides were normalized to 100%.

pink-orange tephra, black tephra, and ash C, and establishes correlations.

Section UFO

Section UFO is located at the northwest corner of Iliamna Lake (Fig. 38). A sequence of Holocene eolian deposits, including tephra, overlies glacial-lacustrine sand and silt, beach gravel, glacial-fluvial sand and silt, and diamicton (Fig. 41; Chapters 2 and 3). A silty, 1- to 3-cm-thick, pink-orange tephra (UFO-2C; Fig. 42) lies ~10 cm above the diamicton. Organic-rich silt at 28.5 m provides a minimum-limiting age of 1860 ± 50 ^{14}C yr BP (Table 10) for this tephra.

Section KV

The Kvichak River section (KV) is located on the right bank of the Kvichak River approximately 40 km downstream of Iliamna Lake (Fig. 38). Holocene eolian sediment overlies outwash sand and gravel graded to the type Kvichak moraine (Fig. 43; Chapter 2). A 1-cm-thick, discontinuous layer of fine-grained, pink-orange tephra (KV-7A) directly overlies the outwash gravel, and a ~7-cm-thick block of fine- to medium-grained black tephra (KV-7B) directly overlies the pink-orange tephra (Fig. 39). The black tephra was sampled at its top to avoid contamination with the underlying pink-orange tephra. These two tephra layers form the base of a ~2-m-thick unit of massive silt and sand that is interstratified with two thin (~1 cm), discontinuous organic stringers, two kidney-shaped lenses of organic-rich silt and peat; a thin (~2 cm), laterally continuous, organic-rich horizon; and a third lens of organic-rich silt and peat. The lowermost organic stringer did not contain enough material for a ^{14}C determination. The next-higher organic stringer at ~1 m below the surface contained plant macrofossils that were dated at 9310 ± 70 ^{14}C yr

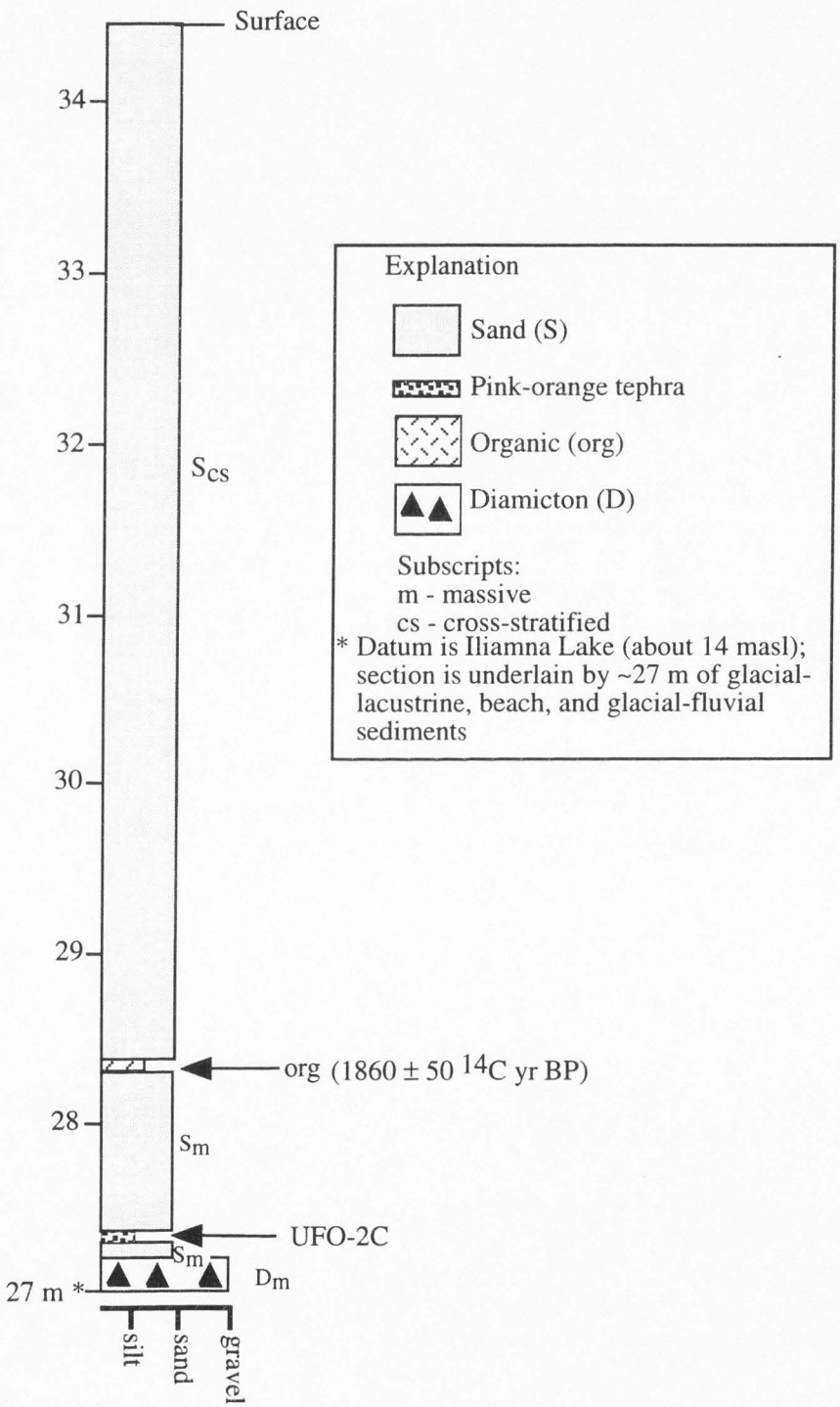

Figure 41. Holocene portion of stratigraphic section UFO at the northwest corner of Iliamna Lake (Fig. 38).

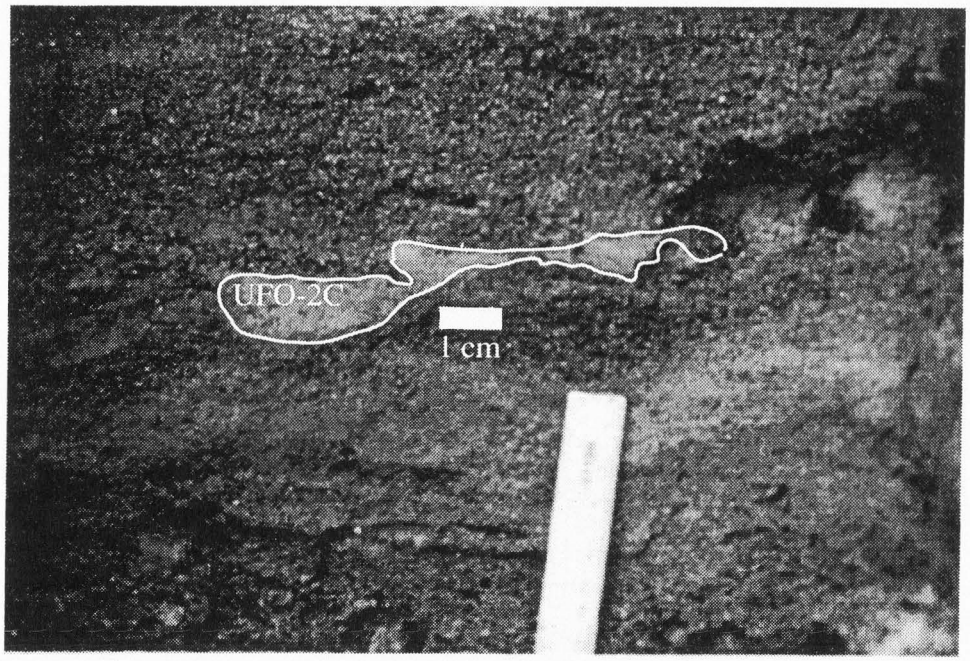

Figure 42. Pink-orange tephra (UFO-2C) outlined in white found ~27.3 m above lake level at section UFO.

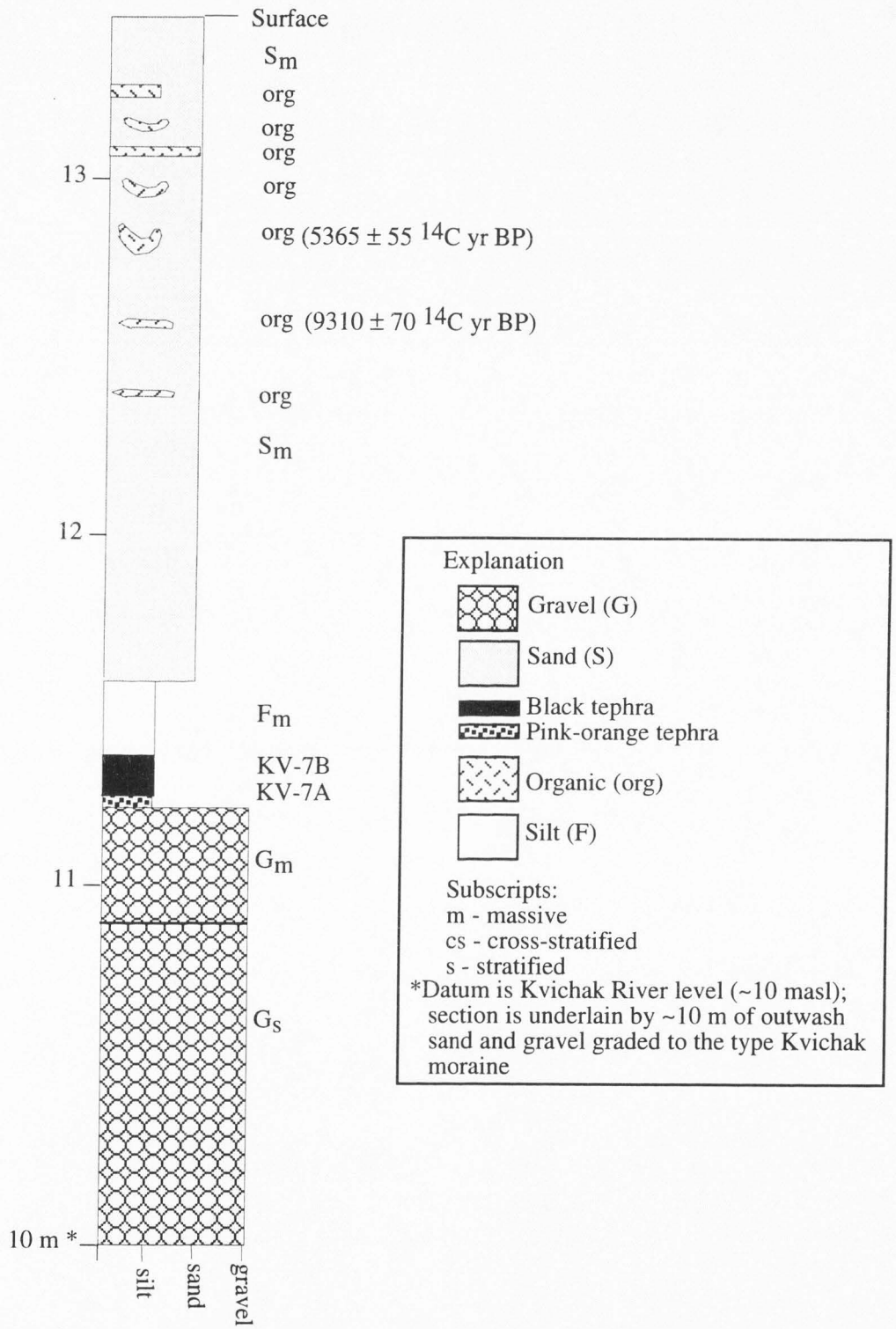

Figure 43. Kvichak River section (KV) on the right bank of the Kvichak River ~40 km downstream of Iliamna Lake (Fig. 38).

BP (Table 10), providing a minimum-limiting age on both the pink-orange and black tephra layers. The overlying kidney-shaped organic layer also contained plant macrofossils that were dated at 5365 ± 55 ^{14}C yr BP (Table 10), and this age demonstrates that the ^{14}C ages decrease upsection. Organic matter from higher organic units was not submitted for ^{14}C dating.

Section LC

The Leader Creek section (LC), located on the north side of the Naknek River about 30 km downstream of Naknek Lake (Fig. 38), is underlain by ~40 m of late Wisconsin and older sediments (Fig. 44) (Thompson and others, 1994a). A 3-cm-thick, silty, pink-orange tephra (LC-3C; Fig. 45a) was sampled ~2 m below the surface. A laterally continuous (~3-4 cm thick) organic-rich horizon overlies the pink-orange tephra. Above the organic horizon are a thin (~2 cm), massive, sand layer and a 3-cm-thick, sandy, laterally continuous black tephra (LC-3A and LC-3B[4]; Fig. 45b). About 1.5 m of cross-stratified eolian sand interstratified with late Holocene tephras form a cliff-head dune that caps the section. Plant macrofossils within the organic-rich horizon were dated at 8005 ± 70 ^{14}C yr BP (Table 10) and provide a minimum-limiting age on the pink-orange tephra, and a maximum-limiting age on the black.

---

4 Two samples were analyzed from this tephra layer; LC-3A a pumice-rich magnetic fraction, and LC-3B a glass-rich, nonmagnetic fraction.

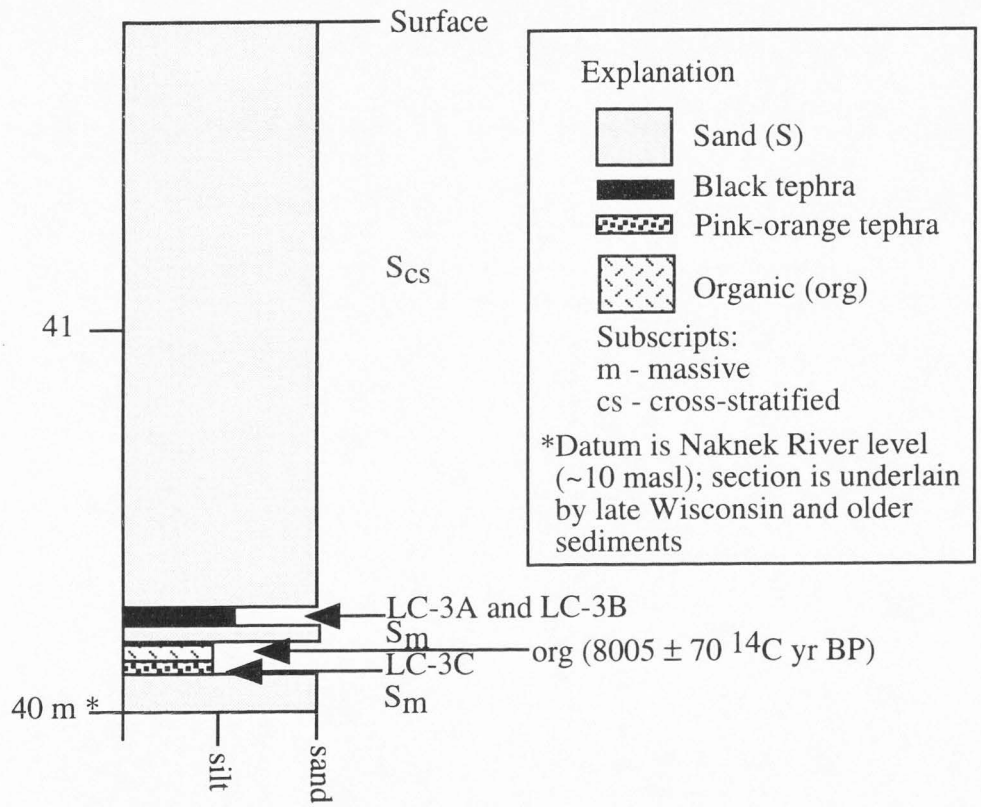

Figure 44. Leader Creek section (LC) on the north side of the Naknek River about 30 km downstream of Naknek Lake (Fig. 38).

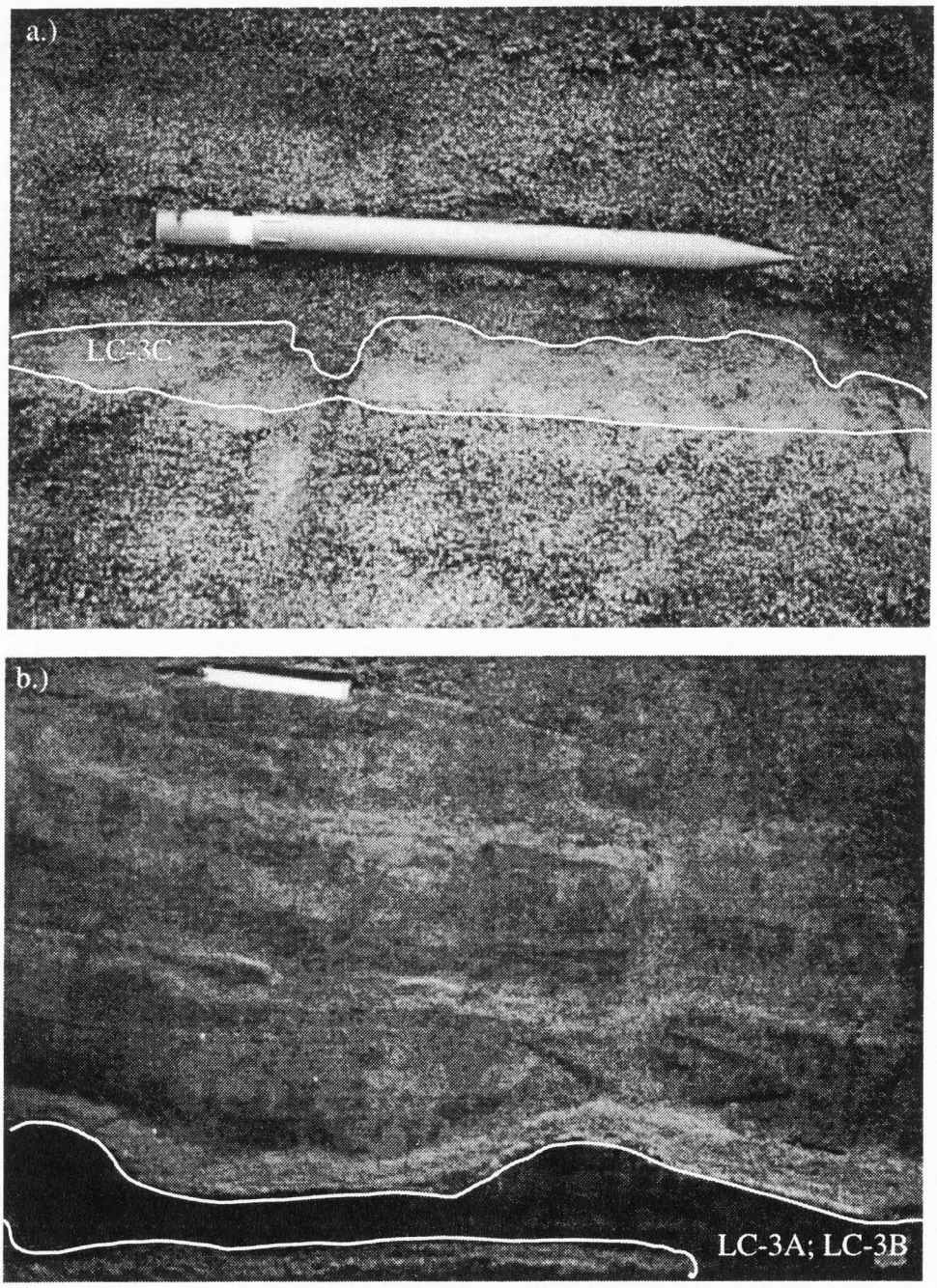

Figure 45. Tephras at Leader Creek section (LC). (a) Pink-orange tephra (LC-3C); pen in photo is approximately 15 cm, and (b) black tephra (LC-3A and LC-3B); knife in photo is ~5 cm.

Sections JH and HB

The Johnston Hill section (JH) is located along the east shore of Kvichak Bay about 25 km south of the mouth of the Naknek River (Fig. 38). The Halfmoon Bay section (HB) is situated on the west side of Kvichak Bay, ~30 km west of the Naknek River mouth (Fig. 38). Tephra samples from these two localities were collected by Peter Lea (Bowdoin College), who did not provide detailed stratigraphic information. The ages of two fine-grained, pink-orange tephra layers, samples JH-11 and HB-1, are constrained by unpublished minimum-limiting ^{14}C ages of 12.7 ka and 12.8 ka, respectively (Peter Lea, personal communication, 1994).

Test Pit BL

The Lake Brooks moraine test pit (BL) was dug at the crest of the moraine ridge forming the western end of Lake Brooks (Figs. 38 and 46). Compact, matrix-supported diamicton containing angular cobbles is found at the base of the 1.1-m-deep pit. The diamicton is overlain by ~60 cm of unoxidized sand and silt with scattered pebbles derived from below. At ~93 cm below the surface (~28 cm below the depth of soil oxidation) is a 1-cm-thick, fine-grained, lens-like pink-orange tephra (BL-4A). The pink-orange tephra, in turn, is overlain by a 0.5-cm-thick, sandy, discontinuous black tephra (BL-4B). The black tephra is buried by ~30 cm of oxidized silt and fine sand containing three additional tephra layers that were not analyzed. Gray tephra, probably ash C of Dumond (1981), a buried organic-rich horizon (perhaps ash B), Mt. Katmai ash, and a 5-cm-thick tundra mat overlie the oxidized silt and fine sand.

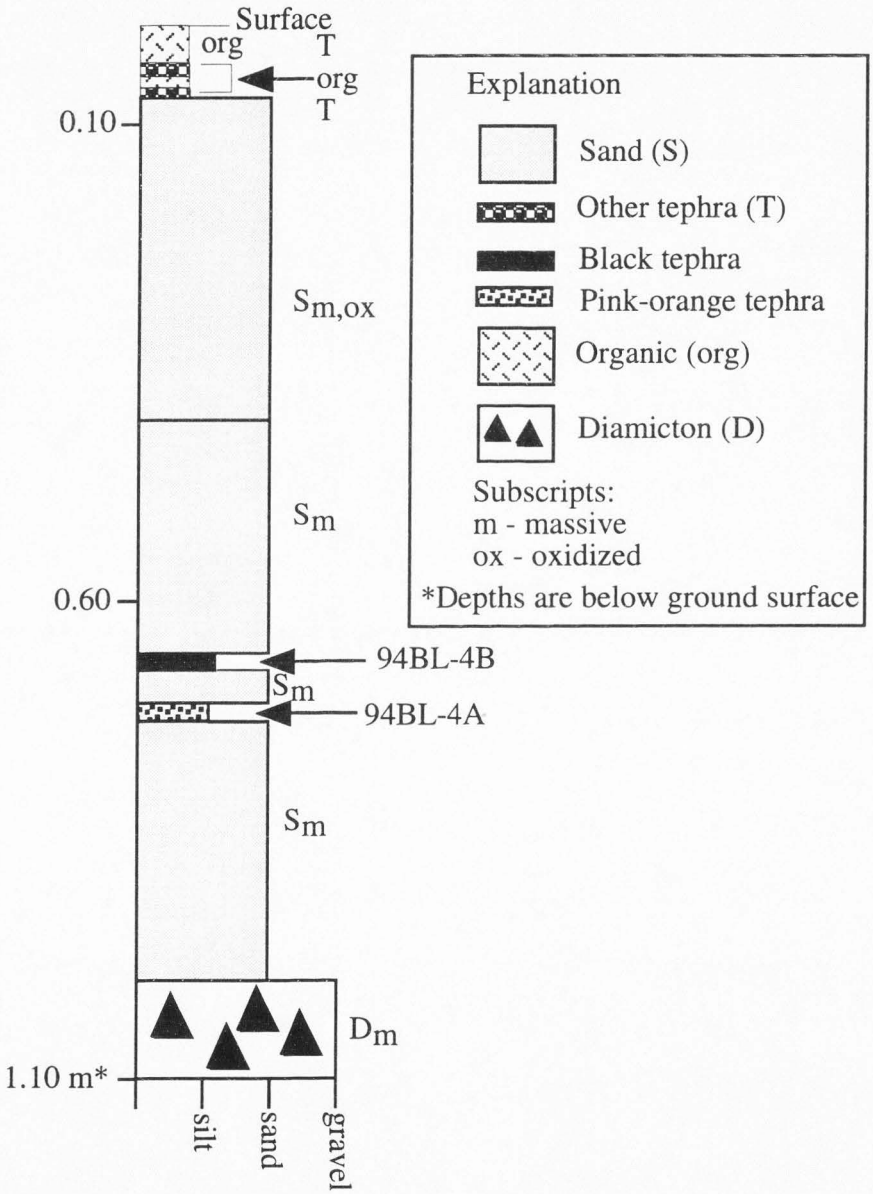

Figure 46. Test pit BL dug into the Lake Brooks moraine (Fig. 38).

Test Pit NL

The Naknek lake test pit (NL) was dug into the type Iliuk moraine located at the western edge of Iliuk Arm of Naknek Lake (Figs. 38 and 47). The lowermost 10 cm of the 1.2-m-deep pit penetrated gray sand, which is overlain by 80 cm of oxidized sand. At ~80 cm depth is a discontinuous, 2-cm-thick, fine-grained, black tephra layer (NL-4B), which is overlain by a 4-cm-thick, prominent, laterally continuous, fine-grained, yellow tephra layer. The tephra layers, in turn, are overlain by ~50 cm of oxidized sand, and the section is capped by a suite of late Holocene tephra and organic layers. The lowermost of these organic horizons is 3 cm thick, and is overlain by a 2-cm-thick gray tephra, and ash C. At its base, ash C is comprised of a 1-cm-thick yellow horizon (NL-3B), followed by a 4-cm-thick organic-rich horizon, and a 2-cm-thick gray horizon (NL-3C). Another thin organic-rich horizon overlies ash C (possibly ash B), followed by ~20 cm of white, fine-grained Mt. Katmai ash (ash A), and ~2 cm of modern tundra.

Test Pit BC

The Brooks Camp test pit (BC) is located at the northeastern corner of Lake Brooks, on the south side of Brooks River that connects Lake Brooks to Naknek Lake (Fig. 38). Archaeologists Donald Dumond (University of Oregon), Richard Bland, and Patricia McClennahan (both of the National Park Service, King Salmon) excavated a shallow test pit on the east side of Lake Brooks adjacent to the National Park Service cabin in August 1994 (Figs. 38 and 40a,b). At its base, the pit showed a black, ~3.5-cm-thick, fine-grained tephra (probably ashes D, E, and F), interspersed with peat, which was overlain by a 1-cm-thick, fine-grained yellow horizon of ash C (BC-3H), a 1-cm-thick, fine-grained black color horizon of ash C (BC-3F), and a 1-cm-thick, fine-grained gray

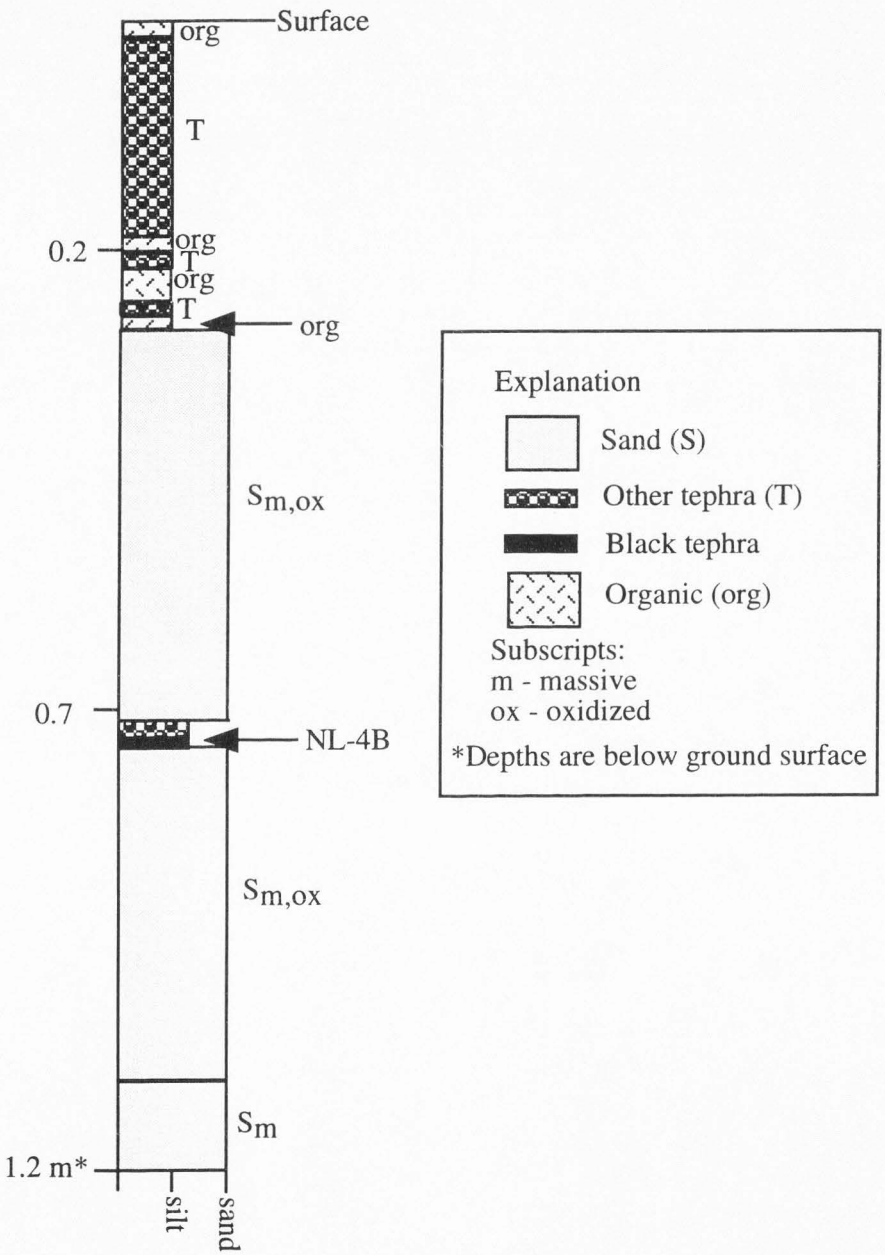

Figure 47. Test pit NL dug into the type Iliuk moraine (Fig. 38).

color horizon of ash C (BC-3C), an organic-rich silt and peat horizon (ash B), and ~15 cm of white Mt. Katmai ash.

Summary of Tephra Stratigraphy and Chronology

Samples collected from stratigraphic sections and test pits fall into three categories. Category (1) is pink-orange tephra that typically underlies black tephra layers. At two sites (JH and HB), these tephra are older than 12.7-12.8 ka, and at two other sites (KV and LC) they are older than 8-9 ka. Category (2) is black tephra that typically overlies a pink-orange tephra layer and, in general, is of early Holocene age (for example, LC-3A and LC-3B are younger than ~8 ka, and KV-7B is older than ~9.3 ka). And category (3) is three color zones of Dumond's (1981) ash C (Table 12). The following discussion is subdivided accordingly: (1) pink-orange tephra, (2) black tephra, and (3) ash C.

TABLE 12. SIXTEEN TEPHRA SAMPLES ANALYZED IN THIS STUDY, SUBDIVIDED INTO THREE CATEGORIES

Pink-orange	Black	Ash C
BL-4A	BL-4B	BC-3C (gray)
HB-1	KV-7B	BC-3F (black)
JH-11	LC-3A	BC-3H (yellow)
KV-7A	LC-3B	NL-3B (yellow)
LC-3C	NL-4B	NL-3C (gray)
UFO-2C		

RESULTS AND DISCUSSION

Pink-Orange Tephra

Field characteristics of all six pink-orange tephra layers (Table 12) are similar: pink-orange color, 1-2 cm thickness, fine-grained texture, stratigraphic position beneath black tephra layers near the base of the regional eolian mantle, and above drift. Samples JH-11, HB-1, and BL-4A contain both primary and secondary populations (Table 13). Primary population mean compositions were calculated using an average of 15 shards, whereas secondary populations typically comprised 2-4 shards (Appendix 2). The two modes of each sample are chemically distinct, with the most significant differences found in MgO, Al_2O_3, K_2O, CaO, TiO_2, and FeO. The remaining three pink-orange tephra samples are homogenous, consisting of a single population.

TABLE 13. MAJOR-ELEMENT COMPOSITIONS OF SIX PINK-ORANGE TEPHRAS, AND COARSE AND FINE FRACTIONS OF LETHE TEPHRA (FROM PINNEY AND BEGÉT (1991B)

Sample	Na2O	MgO	Al2O3	SiO2	K2O	CaO	TiO2	FeO	n
JH-11a	4.48 (0.12)	0.67 (0.06)	14.22 (0.15)	71.96 (0.41)	2.48 (0.08)	2.52 (0.15)	0.61 (0.04)	3.05 (0.16)	15
JH-11b	4.45 (0.04)	0.48 (0.02)	13.38 (0.08)	74.18 (0.41)	2.70 (0.02)	1.83 (0.02)	0.55 (0.04)	2.44 (0.27)	2
HB-1a	4.52 (0.11)	0.67 (0.08)	14.26 (0.18)	72.04 (0.46)	2.42 (0.08)	2.48 (0.16)	0.63 (0.04)	2.98 (0.14)	14
HB-1b	4.41 (.012)	0.53 (0.03)	13.46 (0.35)	73.63 (0.25)	2.71 (0.17)	1.95 (0.14)	0.63 (0.05)	2.68 (0.15)	4
KV-7A	4.49 (0.13)	0.63 (0.07)	14.11 (0.33)	72.38 (0.69)	2.49 (0.10)	2.42 (0.21)	0.60 (0.07)	2.87 (0.22)	18
LC-3C	4.50 (0.10)	0.62 (0.11)	13.98 (0.38)	72.72 (1.12)	2.52 (0.10)	2.28 (0.33)	0.06 (0.07)	2.78 (0.34)	16
UFO-2C	4.51 (0.10)	0.66 (0.08)	14.01 (0.30)	72.45 (0.78)	2.47 (0.11)	2.39 (0.23)	0.63 (0.08)	2.88 (0.23)	18
BL-4Aa	4.33 (0.09)	0.11 (0.01)	12.15 (0.05)	77.94 (0.11)	3.46 (0.16)	0.62 (0.03)	0.20 (0.35)	0.20 (0.10)	6
BL-4Ab	4.41 (0.06)	0.32 (0.04)	13.02 (0.21)	75.92 (0.51)	2.75 (0.04)	1.30 (0.05)	0.46 (0.09)	1.82 (0.06)	2
Lethe (coarse)	4.18 (0.11)	0.72 (0.03)	13.90 (0.10)	72.02 (0.27)	2.38 (0.04)	2.60 (0.09)	0.62 (0.03)	3.13 (0.12)	11
Lethe (fine)	4.31 (0.14)	0.70 (0.04)	13.88 (0.13)	72.37 (0.30)	2.34 (0.06)	2.56 (0.09)	0.62 (0.05)	3.07 (0.13)	16

Values are averages of several individual shards (n) after eliminating outliers (Appendix 2).
Reported values are normalized to 100%; values in parentheses are one standard deviation.

Similarity coefficients calculated for each tephra pair demonstrates that the primary population of five of the six samples are correlative (Table 14). The Fe, Mg, and K + Na composition of these samples is strikingly similar (Fig. 48a). Secondary populations of HB-1 and JH-11 are not correlative with the primary populations of any other sample, but an S.C. of 0.95 demonstrates that they are correlative with one another. Neither primary nor secondary populations of sample BL-4A correlate with any other sample (S.C. values range from 0.57-0.84). This tephra layer probably corresponds with one of Dumond's (1981) lowermost ashes, perhaps ash J, which is often light colored (Donald Dumond, personal communication, 1994).

TABLE 14. SIMILARITY COEFFICIENT MATRIX FOR PINK-ORANGE TEPHRAS, INCLUDING THEIR SECONDARY POPULATIONS

Sample	HB-1a	HB-1b	JH-11a	JH-11b	KV-7A	LC-3C	UFO-2C	BL-4Aa	BL-4Ab
HB-1a	1.00								
HB-1b	0.91	1.00							
JH-11a	**0.99**	0.91	1.00						
JH-11b	0.87	**0.95**	0.87	1.00					
KV-7A	**0.97**	0.92	**0.98**	0.89	1.00				
LC-3C	**0.96**	0.94	**0.96**	0.90	**0.98**	1.00			
UFO-2C	**0.98**	0.92	**0.98**	0.88	**0.98**	**0.97**	1.00		
BL-4Aa	0.57	0.61	0.57	0.63	0.58	0.59	0.58	1.00	
BL-4Ab	0.72	0.80	0.73	0.84	0.74	0.76	0.74	0.66	1.00
Lethe (coarse)	**0.96**		**0.97**		**0.95**	0.93	**0.95**		
Lethe (fine)	**0.97**		**0.98**		**0.95**	0.94	**0.96**		

Correlations supported by S.C. >0.95 are shown in bold.
Also shown is similarity coefficient matrix between pink-orange and Lethe tephra, excluding secondary populations and sample BL-4A.

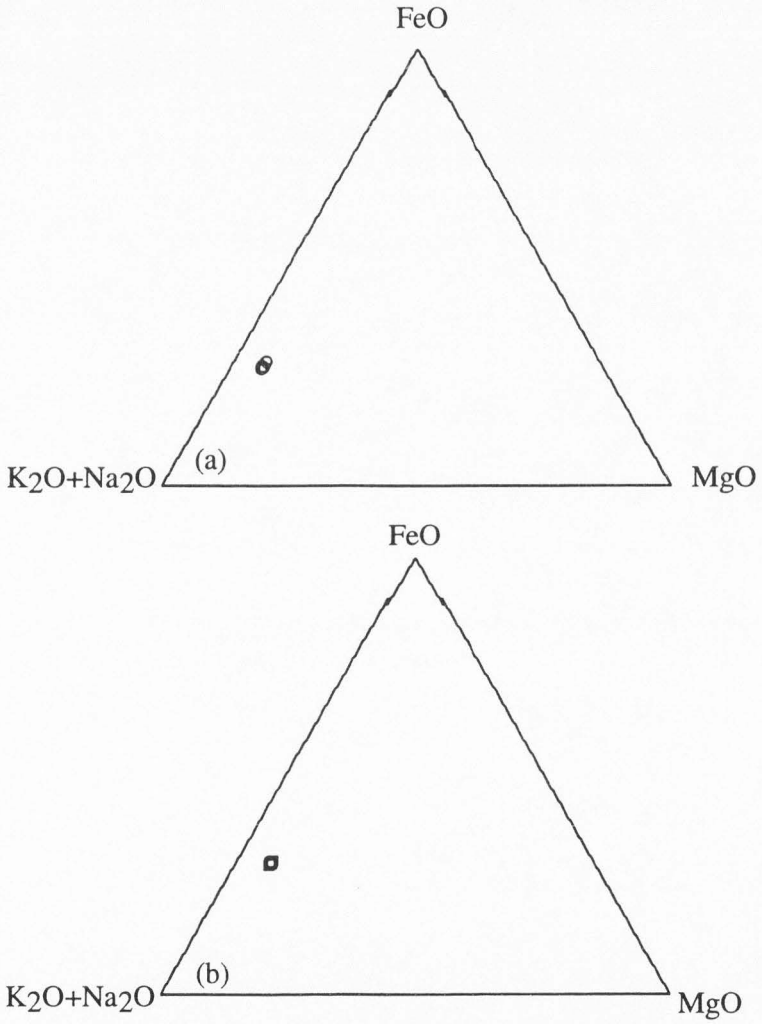

Figure 48. Ternary plot of three major oxides for (a) primary populations of pink-orange tephras, excluding BL-4A, and (b) coarse and fine fractions of Lethe tephra [constructed from published data in Pinney and Begét (1991b)]. Data listed in Table 13.

The age, stratigraphic position, and field characteristics of the five correlative samples (KV-7A, LC-3C, UFO-2C, HB-1a, and JH-11a) suggest that they are correlative with the published chemical compositions of Pinney and Begét's (1991) Lethe tephra that is >12.6 ka. This is supported by the probe data that show all five samples, except LC-3C, have S.C. values of ≥ 0.95, demonstrating that they are correlative with Lethe tephra (Table 14). Although LC-3C has S.C. of 0.94 and 0.93 for the fine and coarse fractions of Lethe tephra, respectively, it is considered correlative with Lethe tephra because it is 96-98% similar to the other four pink-orange tephra samples, which themselves are correlative with Lethe tephra. The secondary mode, which shows up in only two samples, has not been reported, but may be representative of a bimodal eruption.

The areal distribution of the Lethe tephra is here expanded from the original work of Pinney (1993) to encompass each of the five correlative pink-orange tephras analyzed in this study (Fig. 49). This extends the plume ~125 km west of the presumed source area (105 km farther than previously documented), and ~150 km northwestward. Pinney and Reger (personal communication, 1995) have found Lethe tephra ~260 km northeast of the source area, making it an extremely useful, widespread stratigraphic marker in southern Alaska.

Black Tephra

Correlation of black tephra samples is more complex than that of pink-orange tephras. Similarity coefficients calculated between pairs of analyses fails to produce any correlations between samples (Tables 15 and 16). S.C. calculated for all sample pairs ranges broadly (0.22-0.91), and fails to produce any significant correlations (Table 16). This chemical disparity is illustrated by a plot of Fe, Mg, and K + Na composition (Fig. 50).

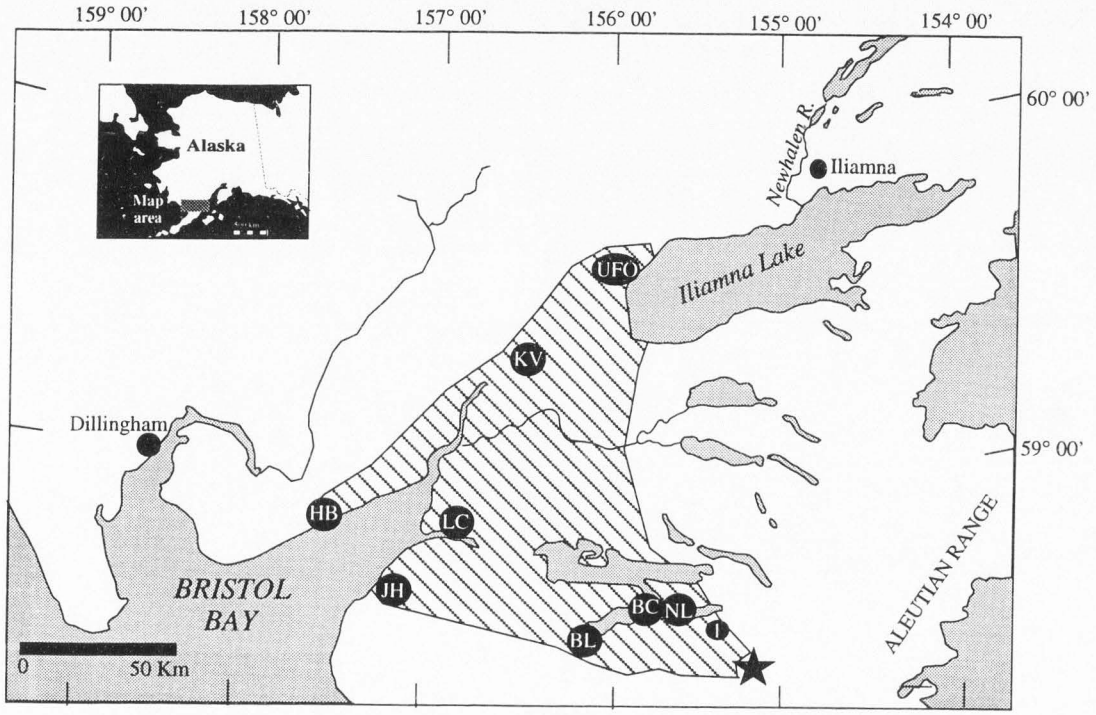

Figure 49. Presently known western distribution of Lethe ash plume. Star = presumed source area (Pinney, 1993).

TABLE 15. MAJOR-ELEMENT COMPOSITIONS OF BLACK TEPHRAS

Sample	Na2O	MgO	Al2O3	SiO2	K2O	CaO	TiO2	MnO	FeO	n	Total
NL-4Ba	4.74 (0.16)	1.74 (0.16)	15.51 (0.34)	64.63 (0.82)	2.48 (0.19)	3.72 (0.30)	1.10 (0.12)	0.24 (0.02)	5.60 (0.29)	8	98.56 (0.70)
NL-4Bb	5.94 (0.21)	0.03 (0.01)	27.35 (0.31)	56.60 (0.31)	0.30 (0.04)	9.35 (0.28)	0.07 (0.02)	0.00 (0.00)	0.56 (0.08)	2	100.88 (0.82)
KV-7Ba	4.61 (0.44)	2.42 (0.23)	16.32 (0.14)	59.56 (1.22)	1.69 (0.15)	5.38 (0.32)	1.21 (0.08)	0.21 (0.04)	7.11 (0.49)	13	98.51 (1.13)
KV-7Bb	4.69 (0.37)	0.59 (0.11)	15.12 (1.78)	69.47 (1.88)	2.59 (0.29)	2.37 (0.48)	0.52 (0.05)	0.10 (0.06)	2.98 (0.35)	4	98.43 (2.06)
BL-4B	3.94 (0.23)	0.15 (0.02)	12.00 (0.01)	72.90 (0.41)	2.78 (0.08)	0.87 (0.02)	0.16 (0.03)	0.03 (0.04)	0.90 (0.02)	3	93.73 (0.58)
LC-3Aa	4.70 (0.19)	2.60 (0.31)	16.05 (0.43)	56.55 (0.83)	1.75 (0.15)	6.23 (0.23)	1.54 (0.08)	0.23 (0.04)	9.04 (0.88)	9	98.70 (1.03)
LC-3Ab	5.14 (0.28)	0.13 (0.03)	28.53 (0.54)	53.94 (0.28)	0.24 (0.06)	11.35 (0.55)	0.13 (0.04)	0.03 (0.02)	0.84 (0.13)	6	100.32 (0.61)
LC-3Ba	5.38 (0.48)	0.06 (0.02)	28.57 (0.53)	54.68 (1.12)	0.26 (0.01)	10.83 (0.83)	0.02 (0.01)	0.02 (0.01)	0.48 (0.02)	4	100.30 (0.37)
LC-3Bb	1.45 (0.06)	0.06 (0.02)	34.37 (0.04)	45.83 (0.22)	0.06 (0.00)	17.86 (0.21)	0.032 (0.04)	0.02 (0.03)	0.64 (0.03)	2	100.32 (0.08)

Values are averages of several individual shards (n) after eliminating outliers (Appendix 2).
Reported values are in weight percent; values in parentheses are one standard deviation.

TABLE 16. SIMILARITY COEFFICIENT MATRIX OF BLACK TEPHRAS

Sample	NL-4Ba	NL-4Bb	KV-7Ba	KV-7Bb	BL-4B	LC-3Aa	LC-3Ab	LC-3Ba	LC-3Bb
NL-4Ba	1.00								
NL-4Bb	0.33	1.00							
KV-7Ba	0.83	0.36	1.00						
KV-7Bb	0.69	0.32	0.60	1.00					
BL-4B	0.46	0.37	0.40	0.56	1.00				
LC-3Aa	0.79	0.37	0.91	0.57	0.39	1.00			
LC-3Ab	0.35	0.65	0.38	0.40	0.63	0.39	1.00		
LC-3Ba	0.33	0.69	0.36	0.33	0.42	0.37	0.74	1.00	
LC-3Bb	0.22	0.49	0.24	0.24	0.38	0.24	0.55	0.68	1.00

Four out of five black tephra samples contained secondary populations, and, on average, 10 analyses were discarded from each sample data set (Appendix 2). This suggests significant contamination by foreign glass shards, minerals, microlites or other components (see methods). Population compositions are calculated from a small number of shards, resulting in unreliable mean values, but note that this is not true for all samples (Appendix 2).

Interestingly, the pumice-rich phase (LC-3A) and the glass-rich phase (LC-3B) of a single sample do not correlate with one another (Table 16). This can be explained in three ways. First, pumice and glass in this tephra layer may have distinctly different major-element chemistries. This hypothesis is weakened by the fact that, in four out of five cases, glass and pumice have comparable major-element chemistries (James Riehle, personal communication, 1994). Second, the tephra layer may be a collection of several tephras deposited by nearly contemporaneous eruptions. Third, significant reworking may have caused multiple tephras to be combined despite the apparent preservation of this tephra

layer, which exhibits sharp bounding contacts (Fig. 45b).

The available ^{14}C ages support the conclusion that at least two of the black tephras are derived from distinct eruptions. The LC black tephra is younger than 8005 ± 70 ^{14}C yr BP (Fig. 44; Table 10), whereas the black tephra in the KV section is older than 9310 ± 70 ^{14}C yr BP (Fig. 43; Table 10). These dates demonstrate that the two black tephras were erupted at least 1300 yr apart.

These data indicate that black tephra layers are less pure and inherently more complicated than pink-orange tephras. This finding agrees with that of D. Pinney (personal communication, 1995), who also recognized a number of black tephra layers in the area, but was unable to successfully correlate them. Apparently, either multiple eruptions of chemically distinct black tephras took place on the upper Alaska Peninsula, or the samples have been contaminated by reworking.

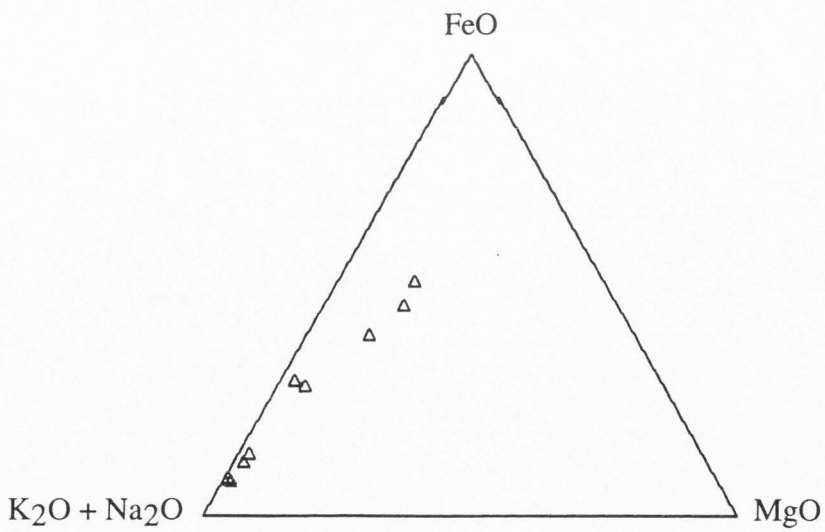

Figure 50. Ternary plot of three major oxides for black tephras.

Ash C

Five samples of ash C, a prominent ash horizon around Brooks Camp, exhibit extremely variable glass chemistries between and within its color horizons. Three out of five samples contain both primary and secondary populations, whereas the other two are unimodal (Table 17). The number of discarded analyses ranged from 3 to 11 (Appendix 2).

Seven out of 28 possible sample pairs correlate with S.C. values ranging from 0.95 to 0.98 (Table 18). The secondary population of the gray horizon of ash C (BC-3Cb) sampled at Brooks Camp is correlative with black (BC-3F), yellow (NL-3Bb), and gray (NL-3Ca) zones of ash C. Likewise, the black horizon BC-3F correlates with the secondary population of the gray horizon NL-3Cb. Finally, primary and secondary populations of the yellow horizon NL-3B (NL-3Ba and NL-3Bb) are correlative with secondary and primary populations of the gray horizon NL-3C (NL-3Cb and NL-3Ca, respectively). All other samples have S.C. values ranging from 0.64 to 0.93, which fail to support any correlations.

Because only 25% of the chemical modes contained in the five samples of ash C correlate, it can be concluded that ash C is comprised of more than one ash. The number of distinct tephras, however, is difficult to estimate. For those seven samples that do correlate, only one is between samples of corresponding color. That is, only once does a chemical population in a gray zone (BC-3Cb) correlate with a mode in another gray zone (NL-3Ca). In the remaining six cases, correlations are between different color zones, demonstrating that the gray, black, and yellow color zones of ash C do not represent unique ashes as originally purported. This finding is consistent with my data on the multiple black tephras, as well as Riehle (undated), who reported many distinct tephras in the area.

Aniakchak volcano, which is located on the western side of the Alaska Peninsula approximately 200 km southwest of the Iliamna/Naknek/Brooks Lake area, has erupted a large number of Holocene tephras of a wide range of compositions. For example, sometimes glass of a single tephra fall is heterogenous and matches glass of other Aniakchak samples having significantly different ages. Samples BC-3C, BC-3F, and NL-3B appear to have an Aniakchak origin; however, this does not necessarily indicate that they are of the same tephrafall (James Riehle, personal communication, 1995).

It is suggested that there has been substantial reworking of tephras within ash C. Additionally, the different color zones of the ash are only ~1-2 cm thick; therefore, there is a possibility that they were cross-contaminated during sampling. The data may be explained by several relatively contemporaneous eruptions in this active volcanic area that would have caused substantial mixing between ashes. Alternatively, the consistent color zonation of ash C may be a postdepositional weathering feature as original suggested by Donald Dumond (personal communication, 1994).

TABLE 17. MAJOR-ELEMENT COMPOSITIONS OF ASH C SAMPLES

Sample	Color	Na2O	MgO	Al2O3	SiO2	K2O	CaO	TiO2	MnO	FeO	n	Total
BC-3H	yellow	4.99 (0.17)	1.19 (0.11)	16.15 (0.32)	65.74 (0.51)	2.52 (0.22)	3.41 (0.23)	0.89 (0.10)	0.17 (0.02)	4.37 (0.31)	10	99.43 (0.60)
BC-3Ca	gray	4.74 (0.08)	1.44 (0.25)	15.20 (0.40)	64.49 (1.45)	2.38 (0.18)	3.67 (0.53)	0.84 (0.08)	0.17 (0.02)	4.90 (0.64)	5	97.82 (0.92)
BC-3Cb	gray	4.52 (0.34)	2.75 (0.45)	16.49 (0.66)	58.35 (1.07)	1.55 (0.19)	6.46 (0.36)	1.10 (0.05)	0.16 (0.05)	7.37 (0.85)	4	98.74 (0.67)
BC-3F	black	4.31 (0.19)	2.89 (0.24)	16.45 (0.13)	58.62 (1.17)	1.64 (0.12)	6.36 (0.43)	1.14 (0.08)	0.18 (0.03)	7.92 (0.60)	17	99.51 (0.53)
NL-3Ba	yellow	5.01 (0.14)	0.85 (0.11)	15.26 (0.19)	68.10 (0.60)	2.80 (0.12)	2.56 (0.19)	0.79 (0.12)	0.17 (0.02)	3.66 (0.61)	8	99.19 (0.74)
NL-3Bb	yellow	4.33 (0.15)	2.83 (0.22)	16.45 (0.11)	59.11 (1.24)	1.68 (0.13)	6.23 (0.42)	1.14 (0.06)	0.20 (0.04)	7.64 (0.62)	7	99.60 (0.39)
NL-3Ca	gray	4.43 (0.10)	2.66 (0.25)	16.24 (0.24)	59.65 (1.05)	1.76 (0.15)	5.91 (0.49)	1.08 (0.08)	0.18 (0.02)	7.48 (0.62)	13	99.38 (0.64)
NL-3Cb	gray	4.98 (0.21)	0.87 (0.04)	15.42 (0.45)	67.81 (0.33)	2.75 (0.18)	2.54 (0.11)	0.80 (0.10)	0.12 (0.03)	3.65 (0.43)	4	98.93 (0.34)

Values are averages of several individual shards (n) after eliminating outliers (Appendix 2).
Reported values are in weight percent; values in parentheses are one standard deviation.

TABLE 18. SIMILARITY COEFFICIENT MATRIX OF ASH C SAMPLES. S.C. VALUES ≥ 0.95 ARE SHOWN IN BOLD

Sample	BC-3H	BC-3Ca	BC-3Cb	BC-3F	NL-3Ba	NL-3Bb	NL-3Ca	NL-3Cb
BC-3H	1.00							
BC-3Ca	0.93	1.00						
BC-3Cb	0.75	0.77	1.00					
BC-3F	0.73	0.76	**0.96**	1.00				
NL-3Ba	0.89	0.86	0.68	0.66	1.00			
NL-3Bb	0.73	0.75	**0.95**	0.67	0.67	1.00		
NL-3Ca	0.76	0.79	**0.95**	**0.98**	0.70	**0.96**	1.00	
NL-3Cb	0.86	0.83	0.66	**0.96**	**0.96**	0.64	0.66	1.00

SUMMARY AND CONCLUSION

Sixteen tephra layers sampled on the upper Alaska Peninsula fall into three distinct categories: latest Pleistocene pink-orange, early Holocene black, and late Holocene ash C. Five of the six pink-orange tephra samples are correlative with Pinney and Begét's (1991b) Lethe tephra, which is older than 12.6 ka and younger than the Iliuk stade of the Brooks Lake glaciation. These findings extend the ash plume 125 km westward and 150 km northwestward from its presumed source area near the Valley of Ten Thousand Smokes. Two unpublished ^{14}C dates of 12.7 and 12.8 ka (Peter Lea, personal communication, 1994) increase the minimum-limiting age on Lethe tephra by 1-2 ka. Furthermore, a new, previously unreported secondary population of Lethe tephra is now recognized.

Black tephra layers are significantly more chemically diverse than pink-orange tephra layers. No correlations between black tephra layers emerged from this study. Two

^{14}C ages and glass chemistry suggest that multiple black tephras are present in the study area all of early Holocene age, or that the tephra was contaminated.

The major-element chemistry of three color zones of ash C demonstrates that it is comprised of multiple ashes. The color zones, however, do not represent single tephras; rather, multiple ashes are scattered throughout the thickness of the layer. These findings, along with those of Riehle (undated), indicate that caution should be used when using ash color to correlate tephra layers.

CHAPTER 5
CONCLUSION

The Alaska Peninsula glacial record not only reflects regional climate change in Alaska, but also global climate cooling associated with marine oxygen-isotope stage 2. This record exhibits evidence for five stades, which is more than any other glacial sequence yet recognized in Alaska. This thesis demonstrates that two glacial systems responded uniquely to climate change. The Iliamna Lake valley was fed by an outlet lobe of the Cordilleran Ice Sheet, whereas the Naknek Lake valley was fed by a coalescent system of local-mountain glaciers. Apparently the different source areas created different patterns of moraines in the two valleys.

Following deglaciation of the lake basins, lake levels lowered, forming a suite of shorelines rimming Iliamna and Naknek lakes. Surprisingly, these terraces are not tilted in an east-west direction as a result of glacial-isostatic rebound or regional tectonism. Geochronology indicates that most of the terraces were formed during the Pleistocene-Holocene transition. The presence of broad, prominent terraces approximately halfway between present-day lake level and the highest terrace at both Iliamna and Naknek lakes suggests some climate control on lake-level fluctuations.

Electron-microprobe analysis of six late-Pleistocene tephra samples allows five to be correlated with latest-Pleistocene Lethe tephra of Pinney and Begét (1991a,b), extending the Lethe plume westward across Bristol Bay and northwestward into the Iliamna Lake valley and providing a valuable ~12.6-12.8 ka marker horizon throughout the Bristol Bay region.

The Iliamna/Naknek/Brooks Lake area contains a storehouse of evidence for both

regional and global climate change. The glacial record was clearly climatically controlled, whereas climate appears to have also influenced lake-level fluctuations. Lethe tephra, organic matter, correlations, and stratigraphic relations help to constrain the ages of the five stades of the Brooks Lake glaciation and lake-level fluctuations and place them in a regional and global context.

REFERENCES

American Association of Petroleum Geologists, 1983, North American stratigraphic code: American Association of Petroleum Geologists Bulletin, v. 67, p. 841-845.

Andrews, J.T., 1975, Glacial systems, An approach to glaciers and their environments: North Scituate, Massachusetts, Duxbury Press, 191 p.

Ashley, G.M., Shaw, J., and, Smith, N.D., eds., 1985, Glacial sedimentary environments: Tulsa, Oklahoma, Society of Paleontologists and Mineralogists SEPM Short Course no. 16, 246 p.

Begét, J., Edwards, M., Hopkins, D., Keskinen, M., and Kukla, G., 1991, Old Crow Tephra found at the Palisades of the Yukon, Alaska: Quaternary Research, v. 35, p. 291-297.

Begét, J., Mason, O., and Anderson, P., 1992, Age, extent and climatic significance of the 3400 ^{14}C yr BP Aniakchak tephra, Western Alaska, USA: The Holocene, v. 2, p. 51-56.

Birkeland, P.W., 1984, Soils and geomorphology: New York, New York, Oxford University Press, p. 3-37.

Birkeland, P.W., Colman, S.M., Burke, R.M., Shroba, R.R, and Meierding, T.C., 1979, Nomenclature of alpine glacial deposits, or, What's in a name?: Geology, v. 7, p. 532-536.

Borchardt, G.A., Aruscavage, P.J., and Millard, H.T., Jr., 1972, Correlation of the Bishop Ash, a Pleistocene marker bed, using instrumental neutron activation analysis: Journal of Sedimentary Petrology, v. 42, p. 301-306.

Broecker, W.S., 1994, Massive iceberg discharges as triggers for global climate change: Nature, v. 372, p. 421-424.

Burke, R.M., and Birkeland, P.W., 1979, Reevaluation of multiparameter relative dating techniques and their application to the glacial sequence along the eastern escarpment of the Sierra Nevada, California: Quaternary Research, v. 11, p. 21-51.

Clark, J.A., Hendriks, M., Timmermans, T.J., Struck, C., and Hilverda, K.J., 1994, Glacial isostatic deformation of the Great Lakes region: Geological Society of America Bulletin, v. 106, p. 19-31.

Colman, S.M., and Pierce, K.L., 1986, Glacial sequence near McCall, Idaho -- weathering rinds, soil development, morphology, and other relative-age criteria: Quaternary Research, v. 25, p. 25-42.

Dansgaard, W., Johnsen, S.J., Clausen, H.B., Dahl-Jensen, D., Gundestrup, N.S.,

Hammer, C.U., Hvidberg, C.S., Steffensen, J.P., Sveinbjornsdottir, A.E., Jouzel, J., and Bond, B., 1993, Evidence for general instability of past climate from a 250-kyr ice-core record: Nature, v. 364, p. 218-220.

Dawson, A.G., 1992, Ice age earth: New York, Routledge, 293 p.

Denton, G.H., 1974, Quaternary glaciations of the White River valley, Alaska, with a regional synthesis for the northern St. Elias Mountains, Alaska and Yukon territory: Geological Society of America Bulletin, v. 85, p. 871-892.

Detterman, R.L., 1986, Glaciation of the Alaska Peninsula, *in* Hamilton, T.D., Reed, K.M., and Thorson, R.M., eds., Glaciation in Alaska -- The geologic record: Anchorage, Alaska, Alaska Geological Society, p. 151-169.

Detterman, R.L., Bowsher, A.L., and Dutro, J.T., Jr., 1958, Glaciation on the Arctic slope of the Brooks Range, northern Alaska: Arctic, v. 11, p. 43-61.

Detterman, R.L., and Reed, B.L., 1973, Surficial deposits of the Iliamna Quadrangle, Alaska: U.S. Geological Survey Bulletin 1368-A, 64 p.

Detterman, R.L., Reed, B.L., and Rubin, M., 1965, Radiocarbon dates from Iliamna Lake, Alaska: U.S. Geological Survey Professional Paper 525-D, p. D34-D36.

Dumond, D.E., 1981, Archaeology on the Alaska Peninsula -- the Naknek Region, 1960-1975: Eugene, Oregon, University of Oregon Anthropological Papers, no. 21, 276 p.

Grootes, P.M., Stuiver, M., White, J.W.C., Johnsen, S., and Jouzel, J., 1993 Comparison of oxygen isotope records from the GISP2 and GRIP Greenland ice cores: Nature, v. 366, p. 552-554.

Hamilton, T.D., 1982, A late Pleistocene glacial chronology for the southern Brooks Range -- stratigraphic and regional significance: Geological Society of America Bulletin, v. 93, p. 700-716.

Hamilton, T.D., 1986, Late Cenozoic glaciation of the central Brooks Range, *in* Hamilton, T.D., Reed, K.M., and Thorson, R.M., eds., Glaciation in Alaska -- The geologic record: Anchorage, Alaska, Alaska Geological Society, p. 9-49.

Hamilton, T.D., 1994, Late Cenozoic glaciation of Alaska, *in* Plafker, G., and Berg, H.C., eds., The geology of Alaska: Boulder, Colorado, Geological Society of America, The Geology of North America, v. G-1, p. 813-884.

Hamilton, T.D., and Porter, S.C., 1975, Itkillik glaciation in the Brooks Range, northern Alaska: Quaternary Research, v. 5, p. 471-497.

Karlstrom, T.N.V., 1964, Surficial geology of the Kenai lowland and glacial history of the

Cook Inlet region, Alaska: U.S. Geological Survey Professional Paper 443, 69 p.

Kaufman, D.S., and Calkin, P.E., 1988, Morphometric analysis of Pleistocene glacial deposits in the Kigluaik Mountains, northwestern, Alaska, U.S.A.: Arctic and Alpine Research, v. 20, p. 273-284.

Kaufman, D.S., and Hopkins, D.M., 1986, Glacial history of the Seward Peninsula, *in* Hamilton, T.D., Reed, K.M., and Thorson, R.M., eds., Glaciation in Alaska -- The geologic record: Anchorage, Alaska, Alaska Geological Society, p. 51-76.

Kaufman, D.S., Lea, P.D., and Forman, S.L., 1994, Early Stage 5 glaciation, NE Bristol Bay, Alaska: Geological Society of America Abstracts with Programs, v. 26, no. 7, A-514.

Kline J.T., and Bundtzen, T.K., 1986, Two glacial records from west-central Alaska, *in* Hamilton, T.D., Reed, K.M., and Thorson, R.M., eds., Glaciation in Alaska -- The geologic record: Anchorage, Alaska, Alaska Geological Society, p. 123-150.

Larsen, C.E., 1987, Geological history of glacial Lake Algonquin and the upper Great Lakes: U.S. Geological Survey Bulletin 1801, 36 p.

Lea, P.D., 1984, Paleoclimatic implication of late Pleistocene glacial asymmetry, Ahklun Mountains, southwestern Alaska: Geological Society of America Abstracts with Programs, v. 16, no. 6, p. 572.

Lea, P.D., 1989, Quaternary environments and depositional systems of the Nushagak lowland, southwestern Alaska [Ph.D. thesis]: Boulder, Colorado, University of Colorado.

Lea, P.D., Elias, S.A., and Short, S.K., 1991, Stratigraphy and paleoenvironments of Pleistocene nonglacial deposits in the southern Nushagak Lowland, southwestern Alaska, U.S.A.: Arctic and Alpine Research, v. 23, p. 375-391.

Lea, P.D., and Waythomas, C.F., 1990, Late-Pleistocene eolian sand sheets in Alaska: Quaternary Research, v. 34, p. 269-281.

Leonard, D.M., 1989, Climatic change in the Colorado Rocky Mountains -- estimates based on modern climate at late Pleistocene equilibrium lines: Arctic and Alpine Research, v. 21, p. 245-255.

Mann, D.H., 1986, Wisconsin and Holocene glaciation of southeast Alaska, *in* Hamilton, T.D., Reed, K.M., and Thorson, R.M., eds., Glaciation in Alaska -- The geologic record: Anchorage, Alaska, Alaska Geological Society, p. 237-265.

Mann, D.H., and Peteet, D.M., 1994, Extent and timing of the Last Glacial Maximum in southwestern Alaska: Quaternary Research, v. 42, p. 136-148.

Meierding, T.C., 1982, Late Pleistocene glacial equilibrium-line altitudes in the Colorado Front Range -- a comparison of methods: Quaternary Research, v. 18, p. 289-310.

Muller, E.H., 1952, The glacial geology of the Naknek District, the Bristol Bay Region, Alaska [Ph.D. thesis]: Urbana, Illinois, University of Illinois.

Nowak, M., 1968, Archeological dating by means of volcanic ash strata [Ph.D. thesis]: Eugene, Oregon, University of Oregon.

Peck, B.J., Kaufman, D.S., and Calkin, P.E., 1990, Relative dating of moraines using moraine morphometric and boulder weathering criteria, Kigluaik Mountains, Alaska: Boreas, v. 19, p. 227-239.

Péwé, T.L., 1975 Quaternary geology of Alaska: US Geological Survey Professional Paper 835, 145 p.

Pinney, D.S., 1993, Late Quaternary glacial and volcanic stratigraphy near Windy Creek, Katmai National Park, Alaska [M.Sc. thesis]: Fairbanks, Alaska, University of Alaska.

Pinney, D.S., and Begét, J.E., 1991a, Deglaciation and latest Pleistocene and early Holocene glacier readvances on the Alaska Peninsula -- records of rapid climate change due to transient changes in solar intensity and atmospheric CO_2 content?, *in* Weller, G., Wilson, C.L., and Severing, B.A.B., eds., International Conference on the role of polar regions in global change: Fairbanks, Alaska, University of Alaska, p. 634-640.

Pinney, D.S., and Begét, J.E., 1991b, Late Pleistocene volcanic deposits near the Valley of Ten Thousand Smokes, Katmai National Park, Alaska, *in* Reger, R.D., ed., Short notes on Alaska geology: Fairbanks, Alaska, Alaska Department of Natural Resources Professional Report 111, p. 45-53.

Porter, S.C., Pierce, K.L., and Hamilton, T.D., 1983, Late Wisconsin mountain glaciation in the western United States, *in* Wright, H.E., Jr., and Porter, S.C., eds., Late Quaternary environments of the United States, vol. the Late Pleistocene: Minneapolis, Minnesota, University of Minnesota Press, p. 71-111.

Riehle, J.R., undated, Description and correlation among late Holocene tephra samples from cultural sites at Brooks Camp, Katmai National Park -- A progress report: Anchorage, Alaska, unpublished report to the National Park Service, 15 p.

Riehle, 1994, Heterogeneity, correlatives, and proposed stratigraphic nomenclature of Hayes tephra set H, Alaska: Quaternary Research, v. 41, p. 285-288

Riehle, J.R., and Detterman, R.L., 1993, Quaternary geologic map of the Mount Katmai Quadrangle and adjacent portions of the Naknek and Afognak quadrangles, Alaska: U.S. Geological Survey Miscellaneous Geologic Investigation Map I-2032.

Rodbell, D.T., 1992, Late Pleistocene equilibrium-line reconstructions in the northern Peruvian Andes: Boreas, v. 21, p. 43-52.

Sarna-Wojcicki, A.M., and Davis, J.O., 1991, Quaternary tephrochronology, *in* Morrison, R.B., ed., Quaternary nonglacial geology -- Conterminous US: Boulder, Colorado, Geological Society of America, The Geology of North America, v. K-2, p. 93-115.

Schmoll, H.R., Szabo, B.J., Rubin, M., and Dobrovolny, E., 1972, Radiometric dating of marine shells from the Bootlegger Cove Clay, Anchorage area, Alaska: Geological Society of America Bulletin, v. 83, p. 1107-1113.

Taylor, L.D., 1990, Evidence of high glacial-lake levels in the northeastern Lake Michigan basin and their relation to the Glenwood and Calumet phases of glacial Lake Chicago, *in* Schneider, A.F., and Fraser, F.S., eds, Late Quaternary history of the Lake Michigan basin: Boulder, Colorado, Geological Society of America Special Paper 251, p. 91-109.

TenBrink, N.W., and Waythomas, C.F., 1985, Late Wisconsin glacial chronology of the north-central Alaska Range - A regional synthesis and its implications for early human settlements, *in* Powers, W.R., ed., North Alaska Range early man project: Washington D.C., National Geographic Society Research Reports, v. 19, p. 15-32.

Thompson, C.H., Kaufman, D.S., and Forman, S.L., 1994a, Quaternary glaciogenic sediments, Naknek River valley, sw Alaska: Geological Society of America Abstracts with Programs, v. 26, no. 7, p. A-126.

Thompson, C.H., Lea, P.D., and Kaufman, D.S., 1994b, Late (?) Wisconsin glaciation in the Wood River Range, southwestern Alaska [abs]: Proceedings, 24th Arctic and Alpine Workshop, Boulder, Colorado, University of Colorado, p. 163-164.

Thorson, R.M., 1986, Late Cenozoic glaciation of the northern Nenana valley, *in* Hamilton, T.D., Reed, K.M., and Thorson R.M., eds., Glaciation in Alaska -- The geologic record: Anchorage, Alaska, Alaska Geological Society, p. 99-121.

Torsnes, I., Rye, N., and Nesje, A., 1993, Modern and Little Ice Age equilibrium-line altitudes on outlet valley glaciers from Jostedalsbreen, western Norway -- An evaluation of different approaches to their calculation: Arctic and Alpine Research, v. 25, p. 106-116.

Weber, F.R., 1986, Glacial geology of the Yukon-Tanana upland, *in* Hamilton, T.D., Reed, K.M., and Thorson, R.M., eds., Glaciation in Alaska -- The geologic record: Anchorage, Alaska, Alaska Geological Society, p. 79-98.

Werner, A., 1995, Glacial history of the McKinley River area, Denali National Park and Preserve, Alaska: Geological Society of America Abstracts with Programs, v. 27, no. 5, p. 83.

APPENDICES

APPENDIX 1. RAW RELATIVE-AGE DATA

Location (Fig. 3)	Stade	Proximal length (m)	Slope angle (°)	Distal length (m)	Slope angle (°)	Crest width (m)	Oxidation thickness (cm)	Muncell color	Granite				Diorite				Coarse-grained weathering index	Basalt				Andesite				Fine-grained weathering index
									1	2	3	4	1	2	3	4		1	2	3	4	1	2	3	4	
1	Ukak	8	19	11	11	21																				
		8	18	12	20	18																				
		22	24	11	19	13																				
		13 ± 8	**20 ± 3**	**11 ± 1**	**17 ± 5**	**17 ± 4**	14	10YR 3/4																		
1	Ukak	17	20	15	16	19																				
		15	22	11	22	16																				
		5	19	11	23	23																				
		20 ± 6	**20 ± 2**	**12 ± 2**	**20 ± 4**	**19 ± 4**	8	10 YR 3/4																		
2	Iliuk	50	19	30	19	98																				
		50	17	30	20	90																				
		25	23	20	19	90																				
		42 ± 14	**20 ± 3**	**27 ± 6**	**19 ± 1**	**93 ± 5**	39	7.5 YR 4/3																		
2	Iliuk	30	14	50	20	30																				
		50	19	30	20	25																				
		55	21	40	19	19																				
		45 ± 13	**18 ± 4**	**40 ± 10**	**20 ± 1**	**25 ± 6**	73	10YR 3/4																		
2	Iliuk	17	21	16	20	16																				
		27	16	15	10	31																				
		22 ± 7	**19 ± 4**	**16 ± 1**	**15 ± 7**	**24 ± 11**	53	10YR 3/4																		
3	Newhalen	18	29	37	11	18																				
		28	30	19	20	12																				
		27	23	20	14	35																				
		24 ± 6	**27 ± 4**	**25 ± 10**	**15 ± 5**	**22 ± 12**	33	10YR 3/4																		
3	Newhalen	45	6	38	12	42																				
		10	20	14	22	16																				
		13	21	9	24	22																				
		23 ± 19	**16 ± 8**	**20 ± 16**	**19 ± 6**	**27 ± 14**	16	10YR 3/4																		
4	Early-late-		14	28	14	20																				
	Wisconsin	13	20	13	14	26																				
	stades	13	17	15	11	26																				
		12 ± 2	**17 ± 3**	**19 ± 8**	**13 ± 2**	**24 ± 3**	12	10YR 3/6	2	6	10	0	0	0	0	0	2.44	1	2	2	2	0	0	0	0	2.71
4	Early-late-	35	12	40	12	26																				
	Wisconsin	8	16	29	15	22																				
	stades	10	10	15	13	18																				
		18 ± 15	**13 ± 3**	**28 ± 13**	**13 ± 2**	**22 ± 4**	19	10YR 3/4	1	5	12	2	0	0	0	0	2.75	0	0	2	1	0	0	0	0	3.33
4	Early-late-		17	25	6	33																				
	Wisconsin	20	12	31	18	25																				
	stades	15	9	90	12	27																				
		22 ± 8	**13 ± 4**	**49 ± 36**	**12 ± 6**	**28 ± 4**	6	10YR 3/6	4	6	10	0	0	0	0	0	2.32	2	0	1	0	0	1	1	0	1.67
4	Early-late-	10	9	17	16	25																				
	Wisconsin	15	13	12	12	23																				
	stades	17	7	16	18	30																				
		14 ± 4	**10 ± 3**	**15 ± 3**	**15 ± 3**	**26 ± 4**	10	10YR 3/3	1	11	11	1	0	0	0	0	2.50	0	0	0	0	0	0	0	0	0.00
5	Kvichak	15	16	33	14	26																				
		14	10	18	16	36																				
		15	16	24	16	36																				
		15 ± 1	**14 ± 3**	**25 ± 8**	**15 ± 1**	**33 ± 6**	39	10YR 3/4	0	19	0	0	0	1	0	0	2.00	7	4	3	1	0	1	1	0	1.94
5	Kvichak	15	12	35	11	19																				
		9	17	30	9	32																				
		16	14	7	12	24																				
		13 ± 4	**14 ± 3**	**24 ± 15**	**11 ± 2**	**25 ± 7**	35	10YR 3/3	0	13	3	0	0	0	0	0	2.19	2	2	2	1	2	1	1	0	2.09
5	Kvichak	30	22	32	12	17																				
		17	9	36	8	48																				
		24	18	17	12	42																				
		24 ± 7	**16 ± 7**	**28 ± 10**	**11 ± 2**	**36 ± 16**	16	10YR 3/4	0	5	4	0	0	0	0	0	2.44	3	3	4	0	2	1	3	0	2.13
6	Iliamna	38	6	16	11																					
		60	5	18	11																					
		49 ± 16	**6 ± 1**	**17 ± 1**	**11 ± 0**		24	10YR 2/2																		
6	Iliamna	30	15	30	14	22																				
		13	12	12	10	20																				
		12	20	9	6	30																				
		18 ± 10	**16 ± 4**	**17 ± 11**	**10 ± 4**	**24 ± 5**	28	10YR 3/4	1	2	0	0	0	0	0	0	1.67	10	9	2	0	0	1	0	0	1.64
7	Iliamna	20	10	12	16	22																				
		7	10	8	8	20																				
		9	9	8	8	28																				
		12 ± 7	**10 ± 1**	**9 ± 2**	**11 ± 5**	**23 ± 4**	22	10YR 4/4	2	4	6	0	1	1	0	0	2.21	0	1	1	0	2	4	3	0	2.18
7	Iliamna	9	11	9	16	18																				
		7	8	14	14	35																				
		14	12	9	6	32																				
		10 ± 4	**10 ± 2**	**10 ± 3**	**11 ± 5**	**28 ± 9**	11	10YR 4/3	0	11	2	0	1	1	0	0	2.07	2	1	0	0	3	3	1	0	1.6
7	Iliamna	30	16	9	13	27																				
		10	12	40	12	22																				
		50	12	39	11	26																				
		30 ± 20	**13 ± 2**	**29 ± 18**	**12 ± 1**	**25 ± 3**	7	10YR 3/4																		
8	Newhalen	28	23	45	16	31																				
		19	17	22	20	14																				
		9	22	14	23	19																				
		19 ± 10	**21 ± 3**	**27 ± 16**	**20 ± 4**	**21 ± 9**	17		2	8	9	1	0	0	0	0	2.45	1	0	0	0	2	0	0	0	1.00
8	Newhalen	12	20	20	18	19																				
		34	19	30	17	22																				
		25	18	38	27	15																				
		24 ± 11	**19 ± 1**	**29 ± 9**	**21 ± 6**	**19 ± 4**	36		7	9	3	0	1	0	0	0	1.75	1	0	0	0	0	2	1	0	2.00
8	Newhalen	12	17	6	15	6																				
		12	19	27	18	28																				
		30	14	30	10	20																				
		18 ± 10	**17 ± 3**	**21 ± 13**	**14 ± 4**	**18 ± 11**	22		7	7	2	0	1	0	0	0	1.65	2	1	0	0	1	3	1	0	1.75

APPENDIX 2. MAJOR-ELEMENT CHEMISTRY FOR TEPHRA SAMPLES[5]

[5] Standard used during analyses. Every table shows primary and secondary populations, and discarded analyses. Samples first organized by category: (1) pink-orange tephra, (2) black tephra, and (3) ash C, and within categories, alphabetically. Pink-orange data are normalized to 100% following Pinney and Begét (1991b), whereas black and ash C data are given in weight percent. Analyst: Charles Meyer (USGS Menlo Park).

	Na2O	MgO	Al2O3	SiO2	K2O	CaO	TiO2	MnO	FeO	Total
Reported	5.25	0.05	11.44	75.70	4.53	0.12	0.21	0.15	2.12	99.60

10 micron beam. GLMP basalt for Mg,Ca,Fe; VG568, Yellowstone Rhyo (RLS-132), for other elements.

	Na2O	MgO	Al2O3	SiO2	K2O	CaO	TiO2	FeO	Total
					BL-4Aa (n=6)				
	4.17	0.09	12.17	77.87	3.53	0.61	0.18	1.37	100.00
	4.38	0.10	12.18	78.02	3.40	0.64	0.17	1.10	100.00
	4.33	0.11	12.22	77.86	3.51	0.64	0.17	1.15	100.00
	4.30	0.11	12.13	77.81	3.59	0.61	0.19	1.27	100.00
	4.35	0.11	12.08	77.98	3.56	0.58	0.22	1.13	100.00
	4.42	0.12	12.12	78.08	3.16	0.65	0.26	1.20	100.00
Average	**4.33**	**0.11**	**12.15**	**77.94**	**3.46**	**0.62**	**0.20**	**1.20**	**100.00**
Stdev:	**0.09**	**0.01**	**0.05**	**0.11**	**0.16**	**0.03**	**0.04**	**0.10**	**0.00**
					BL-4Ab (n=2)				
	4.37	0.35	13.17	75.55	2.78	1.33	0.52	1.93	100.00
	4.46	0.29	12.88	76.28	2.73	1.27	0.40	1.71	100.00
Average:	**4.41**	**0.32**	**13.02**	**75.92**	**2.75**	**1.30**	**0.46**	**1.82**	**100.00**
Stdev:	**0.06**	**0.04**	**0.21**	**0.51**	**0.04**	**0.05**	**0.09**	**0.16**	**0.00**
					BL-4A Discarded analyses (n=13)				
	2.27	0.11	12.31	79.87	3.21	0.66	0.24	1.33	100.00
	3.97	0.15	12.36	77.09	3.84	1.04	0.21	1.34	100.00
	3.33	0.14	12.96	77.99	3.62	0.91	0.15	0.90	100.00
	4.20	0.14	12.93	77.71	2.89	0.93	0.18	1.01	100.00
	3.95	0.13	12.83	78.13	3.01	0.91	0.19	0.85	100.00
	4.35	0.38	12.95	75.44	2.76	1.57	0.47	2.08	100.00
	4.41	0.37	12.93	75.52	2.69	1.63	0.49	1.98	100.00
	4.59	0.77	14.39	71.43	2.39	2.66	0.67	3.09	100.00
	5.46	0.21	17.61	69.69	1.75	3.70	0.24	1.34	100.00
	5.29	0.06	28.81	53.80	0.14	11.31	0.09	0.51	100.00
	7.76	0.04	24.27	61.03	0.47	6.07	0.03	0.33	100.00
	8.04	0.02	24.15	61.16	0.59	5.71	0.02	0.29	100.00
	8.47	0.02	23.79	61.40	0.50	5.52	0.00	0.30	100.00

	Na2O	MgO	Al2O3	SiO2	K2O	CaO	TiO2	FeO	Total
					HB-1a (n=14)				
	4.62	0.67	14.38	71.63	2.42	2.53	0.60	3.15	100.00
	4.39	0.72	14.48	71.61	2.37	2.63	0.64	3.16	100.00
	4.50	0.58	13.90	72.94	2.56	2.14	0.56	2.82	100.00
	4.43	0.59	13.94	73.08	2.44	2.17	0.65	2.70	100.00
	4.65	0.71	14.20	71.79	2.41	2.64	0.68	2.94	100.00
	4.46	0.48	14.45	72.30	2.54	2.35	0.65	2.77	100.00
	4.63	0.75	14.46	71.60	2.33	2.65	0.58	2.99	100.00
	4.55	0.74	14.27	71.74	2.37	2.61	0.71	3.00	100.00
	4.53	0.69	14.25	72.08	2.42	2.42	0.63	2.99	100.00
	4.47	0.73	14.20	72.00	2.41	2.53	0.59	3.06	100.00
	4.31	0.66	14.21	72.10	2.53	2.45	0.65	3.09	100.00
	4.65	0.70	14.28	71.83	2.34	2.46	0.60	3.14	100.00
	4.63	0.70	14.21	72.05	2.37	2.51	0.61	2.91	100.00
	4.45	0.70	14.46	71.83	2.34	2.57	0.69	2.96	100.00
Average:	**4.52**	**0.67**	**14.26**	**72.04**	**2.42**	**2.48**	**0.63**	**2.98**	**100.00**
Stdev:	**0.11**	**0.08**	**0.18**	**0.46**	**0.08**	**0.16**	**0.04**	**0.14**	**0.00**
					HB-1b (n=4)				
	4.57	0.54	13.71	73.42	2.55	2.06	0.57	2.58	100.00
	4.30	0.53	12.94	73.98	2.78	1.92	0.65	2.91	100.00
	4.42	0.50	13.52	73.66	2.93	1.76	0.61	2.60	100.00
	4.35	0.56	13.65	73.47	2.60	2.05	0.68	2.64	100.00
Average:	**4.41**	**0.53**	**13.46**	**73.63**	**2.71**	**1.95**	**0.63**	**2.68**	**100.00**
Stdev:	**0.12**	**0.03**	**0.35**	**0.25**	**0.17**	**0.14**	**0.05**	**0.15**	**0.00**
					HB-1 Discarded analyses (n=1)				
	4.25	0.36	13.00	75.57	2.78	1.50	0.48	2.07	100.00

	Na2O	MgO	Al2O3	SiO2	K2O	CaO	TiO2	FeO	Total
					JH-11a (n=15)				
	4.53	0.53	14.09	72.64	2.53	2.29	0.54	2.84	100.00
	4.46	0.65	13.91	72.60	2.64	2.30	0.56	2.87	100.00
	4.48	0.62	13.96	72.40	2.60	2.41	0.61	2.92	100.00
	4.65	0.70	14.31	71.68	2.48	2.61	0.63	2.94	100.00
	4.25	0.70	14.07	72.43	2.51	2.40	0.68	2.95	100.00
	4.42	0.64	14.42	71.84	2.42	2.62	0.66	2.97	100.00
	4.61	0.78	14.28	71.63	2.48	2.59	0.63	2.99	100.00
	4.23	0.61	14.16	72.36	2.49	2.52	0.60	3.01	100.00
	4.55	0.67	14.38	71.77	2.37	2.55	0.65	3.06	100.00
	4.50	0.72	14.36	71.67	2.47	2.62	0.57	3.08	100.00
	4.48	0.65	14.28	71.95	2.52	2.39	0.64	3.10	100.00
	4.65	0.73	14.32	71.40	2.35	2.85	0.60	3.10	100.00
	4.48	0.64	14.24	71.91	2.45	2.49	0.65	3.14	100.00
	4.38	0.72	14.34	71.52	2.53	2.51	0.64	3.36	100.00
	4.47	0.71	14.19	71.66	2.39	2.62	0.55	3.40	100.00
Average:	**4.48**	**0.67**	**14.22**	**71.96**	**2.48**	**2.52**	**0.61**	**3.05**	**100.00**
Stdev:	**0.12**	**0.06**	**0.15**	**0.41**	**0.08**	**0.15**	**0.04**	**0.16**	**0.00**
					JH-11b (n=2)				
	4.48	0.49	13.44	73.89	2.68	1.82	0.58	2.62	100.00
	4.42	0.46	13.32	74.47	2.71	1.85	0.52	2.25	100.00
Average:	**4.45**	**0.48**	**13.38**	**74.18**	**2.70**	**1.83**	**0.55**	**2.44**	**100.00**
Stdev:	**0.04**	**0.02**	**0.08**	**0.41**	**0.02**	**0.02**	**0.04**	**0.27**	**0.00**
					JH-11 Discarded analyses (n=1)				
	4.39	0.12	12.13	77.75	3.58	0.64	0.19	1.20	100.00

	Na2O	MgO	Al2O3	SiO2	K2O	CaO	TiO2	FeO	Total
					KV-7A (n=18)				
	4.43	0.64	14.22	72.14	2.50	2.51	0.62	2.95	100.00
	4.36	0.70	13.67	72.71	2.58	2.20	0.64	3.15	100.00
	4.74	0.54	15.08	71.39	2.22	2.92	0.47	2.65	100.00
	4.40	0.64	14.06	72.40	2.49	2.46	0.59	2.96	100.00
	4.42	0.51	13.98	73.27	2.58	2.18	0.63	2.44	100.00
	4.52	0.75	14.22	71.70	2.48	2.60	0.58	3.16	100.00
	4.56	0.73	14.30	71.77	2.43	2.54	0.70	2.97	100.00
	4.55	0.65	14.12	72.12	2.55	2.51	0.64	2.86	100.00
	4.39	0.53	13.58	73.60	2.68	2.17	0.48	2.58	100.00
	4.65	0.62	14.21	72.38	2.44	2.28	0.56	2.87	100.00
	4.67	0.69	14.06	72.29	2.45	2.47	0.64	2.72	100.00
	4.55	0.60	14.05	72.50	2.47	2.32	0.57	2.94	100.00
	4.35	0.53	13.61	73.78	2.62	2.00	0.60	2.52	100.00
	4.54	0.67	14.19	71.93	2.50	2.47	0.68	3.02	100.00
	4.31	0.61	14.08	72.70	2.50	2.45	0.50	2.83	100.00
	4.28	0.58	13.95	72.93	2.61	2.30	0.60	2.73	100.00
	4.58	0.69	14.38	71.54	2.41	2.55	0.66	3.19	100.00
	4.58	0.73	14.13	71.76	2.39	2.62	0.72	3.08	100.00
Average:	**4.49**	**0.63**	**14.11**	**72.38**	**2.49**	**2.42**	**0.60**	**2.87**	**100.00**
Stdev:	**0.13**	**0.07**	**0.33**	**0.69**	**0.10**	**0.21**	**0.07**	**0.22**	**0.00**
					KV-7A Discarded analyses (n=2)				
	4.40	0.31	12.71	76.17	2.79	1.35	0.44	1.83	100.00
	4.20	0.26	12.43	76.77	2.88	1.18	0.41	1.86	100.00

	Na2O	MgO	Al2O3	SiO2	K2O	CaO	TiO2	FeO	Total
					LC-3C (n=16)				
	4.63	0.71	14.17	72.12	2.45	2.44	0.64	2.85	100.00
	4.55	0.68	14.10	72.04	2.51	2.53	0.56	3.04	100.00
	4.56	0.53	13.78	73.32	2.64	2.09	0.54	2.54	100.00
	4.62	0.74	14.63	70.94	2.41	2.69	0.67	3.30	100.00
	4.53	0.71	14.16	72.13	2.36	2.51	0.58	3.02	100.00
	4.27	0.63	14.20	72.43	2.53	2.43	0.58	2.93	100.00
	4.48	0.70	14.30	72.03	2.42	2.52	0.57	2.98	100.00
	4.39	0.46	13.33	74.74	2.64	1.71	0.48	2.26	100.00
	4.56	0.55	13.49	73.24	2.66	2.02	0.74	2.73	100.00
	4.53	0.48	13.49	73.91	2.62	1.89	0.60	2.49	100.00
	4.55	0.72	14.16	71.93	2.44	2.58	0.60	3.01	100.00
	4.49	0.70	14.13	72.30	2.46	2.41	0.59	2.92	100.00
	4.45	0.44	13.63	74.38	2.60	1.77	0.58	2.16	100.00
	4.34	0.45	13.55	74.30	2.65	1.84	0.58	2.28	100.00
	4.49	0.68	14.23	72.15	2.44	2.49	0.58	2.93	100.00
	4.58	0.74	14.38	71.52	2.43	2.59	0.71	3.05	100.00
Average:	**4.50**	**0.62**	**13.98**	**72.72**	**2.52**	**2.28**	**0.60**	**2.78**	**100.00**
Stdev:	**0.10**	**0.11**	**0.38**	**1.12**	**0.10**	**0.33**	**0.06**	**0.34**	**0.00**
					LC-3C Discarded analyses (n=4)				
	5.69	0.18	19.35	66.98	1.56	4.76	0.20	1.29	100.00
	5.76	0.20	18.46	67.96	1.62	4.28	0.34	1.37	100.00
	5.43	0.31	19.67	66.01	1.54	5.22	0.29	1.53	100.00
	4.25	0.40	13.00	75.64	2.69	1.53	0.43	2.05	100.00

	Na2O	MgO	Al2O3	SiO2	K2O	CaO	TiO2	FeO	Total
					UFO-2C (n=18)				
	4.45	0.47	13.48	74.17	2.60	1.82	0.52	2.49	100.00
	4.48	0.58	13.52	73.75	2.64	2.02	0.51	2.50	100.00
	4.36	0.57	13.58	73.77	2.57	2.08	0.62	2.46	100.00
	4.46	0.60	13.69	73.17	2.58	2.16	0.50	2.85	100.00
	4.59	0.54	13.72	72.96	2.55	2.23	0.72	2.68	100.00
	4.31	0.67	14.06	72.46	2.54	2.36	0.69	2.92	100.00
	4.53	0.73	14.46	71.76	2.38	2.47	0.64	3.03	100.00
	4.57	0.72	14.06	72.26	2.45	2.43	0.60	2.90	100.00
	4.46	0.64	13.97	72.40	2.50	2.44	0.66	2.92	100.00
	4.58	0.66	14.37	71.93	2.43	2.52	0.68	2.83	100.00
	4.50	0.65	14.19	72.15	2.47	2.49	0.60	2.95	100.00
	4.58	0.71	13.94	72.24	2.40	2.53	0.64	2.95	100.00
	4.43	0.73	14.18	72.14	2.57	2.53	0.64	2.79	100.00
	4.57	0.68	13.99	71.97	2.32	2.52	0.79	3.16	100.00
	4.75	0.71	14.20	71.87	2.38	2.53	0.57	3.00	100.00
	4.59	0.71	14.27	71.65	2.27	2.59	0.72	3.20	100.00
	4.49	0.71	14.21	71.75	2.32	2.58	0.68	3.26	100.00
	4.52	0.74	14.31	71.71	2.42	2.67	0.64	2.98	100.00
Average:	**4.51**	**0.66**	**14.01**	**72.45**	**2.47**	**2.39**	**0.63**	**2.88**	**100.00**
Stdev:	**0.10**	**0.08**	**0.30**	**0.78**	**0.11**	**0.23**	**0.08**	**0.23**	**0.00**
					UFO-2C Discarded analyses (n=2)				
	4.27	0.08	11.99	78.48	3.36	0.65	0.10	1.07	100.00
	4.16	0.44	13.37	74.60	2.60	1.93	0.50	2.39	100.00

	Na2O	MgO	Al2O3	SiO2	K2O	CaO	TiO2	MnO	FeO	Total
					BL-4B (n=3)					
	3.69	0.16	11.89	72.43	2.83	0.89	0.19	0.08	0.92	93.06
	3.97	0.13	12.08	73.10	2.82	0.87	0.16	0.01	0.92	94.04
	4.15	0.18	12.03	73.18	2.68	0.85	0.13	0.02	0.88	94.10
Average:	**3.94**	**0.15**	**12.00**	**72.90**	**2.78**	**0.87**	**0.16**	**0.03**	**0.90**	**93.73**
Stdev:	**0.23**	**0.02**	**0.10**	**0.41**	**0.08**	**0.02**	**0.03**	**0.04**	**0.02**	**0.58**
					BL-4B Discarded analyses (n=16)					
	4.42	0.05	30.72	52.92	0.15	13.06	0.03	0.00	0.70	102.04
	5.39	0.00	30.09	54.60	0.08	11.43	0.00	0.00	0.12	101.71
	6.60	0.02	27.78	56.30	0.25	9.35	0.01	0.02	0.18	100.49
	0.00	0.00	0.08	99.24	0.00	0.01	0.00	0.00	0.05	99.38
	0.00	0.00	0.01	98.93	0.02	0.04	0.02	0.00	0.00	99.02
	0.01	0.01	0.04	98.94	0.02	0.00	0.03	0.02	0.05	99.11
	0.02	0.00	0.06	99.06	0.02	0.01	0.00	0.00	0.00	99.15
	0.02	0.01	0.01	99.22	0.02	0.02	0.00	0.01	0.00	99.32
	0.91	0.00	18.85	64.21	15.21	0.00	0.00	0.00	0.07	99.25
	2.00	0.07	34.13	47.49	0.06	17.31	0.06	0.01	0.71	101.83
	2.29	0.05	12.39	70.20	5.79	0.58	0.11	0.00	0.93	92.36
	2.35	0.20	11.28	72.42	3.95	0.65	0.11	0.12	0.87	91.94
	2.45	0.05	12.42	70.22	5.87	0.60	0.12	0.05	1.05	92.83
	5.38	0.29	13.72	73.88	2.36	1.31	0.31	0.10	1.63	98.98
	4.35	0.51	13.60	73.18	2.61	1.97	0.52	0.04	2.61	99.39
	4.76	0.24	13.77	73.25	3.61	1.19	0.27	0.07	1.98	99.15

	Na2O	MgO	Al2O3	SiO2	K2O	CaO	TiO2	MnO	FeO	Total
					KV-7Ba (n=13)					
	4.78	2.38	16.25	59.09	1.78	5.33	1.11	0.21	6.96	97.88
	4.58	2.46	16.35	59.41	1.60	5.40	1.11	0.23	7.44	98.57
	4.77	2.28	16.28	59.58	1.83	5.10	1.16	0.19	6.58	97.78
	4.83	2.18	16.46	59.90	1.70	5.15	1.17	0.24	6.25	97.86
	5.09	2.15	16.05	60.87	1.90	5.23	1.17	0.22	7.31	99.99
	4.78	2.20	16.40	61.66	1.84	5.09	1.18	0.27	6.64	100.05
	3.34	2.68	16.45	57.74	1.48	5.69	1.19	0.20	7.39	96.15
	4.52	2.56	16.39	58.49	1.54	5.59	1.21	0.16	7.26	97.71
	4.64	2.22	16.11	60.43	1.81	5.09	1.21	0.13	6.66	98.30
	4.62	2.73	16.59	59.09	1.57	5.83	1.22	0.26	7.63	99.54
	5.01	2.19	16.29	61.32	1.81	4.92	1.25	0.23	6.91	99.93
	4.22	2.76	16.36	58.35	1.56	5.80	1.32	0.21	7.57	98.15
	4.72	2.63	16.26	58.41	1.50	5.78	1.38	0.16	7.88	98.73
Average:	**4.61**	**2.42**	**16.32**	**59.56**	**1.69**	**5.38**	**1.21**	**0.21**	**7.11**	**98.51**
Stdev:	**0.44**	**0.23**	**0.14**	**1.22**	**0.15**	**0.32**	**0.08**	**0.04**	**0.49**	**1.13**
					KV-7Bb (n=4)					
	4.21	0.48	13.13	70.31	2.43	1.78	0.51	0.04	2.53	95.41
	4.62	0.72	14.29	71.72	2.48	2.52	0.59	0.06	3.04	100.04
	4.84	0.53	17.22	67.74	2.43	2.92	0.47	0.13	2.98	99.25
	5.09	0.65	15.83	68.11	3.02	2.27	0.50	0.18	3.37	99.02
Average:	**4.69**	**0.59**	**15.12**	**69.47**	**2.59**	**2.37**	**0.52**	**0.10**	**2.98**	**98.43**
Stdev:	**0.37**	**0.11**	**1.78**	**1.88**	**0.29**	**0.48**	**0.05**	**0.06**	**0.35**	**2.06**
					KV-7B Discarded analyses (n=3)					
	2.25	0.72	14.24	72.22	2.39	2.51	0.54	0.06	3.10	98.02
	4.02	0.10	30.29	51.58	0.14	12.96	0.08	0.02	0.82	99.99
	5.11	1.91	18.58	60.13	1.27	6.37	1.03	0.13	5.89	100.42

	Na2O	MgO	Al2O3	SiO2	K2O	CaO	TiO2	MnO	FeO	Total
					LC-3Aa (n=9)					
	4.73	2.47	15.50	57.45	2.01	5.90	1.52	0.20	7.63	97.41
	5.00	2.34	16.81	58.04	1.66	6.38	1.56	0.18	8.12	100.09
	4.47	2.61	16.44	56.25	1.64	6.13	1.46	0.24	8.64	97.88
	4.73	1.94	16.27	56.81	1.73	5.94	1.46	0.18	8.80	97.87
	4.43	2.87	16.23	55.51	1.65	6.36	1.48	0.28	9.12	97.93
	4.88	2.87	15.70	56.81	2.00	6.08	1.71	0.26	9.26	99.56
	4.67	2.82	15.58	55.67	1.73	6.44	1.60	0.26	9.50	98.26
	4.84	2.86	16.07	55.90	1.69	6.56	1.48	0.24	9.61	99.25
	4.58	2.60	15.88	56.49	1.66	6.32	1.59	0.27	10.64	100.03
Average:	**4.70**	**2.60**	**16.05**	**56.55**	**1.75**	**6.23**	**1.54**	**0.23**	**9.04**	**98.70**
Stdev:	**0.19**	**0.31**	**0.43**	**0.83**	**0.15**	**0.23**	**0.08**	**0.04**	**0.88**	**1.03**
					LC-3Ab (n=6)					
	5.49	0.13	27.67	54.36	0.31	10.53	0.19	0.02	0.79	99.49
	5.36	0.11	28.28	54.01	0.24	11.00	0.09	0.06	0.72	99.87
	5.30	0.18	28.13	54.22	0.30	11.14	0.16	0.05	1.08	100.55
	5.19	0.14	28.66	54.34	0.24	11.24	0.09	0.02	0.89	100.81
	4.77	0.11	29.09	53.69	0.17	12.06	0.13	0.00	0.86	100.88
	4.70	0.11	29.35	53.01	0.20	12.14	0.10	0.03	0.71	100.34
Average:	**5.14**	**0.13**	**28.53**	**53.94**	**0.24**	**11.35**	**0.13**	**0.03**	**0.84**	**100.32**
Stdev:	**0.28**	**0.03**	**0.54**	**0.28**	**0.06**	**0.55**	**0.04**	**0.02**	**0.13**	**0.61**
					LC-3A Discarded analyses (n=5)					
	1.14	0.43	15.33	60.50	2.89	3.78	1.05	0.17	3.24	88.52
	6.19	0.04	27.69	56.80	0.27	9.52	0.03	0.00	0.52	101.05
	4.26	1.97	19.52	54.37	1.11	8.82	1.29	0.20	7.89	99.42
	4.84	1.00	23.82	54.51	0.79	8.73	0.64	0.13	3.86	98.32
	4.73	0.69	25.12	53.40	0.51	9.81	0.46	0.03	2.89	97.64

	Na2O	MgO	Al2O3	SiO2	K2O	CaO	TiO2	MnO	FeO	Total
					LC-3Ba (n=4)					
	5.18	0.06	28.66	54.09	0.25	11.17	0.02	0.00	0.46	99.88
	5.51	0.06	28.58	55.34	0.25	10.47	0.03	0.01	0.47	100.72
	4.85	0.10	29.17	53.44	0.28	11.80	0.02	0.00	0.48	100.13
	5.97	0.04	27.88	55.86	0.25	9.88	0.04	0.06	0.50	100.47
Average:	**5.38**	**0.06**	**28.57**	**54.68**	**0.26**	**10.83**	**0.02**	**0.02**	**0.48**	**100.30**
Stdev:	**0.48**	**0.02**	**0.53**	**1.12**	**0.01**	**0.83**	**0.01**	**0.03**	**0.02**	**0.37**
					LC-3Bb (n=2)					
	1.41	0.05	34.35	45.68	0.05	18.00	0.07	0.04	0.61	100.26
	1.49	0.07	34.40	45.98	0.06	17.71	0.00	0.00	0.66	100.37
Average:	**1.45**	**0.06**	**34.37**	**45.83**	**0.06**	**17.86**	**0.03**	**0.02**	**0.64**	**100.32**
Stdev:	**0.06**	**0.02**	**0.04**	**0.22**	**0.00**	**0.21**	**0.04**	**0.03**	**0.03**	**0.08**
					LC-3B Discarded analyses (n=14)					
	6.77	0.05	26.26	57.73	0.43	8.54	0.12	0.02	0.54	100.45
	7.24	0.08	18.40	58.13	0.67	1.07	0.00	0.03	0.01	85.64
	9.49	0.02	19.47	59.75	0.07	0.96	0.24	0.04	0.06	90.09
	0.00	0.02	0.02	97.47	0.02	0.02	0.00	0.01	0.01	97.57
	0.04	0.00	0.06	96.14	0.03	0.02	0.00	0.00	0.03	96.32
	0.06	0.00	0.07	98.63	0.04	0.02	0.00	0.01	0.00	98.82
	0.84	0.00	22.62	54.11	0.06	11.38	0.00	0.00	0.00	89.01
	6.72	0.01	21.05	55.40	0.09	3.61	0.00	0.04	0.00	86.92
	0.91	2.04	16.91	69.18	0.62	4.82	0.01	0.00	0.07	94.56
	0.41	0.01	12.07	69.11	2.84	3.71	0.00	0.04	0.02	88.20
	4.67	0.23	11.86	75.30	2.46	0.86	0.00	0.02	0.73	96.11
	2.97	0.00	22.49	54.96	0.08	9.49	0.05	0.02	0.00	90.06
	3.38	0.11	31.20	50.45	0.30	13.81	0.06	0.00	0.67	99.98
	4.51	0.10	29.90	52.43	0.21	12.24	0.09	0.00	0.71	100.17

	Na2O	MgO	Al2O3	SiO2	K2O	CaO	TiO2	MnO	FeO	Total
					NL-4Ba (n=8)					
	4.68	1.51	16.47	63.25	2.32	4.10	1.00	0.20	5.04	99.17
	4.86	1.65	15.79	63.47	2.35	3.80	0.97	0.19	5.15	99.75
	4.88	1.50	16.03	63.88	2.53	3.69	1.15	0.18	5.33	98.22
	5.22	1.34	15.96	64.72	2.13	3.73	1.23	0.20	5.00	98.78
	4.98	1.22	15.91	64.88	2.47	3.61	0.95	0.14	4.62	98.27
	4.84	1.29	15.41	65.14	2.75	3.29	0.98	0.18	4.62	98.49
	5.01	1.51	15.73	65.18	2.50	3.46	1.20	0.17	5.31	99.52
	4.80	1.22	15.45	65.28	2.54	3.13	0.92	0.19	4.74	100.06
Average:	**4.74**	**1.74**	**15.51**	**64.63**	**2.48**	**3.72**	**1.10**	**0.24**	**5.60**	**98.56**
Stdev:	**0.16**	**0.16**	**0.34**	**0.82**	**0.19**	**0.30**	**0.12**	**0.02**	**0.29**	**0.70**
					NL-4Bb (n=2)					
	5.79	0.04	27.57	56.38	0.27	9.56	0.08	0.00	0.62	100.30
	6.09	0.03	27.13	56.82	0.33	9.15	0.06	0.00	0.51	101.45
Average:	**5.94**	**0.03**	**27.35**	**56.60**	**0.30**	**9.35**	**0.07**	**0.00**	**0.56**	**100.88**
Stdev:	**0.21**	**0.01**	**0.31**	**0.31**	**0.04**	**0.28**	**0.02**	**0.00**	**0.08**	**0.82**
					NL-4B Discarded analyses (n=10)					
	0.08	0.03	0.63	2.00	0.07	0.17	0.03	0.02	0.12	3.15
	3.05	1.82	15.42	64.73	2.48	3.67	1.15	0.17	5.36	97.85
	6.98	0.02	18.93	66.29	2.40	2.62	0.16	0.00	0.73	98.13
	4.39	0.34	14.06	74.07	1.73	2.58	0.32	0.02	1.49	99.83
	4.79	0.03	29.59	54.01	0.39	11.81	0.01	0.06	0.77	100.12
	5.15	0.10	26.09	59.17	0.62	9.21	0.16	0.00	0.80	101.29
	4.06	0.20	13.17	75.32	3.13	1.54	0.50	0.06	1.86	95.03
	5.01	0.22	14.29	67.51	3.28	1.75	0.63	0.06	2.30	100.06
	5.30	0.62	15.07	70.26	3.27	1.95	0.47	0.16	2.96	99.43
	5.39	0.37	16.32	69.29	3.01	2.12	0.49	0.11	2.34	98.99

	Na2O	MgO	Al2O3	SiO2	K2O	CaO	TiO2	MnO	FeO	Total
					BC-3Ca (n=5)					
	4.72	1.12	14.60	65.43	2.46	3.09	0.77	0.16	4.10	96.44
	4.85	1.51	15.58	64.00	2.37	3.86	0.95	0.19	5.17	98.49
	4.70	1.66	15.47	63.74	2.19	4.17	0.87	0.16	5.51	98.46
	4.69	1.66	15.37	62.82	2.23	4.11	0.86	0.19	5.38	97.31
	4.78	1.23	14.98	66.46	2.62	3.11	0.75	0.15	4.32	98.42
Average:	**4.75**	**1.44**	**15.20**	**64.49**	**2.38**	**3.67**	**0.84**	**0.17**	**4.90**	**97.82**
Stdev:	**0.07**	**0.25**	**0.40**	**1.45**	**0.18**	**0.53**	**0.08**	**0.02**	**0.64**	**0.92**
					BC-3Cb (n=4)					
	4.23	3.03	16.26	57.82	1.56	6.77	1.10	0.19	7.85	98.82
	4.37	3.17	16.23	57.18	1.51	6.68	1.12	0.22	8.26	98.72
	4.48	2.61	15.99	58.76	1.79	5.98	1.15	0.14	6.99	97.89
	5.01	2.18	17.47	59.63	1.33	6.42	1.02	0.11	6.36	99.53
Average:	**4.52**	**2.75**	**16.49**	**58.35**	**1.55**	**6.46**	**1.10**	**0.16**	**7.37**	**98.74**
Stdev:	**0.34**	**0.45**	**0.66**	**1.07**	**0.19**	**0.36**	**0.05**	**0.05**	**0.85**	**0.67**
					BC-3C Discarded analyses (n=11)					
	6.47	0.11	25.58	57.49	0.55	8.20	0.10	0.02	0.80	99.31
	6.02	0.21	24.73	58.20	0.80	8.27	0.22	0.06	1.33	99.83
	6.94	0.06	25.79	57.86	0.43	8.09	0.07	0.00	0.60	99.84
	5.97	0.07	27.31	55.88	0.30	9.76	0.04	0.01	0.64	99.98
	4.16	4.41	14.10	59.79	1.74	5.20	0.99	0.27	8.18	98.85
	5.71	0.08	26.47	54.23	0.30	9.88	0.06	0.01	0.76	97.50
	5.16	1.21	19.09	61.22	1.54	5.91	0.62	0.13	4.11	98.97
	5.17	0.46	15.11	69.59	2.98	1.66	0.55	0.19	2.41	98.12
	5.23	0.94	20.73	59.70	1.31	6.78	0.44	0.05	3.60	98.78
	5.08	0.99	15.93	65.98	2.36	3.16	0.72	0.14	3.97	98.32
	5.42	0.95	18.12	64.08	1.92	4.50	0.75	0.16	3.26	99.14

	Na2O	MgO	Al2O3	SiO2	K2O	CaO	TiO2	MnO	FeO	Total
					BC-3F (n=17)					
	4.29	3.20	16.33	57.23	1.47	6.84	1.31	0.19	8.36	99.21
	4.36	2.84	16.51	58.48	1.59	6.45	1.15	0.12	7.37	98.87
	4.29	3.00	16.08	57.02	1.54	6.57	1.27	0.21	8.16	98.13
	4.46	2.57	16.42	60.03	1.74	5.86	1.05	0.18	7.31	99.62
	4.42	2.74	16.42	59.20	1.74	6.03	1.19	0.13	7.61	99.47
	4.55	2.60	16.42	60.08	1.72	5.88	1.08	0.18	7.46	99.96
	4.25	3.18	16.56	57.58	1.54	6.65	1.02	0.19	8.42	99.39
	3.97	3.10	16.41	57.80	1.51	6.83	1.14	0.19	8.37	99.32
	4.11	2.80	16.59	58.89	1.69	6.30	1.10	0.16	7.50	99.12
	4.21	3.10	16.48	57.80	1.63	6.56	1.22	0.17	8.43	99.59
	4.69	2.48	16.35	60.71	1.88	5.51	1.11	0.20	6.94	99.87
	4.24	2.97	16.58	58.13	1.55	6.62	1.14	0.21	8.31	99.74
	4.25	2.93	16.37	58.86	1.68	6.52	1.00	0.23	8.60	100.44
	4.18	3.23	16.53	57.23	1.52	6.91	1.11	0.14	8.91	99.77
	4.46	2.67	16.54	60.31	1.81	5.82	1.16	0.18	7.25	100.20
	4.08	3.05	16.51	57.82	1.55	6.74	1.20	0.20	8.36	99.51
	4.54	2.68	16.59	59.32	1.74	5.96	1.16	0.13	7.34	99.46
Average:	**4.31**	**2.89**	**16.45**	**58.62**	**1.64**	**6.36**	**1.14**	**0.18**	**7.92**	**99.51**
Stdev:	**0.19**	**0.24**	**0.13**	**1.17**	**0.12**	**0.43**	**0.08**	**0.03**	**0.60**	**0.53**
					BC-3F Discarded analyses (n=3)					
	4.73	1.43	15.69	66.24	2.38	3.72	0.77	0.21	4.88	100.04
	4.38	2.66	17.89	57.97	1.38	7.08	1.19	0.19	7.68	100.43
	4.69	2.24	16.38	61.12	1.97	5.09	1.04	0.16	6.34	99.01

	Na2O	MgO	Al2O3	SiO2	K2O	CaO	TiO2	MnO	FeO	Total
					BC-3H (n=10)					
	5.19	1.02	15.96	66.61	2.52	2.96	0.74	0.17	3.84	98.99
	4.92	1.28	16.28	66.21	2.55	3.43	0.91	0.15	4.54	100.27
	4.87	1.20	15.73	65.02	2.47	3.34	1.00	0.16	4.47	98.26
	4.84	1.29	15.79	65.97	2.66	3.43	0.88	0.19	4.65	99.69
	4.81	1.22	16.08	65.49	2.61	3.38	0.89	0.18	4.66	99.32
	5.07	1.12	16.39	65.94	2.43	3.49	0.95	0.13	4.12	99.63
	5.23	1.06	16.56	65.82	2.32	3.61	0.87	0.15	4.02	99.65
	4.80	1.22	15.95	65.32	2.86	3.18	0.93	0.13	4.73	99.13
	4.98	1.11	16.70	65.04	2.43	3.78	0.73	0.19	4.17	99.14
	5.23	1.34	16.06	66.02	2.32	3.53	1.02	0.20	4.49	100.19
Average:	**4.99**	**1.19**	**16.15**	**65.74**	**2.52**	**3.41**	**0.89**	**0.17**	**4.37**	**99.43**
Stdev:	**0.17**	**0.11**	**0.32**	**0.51**	**0.16**	**0.23**	**0.10**	**0.02**	**0.31**	**0.60**
					BC-3H Discarded analyses (n=10)					
	4.42	2.52	16.38	60.43	1.81	5.71	1.05	0.20	7.04	99.57
	4.42	2.30	16.00	57.34	1.78	5.21	1.15	0.12	6.67	94.98
	5.16	0.81	15.34	68.88	2.92	2.45	0.72	0.12	3.34	99.74
	5.07	0.77	15.64	69.34	2.85	2.31	0.69	0.07	3.46	100.20
	4.88	1.64	15.74	64.80	2.51	3.52	0.89	0.18	4.73	98.88
	5.13	0.09	29.32	54.21	0.18	11.58	0.09	0.04	0.66	101.29
	5.26	0.58	18.96	65.72	2.11	4.44	0.58	0.06	2.57	100.28
	4.25	2.12	21.86	54.44	0.58	10.00	0.82	0.15	6.20	100.40
	2.89	10.76	10.43	58.04	0.79	3.23	0.29	0.37	12.27	99.07
	4.69	0.07	29.86	53.65	0.15	12.34	0.02	0.00	0.58	101.36

	Na2O	MgO	Al2O3	SiO2	K2O	CaO	TiO2	MnO	FeO	Total
					NL-3Ba (n=8)					
	4.94	0.73	15.10	68.35	2.70	2.46	0.72	0.17	3.30	98.47
	5.24	0.76	15.45	68.47	2.66	2.44	0.66	0.15	3.41	99.24
	5.12	0.79	15.05	67.93	2.77	2.40	0.72	0.21	3.33	98.32
	5.04	0.80	15.23	68.09	2.81	2.47	0.77	0.18	3.38	98.78
	4.98	0.84	15.62	69.04	2.77	2.45	0.73	0.17	3.47	100.05
	5.03	0.84	15.24	68.39	2.71	2.52	0.75	0.17	3.16	98.81
	4.79	1.00	15.16	67.21	2.98	2.87	0.96	0.16	4.37	99.49
	4.91	1.02	15.21	67.35	3.00	2.87	1.01	0.15	4.85	100.37
Average:	**5.01**	**0.85**	**15.26**	**68.10**	**2.80**	**2.56**	**0.79**	**0.17**	**3.66**	**99.19**
Stdev:	**0.14**	**0.11**	**0.19**	**0.60**	**0.12**	**0.19**	**0.12**	**0.02**	**0.61**	**0.74**
					NL-3Bb (n=7)					
	4.24	3.14	16.40	57.21	1.50	6.92	1.18	0.23	8.53	99.34
	4.37	2.98	16.58	58.37	1.58	6.49	1.11	0.25	8.14	99.88
	4.10	2.94	16.38	58.68	1.64	6.30	1.06	0.16	7.81	99.05
	4.40	2.61	16.60	59.82	1.85	5.88	1.10	0.23	6.92	99.43
	4.34	2.67	16.38	60.10	1.80	5.92	1.21	0.15	7.21	99.77
	4.53	2.61	16.37	60.46	1.67	5.86	1.17	0.19	7.24	100.10
Average:	**4.33**	**2.83**	**16.45**	**59.11**	**1.68**	**6.23**	**1.14**	**0.20**	**7.64**	**99.60**
Stdev:	**0.15**	**0.22**	**0.11**	**1.24**	**0.13**	**0.42**	**0.06**	**0.04**	**0.62**	**0.39**
					NL-3B Discarded analyses (n=6)					
	4.70	1.34	15.99	65.92	2.64	3.50	0.97	0.16	5.04	100.26
	4.75	1.85	16.01	63.64	2.12	4.38	0.81	0.16	5.59	99.31
	4.70	1.87	15.47	61.76	2.16	4.55	1.21	0.22	7.36	99.30
	2.21	0.50	5.88	25.14	0.98	34.97	0.30	0.15	1.54	71.67
	5.27	0.47	15.20	70.51	3.06	1.68	0.49	0.13	2.40	99.21
	5.79	0.56	18.97	66.60	2.00	4.23	0.55	0.12	2.55	101.37

	Na2O	MgO	Al2O3	SiO2	K2O	CaO	TiO2	MnO	FeO	Total
					NL-3Ca (n=13)					
	4.50	2.16	15.87	61.73	2.00	4.93	0.91	0.15	6.26	98.52
	4.30	2.39	15.78	59.73	1.95	5.36	1.09	0.15	7.04	97.80
	4.48	2.60	16.50	60.13	1.78	5.80	1.10	0.19	7.09	99.67
	4.44	2.44	16.52	60.61	1.90	5.48	0.99	0.18	7.17	99.73
	4.41	2.62	16.06	59.78	1.81	5.87	1.18	0.20	7.19	99.13
	4.54	2.59	16.28	60.17	1.79	5.91	1.05	0.20	7.35	99.86
	4.45	2.66	16.16	60.31	1.73	5.82	1.02	0.17	7.40	99.71
	4.55	2.67	16.11	59.79	1.74	5.88	1.02	0.21	7.46	99.42
	4.36	2.69	16.20	59.16	1.72	5.96	1.08	0.20	7.59	98.95
	4.52	2.74	16.46	59.39	1.76	6.06	1.17	0.18	7.71	99.99
	4.52	2.85	16.33	58.76	1.59	6.45	1.13	0.18	7.83	99.63
	4.32	3.06	16.41	58.04	1.58	6.68	1.10	0.20	8.65	100.04
	4.25	3.09	16.42	57.86	1.47	6.62	1.17	0.14	8.51	99.52
Average:	**4.43**	**2.66**	**16.24**	**59.65**	**1.76**	**5.91**	**1.08**	**0.18**	**7.48**	**99.38**
Stdev:	**0.10**	**0.25**	**0.24**	**1.05**	**0.15**	**0.49**	**0.08**	**0.02**	**0.62**	**0.64**
					NL-3Cb (n=4)					
	5.07	0.86	15.39	68.08	2.65	2.65	0.72	0.08	3.61	99.11
	5.00	0.86	15.65	67.92	2.65	2.39	0.71	0.12	3.39	98.68
	5.17	0.82	15.84	67.91	2.69	2.57	0.84	0.14	3.33	99.33
	4.69	0.92	14.80	67.32	3.02	2.54	0.91	0.14	4.28	98.61
Average:	**4.98**	**0.87**	**15.42**	**67.81**	**2.75**	**2.54**	**0.80**	**0.12**	**3.65**	**98.93**
Stdev:	**0.21**	**0.04**	**0.45**	**0.33**	**0.18**	**0.11**	**0.10**	**0.03**	**0.43**	**0.34**
					NL-3C Discarded analyses (n=3)					
	6.50	0.04	26.31	58.10	0.42	8.61	0.00	0.00	0.50	100.49
	4.58	1.09	14.71	65.11	2.82	2.94	0.97	0.17	4.50	96.89
	4.80	1.60	15.82	63.06	2.25	4.11	1.01	0.23	5.32	98.19